



Dissertations

Graduate College

12-2007

MAPK Survival Signaling in Melanoma

Matthew W. VanBrocklin
Western Michigan University

Follow this and additional works at: <https://scholarworks.wmich.edu/dissertations>



Part of the Biology Commons, Cell and Developmental Biology Commons, and the Physiology Commons

Recommended Citation

VanBrocklin, Matthew W., "MAPK Survival Signaling in Melanoma" (2007). *Dissertations*. 923.
<https://scholarworks.wmich.edu/dissertations/923>

This Dissertation-Open Access is brought to you for free and open access by the Graduate College at ScholarWorks at WMU. It has been accepted for inclusion in Dissertations by an authorized administrator of ScholarWorks at WMU. For more information, please contact wmu-scholarworks@wmich.edu.



MAPK SURVIVAL SIGNALING IN MELANOMA

by

Matthew W. VanBrocklin

A Dissertation
Submitted to the
Faculty of The Graduate College
in partial fulfillment of the
requirements for the
Degree of Doctor of Philosophy
Department of Biological Sciences
Dr. Bruce Bejcek, Advisor

Western Michigan University
Kalamazoo, Michigan
December 2007

MAPK SURVIVAL SIGNALING IN MELANOMA

Matthew W. VanBrocklin, Ph.D.

Western Michigan University, 2007

Extracellular signals activate mitogen-activated protein kinase (MAPK) cascades potentiating biological activities such as cell proliferation, differentiation, and survival. Constitutive activation of MAPK signaling pathways is implicated in the development and progression of many human cancers, including melanoma. Mutually exclusive activating mutations in NRAS or BRAF are found in ~85% of all melanomas resulting in constitutive activation of the MAPK pathway (RAS-BRAF-MEK-ERK-RSK). We have previously demonstrated that inhibition of this pathway with small molecule MEK inhibitors selectively induces apoptosis in human melanoma cells both in vitro and in vivo, but not in normal melanocytes. These results support the notion that the MAPK pathway represents a tumor-specific survival signaling pathway in melanoma, and that targeting members of this pathway may be an effective therapeutic intervention strategy for treating melanoma. Understanding the mechanisms by which constitutive MAPK activation promotes survival and defining the minimal vital MAPK pathway components required for the development and progression of melanoma may have direct translational implications. The overall objective of this Doctoral Thesis was to define the

molecular mechanism(s) by which the MAPK pathway mediates melanoma-specific survival signals. In doing so, several new promising therapeutic targets (Bcl-2, Bcl-xL and Mcl-1) have emerged and a novel small molecule inhibitor (TW37) of these has been developed. Combined targeting of MAPK and these Bcl-2 pro-survival members was synergetic in vitro and in vivo. Additionally, the ability of RAS, BRAF and RSK to transform normal mouse melanocytes was evaluated revealing that NRAS and BRAF are very efficient while RSK required secondary genetic events for progression. Upon investigation, high level intrachromosomal gene amplification of Met, a growth factor receptor tyrosine kinase implicated in melanoma progression. MET expression is rarely detected in primary human melanoma, but is frequently observed in advanced metastatic disease and therefore may be an additional attractive therapeutic target to prevent disease progression.

UMI Number: 3293193

INFORMATION TO USERS

The quality of this reproduction is dependent upon the quality of the copy submitted. Broken or indistinct print, colored or poor quality illustrations and photographs, print bleed-through, substandard margins, and improper alignment can adversely affect reproduction.

In the unlikely event that the author did not send a complete manuscript and there are missing pages, these will be noted. Also, if unauthorized copyright material had to be removed, a note will indicate the deletion.

UMI[®]

UMI Microform 3293193

Copyright 2008 by ProQuest Information and Learning Company.

All rights reserved. This microform edition is protected against unauthorized copying under Title 17, United States Code.

ProQuest Information and Learning Company
300 North Zeeb Road
P.O. Box 1346
Ann Arbor, MI 48106-1346

ACKNOWLEDGMENTS

This dissertation is dedicated to the memory of Dr. Han-Mo Koo, in whose lab this work began, who lost his battle with cancer in May 2004. He was a respected scientist and friend, devoted husband and father (1963-2004). I would like to thank my beautiful wife, Sheri Holmen, Ph.D., for her undying commitment and continuous support during this process. I am grateful for our past and current scientific collaborations as well as family additions Brooke and Evan. Additionally I would like to acknowledge the tremendous support I have received from Dr. George Vande Woude and the Van Andel Research Institute.

I would like to acknowledge my advisor, Dr. Bruce Bejcek, for providing me with this opportunity and for his guidance along the way. I would also like to thank my graduate advisory committee members Dr. John Geiser and Dr. Pamela Hoppe for their advice and support.

Matthew W. VanBrocklin

TABLE OF CONTENTS

ACKNOWLEDGMENTS	ii
LIST OF TABLES	ix
LIST OF FIGURES	x
CHAPTER	
I. INTRODUCTION	1
Skin Anatomy and Pigmentation.....	1
Skin Cancer and Melanoma Epidemiology.....	3
Melanoma Classification.....	7
Etiology	8
Current Therapies.....	10
Promising Clinical Trials.....	11
Discussion	13
BIBLIOGRAPHY.....	15
II. DIFFERENTIAL ONCOGENIC POTENTIAL OF ACTIVATED RAS ISOFORMS IN MELANOCYTES	19
Abstract	19
Introduction	20
Materials and Methods.....	22
Isolation of primary melanocytes and melanoma cells.....	22
Cell culture.....	23
Immunohistochemistry	23

Table of Contents—continued

CHAPTER		
	Microarray data generation and analysis	24
	Vector constructs	25
	Virus propagation	26
	Viral infections	27
	Cell lysis and immunoprecipitation	27
	Western blotting.....	28
	Growth in soft agar	28
	Cell proliferation studies.....	29
	<i>In vivo</i> studies	29
	Results	30
	Ink4a/Arf-deficient melanocytes are immortal in culture.....	30
	RAS/MAPK activation induces anchorage-independent growth of melanocytes <i>in vitro</i>	33
	NRAS activation in melanocytes is potently tumorigenic <i>in vivo</i>	34
	NRAS and KRAS both activate the classical MAPK pathway in melanocytes.....	35
	NRAS, but not KRAS, increases the rate of proliferation of melanocytes and prevents GSK3-mediated phosphorylation of Myc.....	37
	Coexpression of KRAS and either MYC or AKT increases the tumorigenicity of melanocytes.....	40
	The proliferation rate of KRAS-expressing melanocytes is increased by MYC expression	43

Table of Contents—continued

CHAPTER		
	Discussion	43
	Acknowledgements	46
	BIBLIOGRAPHY	47
III.	MALIGNANT TRANSFORMATION OF MELANOCYTES BY OVEREXPRESSION OF RSK.....	51
	Abstract	51
	Introduction	52
	Materials and Methods.....	55
	Cell culture.....	55
	Inhibitors	55
	Immunohistochemistry	56
	Vector constructs	57
	Virus production	57
	Viral infections	57
	Western blotting.....	58
	Growth in soft agar	59
	Cell proliferation studies.....	59
	<i>In vivo</i> studies	59
	Metaphase spreads	60
	Reverse DAPI	60
	Spectral karyotyping (SKY)	60
	Fluorescent <i>in situ</i> hybridization (FISH)	61

Table of Contents—continued

CHAPTER		
	Results	62
	RSK is overexpressed and highly activated in human melanoma cells.....	62
	RSK overexpression/activation increases the proliferation of melanocytes.....	63
	Melanocytes expressing wt RSK or RSK-CAII are tumorigenic	66
	Tumor cells expressing wt RSK are aneuploid.....	69
	Increased Met protein levels result from gene amplification.	70
	Discussion	72
	Acknowledgements	74
	BIBLIOGRAPHY.....	75
IV.	A NOVEL BH3 MIMETIC REVEALS A MAPK-DEPENDENT MECHANISM OF MELANOMA CELL DEATH CONTROLLED BY p53 AND REACTIVE OXYGEN SPECIES	79
	Abstract	79
	Introduction	80
	Materials and Methods	83
	Cell culture.....	83
	Reagents.....	84
	Design and binding assays for TW-37.....	84
	Drug treatments and cell viability	85
	Cell cycle analyses.....	86
	Protein immunoblots.....	86

Table of Contents—continued

CHAPTER		
	Stable short hairpin interfering RNA constructs (shRNA).....	87
	Immunofluorescent visualization of activation-dependent conformational changes of BAX	87
	Detection of ROS production by fluorescent microscopy	88
	Indirect measurement of oxidized proteins.....	88
	Melanoma growth <i>in vivo</i> (Mouse xenographs)	89
	Statistics	90
	Mutational status of BRAF and NRAS.....	90
	Primary antibodies.	91
	Results	91
	Identification of melanoma cell lines resistant to inhibition of the MAPK pathway	91
	Anti-apoptotic factors retained after ERK inhibition.	92
	Stable RNA interference for target validation	94
	Pharmacological enhancement of the response of melanoma cells to U0126: Design and validation of new BH3 mimetics.....	96
	Selective and synergistic killing of melanoma cells by U0126 and TW-37.	98
	Mechanistic analyses of the TW-37/U0126 combination. Release of pro-apoptotic factors from the mitochondria	99
	Impact of MEK/ERK inhibition upstream of BAX.	104
	Reactive oxygen species (ROS) modulating the cytotoxic effect of TW-37/U0126.....	105
	ROS-dependent activation of p53 by TW-37/U0126.	107

Table of Contents—continued

CHAPTER	
	p53 and ROS define the tumor cell-selective toxicity of TW-37/U0126..... 108
	General impact of MEK inhibitors on TW-37 mediated cell death. Anti-cancer activity <i>in vivo</i> 112
	Discussion 115
	Acknowledgements 120
	Grant support 120
APPENDIX	
	Animal Protocol Approval 121
BIBLIOGRAPHY 122

LIST OF TABLES

CHAPTER I

1. Current AJCC Staging System for Cutaneous Melanoma..... 8

CHAPTER II

1. Tumorigenicity of *Ink4a/Arf*^{-/-} melanocytes expressing different combinations of oncogenes. 31

CHAPTER III

1. Tumorigenicity of melanocytes expressing different components of the MAPK pathway 67
2. DNA content of melanocytes and tumor cells 70

LIST OF FIGURES

CHAPTER II

1. Gene expression-based evaluation of the melanocytic origin of the D6-MEL cell line.....	32
2. Proposed RAS signaling pathways.....	36
3. <i>In vivo</i> tumor formation.....	36
4. <i>In vitro</i> proliferation of melanocytes expressing different genes.....	38
5. RAS-mediated regulation of c-Myc phosphorylation.....	40
6. Expression of <i>KRAS</i> , <i>AKT</i> and <i>MYC</i> in melanocytes.....	41
7. <i>In vivo</i> tumor formation.....	42

CHAPTER III

1. MAPK (ERK1&2) and RSK activation in melanoma cell lines.....	63
2. Indirect immunofluorescent staining of RSK-1 in human melanoma cells treated with DMSO or PD98059.....	64
3. Oncogene expression in immortal melanocytes.....	65
4. (A) <i>In vitro</i> proliferation of melanocytes expressing different genes.....	66
4. (B) <i>In vivo</i> tumor formation.....	68
5. Spectral karyotyping and <i>Met</i> FISH of melanocytes and tumor cells.....	71

CHAPTER IV

1. Cytostatic effect of the MEK inhibitor U0126 on metastatic melanoma lines.....	93
2. Tumor-cell selectivity of TW-37/U0126.....	95
3. TW-37 as a novel class of BH3 mimetics.....	97

List of Figures—continued

CHAPTER IV

3. TW-37 as a novel class of BH3 mimetics.....	98
4. Synergistic caspase activation by the TW-37/U0126 combination.....	100
5. Genetic inactivation of anti-apoptotic Bcl-2 proteins by lentiviral-mediated RNA interference	101
6. Inhibitory effect of antioxidants on BAX activation	102
7. Classical BH3-mimetic features of TW-37.....	103
7. Classical BH3-mimetic features of TW-37.....	104
8. ROS production modulates the cytotoxic effect of TW-37/U0126	106
8. ROS production modulates the cytotoxic effect of TW-37/U0126	108
9. BH3 Mimetics and MEK inhibition cooperate in the activation of p53	109
10. p53 and ROS define the tumor cell-selective toxicity of TW-37/U0126	111
11. Synergy between TW-37 and MEK inhibitors is not restricted to U0126 and can be visualized <i>in vivo</i>	113
11. Synergy between TW-37 and MEK inhibitors is not restricted to U0126 and can be visualized <i>in vivo</i>	114

CHAPTER I

INTRODUCTION

Skin Anatomy and Pigmentation

The skin is the largest organ in the body and performs many essential functions. It consists of three layers; the epidermis (outermost), dermis and the subcutis. The thin epidermis layer consists primarily of keratinocytes which originate in the basal layer from the division of keratinocyte stem cells. These cells gradually undergo differentiation as they are pushed to the stratum corneum, the outermost layer of the epidermis. There they form an effective barrier of dead highly keratinized squamous cells which are continuously shed. The dermis consists of connective tissue as well as hair follicles, nerves and various glands and is tightly connected to the epidermis by a basement membrane. The thicker subcutis primarily serves as an insulator and energy storage reservoir as it is primarily composed of adipose tissue.

Neural crest derived melanocytes comprise 5 to 10% of the cells in the epidermal layer and reside near the basal layer where they obtain growth factors derived from keratinocytes. Melanocytes are migratory cells that produce the pigment melanin, which is responsible for skin, hair, and eye color. The amount of melanin produced by the melanocytes is regulated by genetic as well as environmental factors such as UV irradiation, which stimulates melanin formation as a protective response and results in the formation of a tan (1). In humans the variety

of skin color is the result of differences in basal melanin production rather than net differences in melanocyte number or melanocyte stimulating hormone (MSH) levels (1). Small nucleotide polymorphisms (SNPs) in the MSH receptor, MC1R, as well as cell surface density plays a crucial role in melanin production and the distinct pigmentation of each ethnic group and race (1, 2). Melanin is exported to nearby keratinocytes resulting in uniform skin color, but can localize to produce freckles, birthmarks or nevi (moles).

The inability of melanocytes to produce adequate melanin results in little or no pigment in the eyes, skin or hair and is identified as albinism. There is a broad range of pigment loss depending on the genetic defect involved, with tyrosinase-related defects being the most common and exhibiting some of the most severe phenotypes. In addition to pigment loss, all people with albinism exhibit some form of vision impairment, and interestingly the primary test for albinism is an eye exam. Albinism is distributed relatively evenly across all races and people with albinism generally live normal life spans with comparable medical problems as their counterparts.

In contrast, vitiligo is a chronic skin condition characterized by the localized loss of skin pigment resulting in irregular pale patches. These de-pigmented patches typically appear on the extremities and are often symmetric. De-pigmentation is a result of melanocyte loss due to autoimmune or inflammatory disorders and generally worsens over time. Immune modulation by corticosteroids is the most common approach to treatment, although new therapies employed to promote melanocyte repopulation are rapidly becoming available.

Skin Cancer and Melanoma Epidemiology

Not surprisingly skin cancer is the most common form of malignancy in the United States with more than 1.5 million new cases diagnosed annually (3). Skin cancers generally develop in the epidermis making them highly visible which allows for early detection. Basal cell carcinoma (BCC) alone accounts for more than 1 million new cases annually, while more than 250,000 people develop squamous cell carcinoma (SCC). BCCs are derived from basal cells that line the deepest layer of the epidermis and are generally found in areas of the body that are most frequently exposed to the sun. SCC develops from squamous cells on the periphery of the skin and like BCC often arises in sun exposed areas, but may also develop in areas of the skin that may have been burned or exhibit chronic inflammation. BCC and SCC incidence increases approaching the equator. The lifetime risk of developing these skin cancers is about one in five for all Americans and one in three for Caucasians. Fortunately, these types of neoplasms rarely metastasize, are easily treated by surgical resection and are associated with a low morbidity.

Although melanoma only accounts for 4% of all skin cancers, it is responsible for 79% of skin cancer deaths and early diagnosis is critical to the successful treatment of the disease. Five-year relative survival rates for localized or metastatic melanoma is 99% and 15%, respectively (4). Unfortunately, the incidence of melanoma is increasing rapidly in the U.S. and is now the sixth most common cancer overall in men and women with a predicted 59,940 new cases diagnosed in 2007 (4).

Currently melanoma is the most common cancer in men and women ages 20-29 and is the leading cause of cancer death in women between the ages of 25-29 (5).

Nevi are clusters of pigmented cells (primarily melanocytes and keratinocytes) that often appear as small, dark brown spots on the torso, face, arms and legs which can give rise to melanoma. Melanoma is a malignant neoplasm which originates from the melanocytes. Melanomas most often arise within epidermal melanocytes of the skin, although they can also derive from noncutaneous melanocytes such as those lining the choroidal layer of the eye and internal organs (2). Most melanomas are black or brown, but can range from skin-colored to pink, red or purple. Accurate diagnosis of melanoma requires experience, as early stages may look identical to harmless moles or not have any color at all. As with most cancers, early detection is paramount for enhanced survival. Likely due to its migratory history, melanomas are highly metastatic resulting in high mortality.

There are several factors, both environmental as well as genetic, that can contribute to an increased risk for melanoma. Probably the most important environmental factor that can lead to an increased risk of melanoma is exposure to sun light. Over the past 60 years there has been a dramatic increase in the melanoma rate in the U.S. due to the increase in skin exposure to sun light that has become culturally desirable. In 1940, when conservative clothing was in vogue, the lifetime risk of developing melanoma in the U.S. was 1 in 1,500 which contrasts sharply with a 2007 predicted rate of 1 in 67 (4, 5). High incidences of skin cancer are also seen in other countries with substantial sun exposure and a fair skinned population such as Australia. Australia has the highest melanoma incidence world wide where the

immigrant white population is 3 to 5 times more likely to develop melanoma than their American or European counterparts (6).

Although sun exposure is a major contributing factor to melanoma development its effects can be mitigated by skin pigmentation. Therefore, race is a major risk factor for developing melanoma with fair-skinned races at greater risk than darker-skinned races. White Americans are 4 and 20 times more likely to develop melanoma than Hispanic and African Americans, respectively and worldwide white populations have the highest risk of developing melanoma. Interestingly, Asian populations have the lowest risk (7). In addition to race, additional relevant risk factors include a fair complexion, red hair, atypical or dysplastic nevi and increased numbers of nevi (8).

Several genetic components have been associated with an increased incidence of melanoma. In 1857, William Norris identified individuals with a family history of melanoma (9) and it is now well established that a family history of the disease can be considered a risk factor although familial forms represent less than 10% of all cases. Familial melanomas share similar histopathology and survival rates with sporadic melanoma (1, 8) but individuals with a family history will generally have a greater number of primary lesions that will develop at an earlier age. Although three genes involved in familial melanoma have been well characterized, they are only present in 40% of all familial melanomas and mutations in these genes are not always predictive.

Germline activating mutations in cyclin-dependent kinase 4 (CDK4), located on chromosome 12q13, are inherited in an autosomal dominant fashion and confer the

highest risk (1). CDK4 is important in regulating cell cycle progression. The CDKN2A locus encodes the remaining two susceptibility genes, which encode two distinct tumor suppressor proteins: Inhibitor of cyclin-dependent kinase 4A (p16^{INK4a}) involved in suppressing cell cycle progression and alternate reading frame (p14^{ARF}) a key regulator of the p53 tumor suppressor pathway. Alternative splicing results in two different gene products, but due to their overlapping coding regions the prevalence of each is equal. CDK4 and p16^{INK4a} / p14^{ARF} mutations are mutually exclusive (2). With greater frequency, non-germline mutations in these genes are found in sporadic melanoma (2).

Rare non-familial genetic disorders lacking racial bias can be the single greatest risk factor for developing melanoma. Xeroderma pigmentosum (XP) is an autosomal recessive genetic disorder characterized by an inability to correctly repair DNA damage caused by UV. Mutations in nucleotide excision repair (NER) genes are the leading cause of XP and results in diminished or inability to repair damaged DNA. Chronic exposure to UV leads to an accumulation of DNA damage ultimately resulting in oncogenesis. In fact, people with XP have a 1,000-fold increase in melanoma incidence with a median onset at 8 years with less than 40% surviving past 20 years (10). In contrast, melanoma occurrence in albinos is extremely rare (11), likely due to a combination of diligent sun avoidance as well as a lack of UVA-melanin intracellular interactions creating free radicals leading to sustained DNA damage in melanocytes.

Melanoma Classification

There are four subtypes of cutaneous invasive melanoma (12). This includes superficial spreading, which accounts for 70% of all cases in the U.S., and is generally located on the lower extremities or back and may appear variably pigmented with a flat or slightly elevated papule with an irregular contour (13). Nodular melanomas generally present as deeply pigmented, small asymmetric nodules on the neck or trunk. Lentigo maligna melanoma (dermis) arises from pre-existing lentigo maligna lesions on the face of the elderly and are deeply pigmented and form slow growing nodules. Acral lentiginous melanoma accounts for less than 5% of all melanomas in caucasians, but is six times more prevalent in African Americans and Asians (14). It is characterized by its appearance and location as deeply pigmented lesions that appear as deep nodules on the palms, soles, fingers, toes and nails.

Melanoma is one of a handful of cancers that are staged in millimeters rather than centimeters due to its very aggressive nature (2). In 1969, the staging of cutaneous melanoma was established by Dr. Wallace Clark and was based on dimension, ulceration, lymph node involvement, and distant metastases (15). There are two important growth phases involved in melanoma progression; radial growth phase (RGP) and vertical growth phase (VGP). During RGP, pagetoid spread of melanocytes occurs and is an early indicator of a precancerous state. Most melanomas undergo RGP for months to years followed by progression into the often very rapid VGP which promotes metastasis to nearby lymph nodes and beyond (16). Clark Level staging was recently updated in 1997 and again in 2001 by the American

Joint Committee on Cancer to include tumor-node-metastasis (TNM) criteria consistent with outcome (17). Like most cancers, there are four distinct stages (I-IV) that can be further subdivided (A-C). Table 1 shows the staging categories for cutaneous melanoma.

Table 1. Current AJCC Staging System for Cutaneous Melanoma

Stage	Characteristics
IA	Tumor ≤ 1.0 mm <i>without</i> ulceration; no lymph node involvement; no distant metastases
IB	Tumor ≤ 1.0 mm <i>with</i> ulceration or Clark level IV or V; tumor 1.01-2.0 mm <i>without</i> ulceration; no lymph node involvement; no distant metastases
IIA	Tumor 1.01-2.0 mm <i>with</i> ulceration; tumor 2.01-4.0 mm <i>without</i> ulceration; no lymph node involvement; no distant metastases
IIB	Tumor 2.01-4.0 mm <i>with</i> ulceration
IIB	Tumor > 4.0 mm <i>without</i> ulceration; no lymph node involvement; no distant metastases
IIC	Tumor > 4.0 mm <i>with</i> ulceration; no nodal involvement; no distant metastases
IIIA	Tumor of any thickness <i>without</i> ulceration with 1 positive lymph
IIIB	Tumor of any thickness <i>without</i> ulceration with 2-3 positive lymph nodes
IIIC	Tumor of any thickness and 4 more metastatic lymph nodes <i>OR</i> matted nodes <i>OR</i> in-transit met(s)/satellite(s) <i>without</i> metastatic lymph nodes, or combinations of in-transit met(s)/satellite(s), <i>OR</i> ulcerated melanoma <i>and</i> metastatic lymph node(s)
IV	Tumor of any thickness with any nodes and any distant metastases

Met(s) = metastases, Ulceration = the absence of an intact epidermis overlying a portion of the primary melanoma based on pathologic microscopic observation of the histologic sections. Source: Adapted from Balch et al., 2001 (17).

Etiology

It is well established that ultraviolet A and B (UVA, UVB) exposure plays a crucial role in promoting all skin cancers including melanoma. All skin cancer

frequencies increase approaching the equator where more direct UV rays are present. Occasional extreme sun exposure resulting in blistering or peeling sunburns greatly enhances the likelihood of developing melanoma, especially prior to age 20 (18). These individuals are twice as likely to develop melanoma as people who work outdoors (18). Gradual sun exposure and tan formation protects melanocytes from the DNA damaging effects of UVA and UVB.

UVB radiation induces DNA damage to cells by causing covalent bonds to form between adjacent thymine bases. This can result in thymine dimer formation, often resulting in misrepair and mutagenesis and/or DNA strand breaks. When basal or squamous cells accrue chromosomal damage, the cells often die or form a nonmalignant neoplasm, such as BCC or SCC. In contrast, these types of mutations are rarely found in melanomas (19). Unlike most cell types in the skin, melanocytes are highly resistant to the cytotoxic effects of UVA and UVB radiation and are able to survive to produce melanin to neutralize the effects of future radiation exposure (20). The ability to endure frequent or severe UVA and UVB exposure allows some melanocytes, especially those clustered in nevi, to accrue UV-induced genetic alterations over time leading to the development of melanoma.

While many genetic alterations have been identified at all stages in melanomagenesis, mutations in several proto-oncogenes have been found with a high frequency. This includes mutually exclusive mutations in NRAS and BRAF, resulting in constitutive activation of the mitogen-activated protein kinase (MAPK) signaling pathway in over 70% of all malignant melanomas (21). Additionally, most of those harboring BRAF mutations also have PTEN loss which results in AKT

signaling deregulation. These two vital signal transduction pathways promote melanoma cell survival and proliferation and promote keratinocyte independence enabling metastasis.

Current Therapies

Complete surgical excision with large margins, often reaching 2 cm, and local nodal biopsy is the standard therapy for cutaneous melanomas. Surgery remains the best treatment for localized melanomas with a cure rate approaching 100%. Similar to most cancers, melanoma generally spreads to local lymph nodes prior to metastasizing to other organs such as the lung, liver or brain. Stage III patients with a melanoma positive lymph node generally undergo radical lymphadenectomy followed by adjuvant therapy, but still have a poor prognosis (22). Stage IV patients with established metastatic melanoma undergo surgery for the primary tumor (if known) followed by aggressive adjuvant care (22). Melanoma is also one of the most common metastatic cancers of unknown primary lesion (2). Cure rates for metastatic disease has seen little increase over the last 30 years (23).

Currently Dacarbazine (DTIC), an alkylating agent, is the only FDA approved chemotherapeutic agent for treating melanoma. Temolozomide is a related drug, but can be taken orally and is often used in place of DTIC. There are many clinical trials that use compounds in combination with DTIC or Temolozomide. Two immunotherapeutic cytokines are also approved for the treatment of Stage II – IV melanoma. While interferon gamma (IFN γ) has a poor overall long term success rate and is associated with unfavorable side effects, some patients are spontaneously cured

(24). Recently IL-2, another inflammatory cytokine, was approved for the treatment of metastatic melanoma and has shown a similar pattern of response as IFN γ . While the response rates are lower for these immunotherapeutics, most patients that do respond have a complete remission that is long-lasting (24). While melanomas are much less sensitive to the apoptosis-inducing effects of radiation, occasionally radiation treatment is the preferred treatment. Often this method is used to treat large (slower growing) facial lentigo melanomas in older patients as opposed to radical surgery. Radiation is generally the best way to target melanoma that has metastasized to the brain.

Promising Clinical Trials

It is quite clear that current therapies used to treat metastatic melanoma are inadequate as the 5-year survival rate has remained at less than 15% for decades with over 8,000 deaths annually (4). Current therapies are not target-specific, but most of the new promising therapies are. By far, the most numerous clinical trials are based on the immunogenicity of melanoma specific antigens. While IFN γ and IL-2 non-specifically activate lymphocytes, most vaccine therapies incorporate small known antigenic melanoma-specific peptides to “educate” the host lymphocytes and direct their activity towards melanomas systemically.

Unfortunately, all of these trials to date have failed to produce a significant survival benefit relative to standard therapies. Most patients respond initially and then quickly progress. Recently, Antigenics presented the results from a Phase III clinical trial of Oncophage (Vitespen) in metastatic melanoma at the annual American

Society of Clinical Oncology (ASCO) meeting. After surgery, the patient's tumors were sent to Anitgenics where isolation and purification of heat shock protein 96 (HSP96) and bound peptides occurred. This tailored vaccine was then reintroduced into the patient to invoke a melanoma-specific immune response. Initial results are promising, especially in pre-stage IV patients where a 50% increase in survival over standard therapy was observed (25).

Targeted therapies based on exploiting prevalent mutations of specific kinases are also increasing as reagents become available. Of note, small molecule inhibitors of the RAS/MAPK pathway have shown promise in early phase I and II clinical trials. While mutations in RAS are prevalent in most cancer types resulting in constitutive MAPK signaling, inhibition of this pathway has little effect on tumor growth, except in melanoma (26-28). BRAF and NRAS mutations are nearly as prominent in nevi as in melanomas and are likely involved in initiating melanomagenesis, but still required for survival. Recent *in vitro* data suggests that MAPK and AKT appear to be vital for melanoma survival (26, 27). Trials involving multiple inhibitors of the MAPK and AKT pathway are currently underway. Targeting cellular components that regulate apoptosis such as the Inhibitor of Apoptosis (IAP) and Bcl-2 family members has recently gained traction as small molecule antagonists. For example, ABT737 developed by Abbott, which targets Bcl-2/Bcl-xL, or the inhibitor YM155 developed by Astellas Pharma, which targets most IAPs including survivin, have recently been developed and are currently in early phase clinical trials. The rationale for this approach is to reduce the threshold of stress (through chemotherapy, etc.) required to induce apoptosis. Despite obvious delivery hurdles to overcome, Oblimersen (Bcl-2

antisense DNA molecule) showed much promise in a Phase III clinical trial in combination with DTIC (29).

Discussion

Developing rational therapeutic targets (genetic and immunogenic) in melanoma is now a possibility as better small molecule agents become available. Like all cancers, though, many genetic mutations are found in melanomas at various stages. It will be necessary to 'sift' through these to find those required for progression, metastasis, and maintenance. Simultaneously, alterations in melanocyte specific melanin production occur during this progression, resulting in altered appearance in color and antigenicity. It will likely be necessary to target several vital components simultaneously (genetic and/or immunogenic), but most current clinical trials involve single agent therapies rather than true combinational therapies. Supportive of this notion are the results from the Oncophage (Vitespen) clinical trial. Probably the best characterized melanoma antigen is gp100 (highly antigenic), which has been targeted extensively immunologically in clinical trials with very little long term success. Oncophage vaccine therapies use many patient melanoma-specific uncharacterized antigens to stimulate an immune response. Similar responses are observed when patient's dendritic cells are removed, exposed to melanoma antigens in the presence of cytokines, expanded and returned to the patient. However, the latter process is expensive and time consuming.

True combination therapies targeting genetic alterations and/or apoptosis regulation are also necessary. Targeting MAPK and Bcl-2 pro-survival members

simultaneously resulted in complete regression of human melanomas resistant to inhibition of either target alone (30). Unfortunately most of these new agents are evaluated as a single agent therapy. Given the high costs associated with clinical trials and FDA approval, another issue facing melanoma and other less prevalent cancers (smaller market potential) is the commitment from pharmaceutical companies. Pfizer, for example initiated a large clinical trial with the small molecule MEK inhibitor CI-1040 directed against pancreatic, breast, colon and lung cancer although *in vitro* data supported melanoma as a much better candidate. The large clinical trial failed, ended abruptly, and Pfizer only recently initiated a phase II clinical trial targeting melanoma with a second generation CI-1040 derivative, which has shown very promising results. The real challenge will be convincing pharmaceutical companies to initiate clinical trials together with their respective novel compounds with intellectual property and associated patents.

BIBLIOGRAPHY

1. Pho, L., Grossman, D., and Leachman, S. A. Melanoma genetics: a review of genetic factors and clinical phenotypes in familial melanoma. *Curr Opin Oncol*, 18: 173-179, 2006.
2. Chin, L., Garraway, L. A., and Fisher, D. E. Malignant melanoma: genetics and therapeutics in the genomic era. *Genes Dev*, 20: 2149-2182, 2006.
3. <http://seer.cancer.gov/>, N. C. I. N. S. E. a. E. R. S.
4. Jemal, A., Siegel, R., Ward, E., Murray, T., Xu, J., and Thun, M. J. Cancer statistics, 2007. *CA Cancer J Clin*, 57: 43-66, 2007.
5. Charlie Guild Melanoma Foundation, R., CA
6. The Cancer Council, P., Australia.
7. Lotze MT, D. R., Kirkwood JM, Flickinger JC. Cutaneous melanoma. In DeVita VT, Rosenberg SA, Hellman S. (eds.), *Principles and Practice of Oncology*, 6 th ed. Philadelphia: Lippincott, 2001.
8. Ford, D., Bliss, J. M., Swerdlow, A. J., Armstrong, B. K., Franceschi, S., Green, A., Holly, E. A., Mack, T., MacKie, R. M., Osterlind, A., and et al. Risk of cutaneous melanoma associated with a family history of the disease. The International Melanoma Analysis Group (IMAGE). *Int J Cancer*, 62: 377-381, 1995.
9. Smith, J. A., Poteet-Smith, C. E., Xu, Y., Errington, T. M., Hecht, S. M., and Lannigan, D. A. Identification of the first specific inhibitor of p90 ribosomal S6 kinase (RSK) reveals an unexpected role for RSK in cancer cell proliferation. *Cancer Res*, 65: 1027-1034, 2005.
10. English, J. S. and Swerdlow, A. J. The risk of malignant melanoma, internal malignancy and mortality in xeroderma pigmentosum patients. *Br J Dermatol*, 117: 457-461, 1987.
11. Ozdemir, N., Cangir, A. K., Kutlay, H., and Yavuzer, S. T. Primary malignant melanoma of the lung in oculocutaneous albino patient. *Eur J Cardiothorac Surg*, 20: 864-867, 2001.
12. Houghton, A. N., Coit, D. G., Daud, A., Dilawari, R. A., Dimaio, D., Gollob, J. A., Haas, N. B., Halpern, A., Johnson, T. M., Kashani-Sabet, M., Kraybill,

- W. G., Lange, J. R., Martini, M., Ross, M. I., Samlowski, W. E., Sener, S. F., Tanabe, K. K., Thompson, J. A., Trisal, V., Urist, M. M., and Walker, M. J. Melanoma. *J Natl Compr Canc Netw*, 4: 666-684, 2006.
13. Hogg, D., Brill, H., Liu, L., Monzon, J., Summers, A., From, L., and Lassam, N. J. Role of the cyclin-dependent kinase inhibitor CDKN2A in familial melanoma. *J Cutan Med Surg*, 2: 172-179, 1998.
 14. Kukita, A. and Ishihara, K. Clinical features and distribution of malignant melanoma and pigmented nevi on the soles of the feet in Japan. *J Invest Dermatol*, 92: 210S-213S, 1989.
 15. Clark, D. E., Errington, T. M., Smith, J. A., Frierson, H. F., Jr., Weber, M. J., and Lannigan, D. A. The serine/threonine protein kinase, p90 ribosomal S6 kinase, is an important regulator of prostate cancer cell proliferation. *Cancer Res*, 65: 3108-3116, 2005.
 16. Chudnovsky, Y., Khavari, P. A., and Adams, A. E. Melanoma genetics and the development of rational therapeutics. *J Clin Invest*, 115: 813-824, 2005.
 17. Balch, C. M., Buzaid, A. C., Soong, S. J., Atkins, M. B., Cascinelli, N., Coit, D. G., Fleming, I. D., Gershenwald, J. E., Houghton, A., Jr., Kirkwood, J. M., McMasters, K. M., Mihm, M. F., Morton, D. L., Reintgen, D. S., Ross, M. I., Sober, A., Thompson, J. A., and Thompson, J. F. Final version of the American Joint Committee on Cancer staging system for cutaneous melanoma. *J Clin Oncol*, 19: 3635-3648, 2001.
 18. Oliveria, S. A., Saraiya, M., Geller, A. C., Heneghan, M. K., and Jorgensen, C. Sun exposure and risk of melanoma. *Arch Dis Child*, 91: 131-138, 2006.
 19. Brash, D. E., Rudolph, J. A., Simon, J. A., Lin, A., McKenna, G. J., Baden, H. P., Halperin, A. J., and Ponten, J. A role for sunlight in skin cancer: UV-induced p53 mutations in squamous cell carcinoma. *Proc Natl Acad Sci U S A*, 88: 10124-10128, 1991.
 20. Wei, Q., Lee, J. E., Gershenwald, J. E., Ross, M. I., Mansfield, P. F., Strom, S. S., Wang, L. E., Guo, Z., Qiao, Y., Amos, C. I., Spitz, M. R., and Duvic, M. Repair of UV light-induced DNA damage and risk of cutaneous malignant melanoma. *J Natl Cancer Inst*, 95: 308-315, 2003.
 21. Davies, H., Bignell, G. R., Cox, C., Stephens, P., Edkins, S., Clegg, S., Teague, J., Woffendin, H., Garnett, M. J., Bottomley, W., Davis, N., Dicks, E., Ewing, R., Floyd, Y., Gray, K., Hall, S., Hawes, R., Hughes, J., Kosmidou, V., Menzies, A., Mould, C., Parker, A., Stevens, C., Watt, S., Hooper, S., Wilson, R., Jayatilake, H., Gusterson, B. A., Cooper, C., Shipley, J., Hargrave, D., Pritchard-Jones, K., Maitland, N., Chenevix-Trench, G.,

- Riggins, G. J., Bigner, D. D., Palmieri, G., Cossu, A., Flanagan, A., Nicholson, A., Ho, J. W., Leung, S. Y., Yuen, S. T., Weber, B. L., Seigler, H. F., Darrow, T. L., Paterson, H., Marais, R., Marshall, C. J., Wooster, R., Stratton, M. R., and Futreal, P. A. Mutations of the BRAF gene in human cancer. *Nature*, 417: 949-954., 2002.
22. Nahabedian, M. Y. Melanoma. *Clin Plast Surg*, 32: 249-259, 2005.
 23. The Melanoma Research Foundation, P., NJ.
 24. Bajetta, E., Del Vecchio, M., Bernard-Marty, C., Vitali, M., Buzzoni, R., Rixe, O., Nova, P., Aglione, S., Taillibert, S., and Khayat, D. Metastatic melanoma: chemotherapy. *Semin Oncol*, 29: 427-445, 2002.
 25. J. Richards, A. T., E. Whitman, G. B. Mann, J. Lutzky, L. Camacho, G. Parmiani, A. Hoos, R. Gupta, P. Srivastava Autologous tumor-derived HSPPC-96 vs. physician's choice (PC) in a randomized phase III trial in stage IV melanoma. . *Journal of Clinical Oncology*, 2006 ASCO Annual Meeting Proceedings Part I. Vol 24, No. 18S (June 20 Supplement), 2006: 8002, 2006.
 26. Eisenmann, K. M., VanBrocklin, M. W., Staffend, N. A., Kitchen, S. M., and Koo, H. M. Mitogen-activated protein kinase pathway-dependent tumor-specific survival signaling in melanoma cells through inactivation of the proapoptotic protein bad. *Cancer Res*, 63: 8330-8337., 2003.
 27. Koo, H. M., VanBrocklin, M., McWilliams, M. J., Leppla, S. H., Duesbery, N. S., and Woude, G. F. Apoptosis and melanogenesis in human melanoma cells induced by anthrax lethal factor inactivation of mitogen-activated protein kinase kinase. *Proc Natl Acad Sci U S A*, 99: 3052-3057., 2002.
 28. Whitwam, T., Vanbrocklin, M. W., Russo, M. E., Haak, P. T., Bilgili, D., Resau, J. H., Koo, H. M., and Holmen, S. L. Differential oncogenic potential of activated RAS isoforms in melanocytes. *Oncogene*, 2007.
 29. Agop Y. Bedikian, M. M., Hubert Pehamberger, Robert Conry, Martin Gore, Uwe Trefzer, Anna C. Pavlick, Ronald DeConti, Evan M. Hersh, Peter Hersey, John M. Kirkwood, Frank G. Haluska Bcl-2 Antisense (oblimersen sodium) Plus Dacarbazine in Patients With Advanced Melanoma: The Oblimersen Melanoma Study Group *Journal of Clinical Oncology*, Vol 24, No 29 (October 10), 2006: pp. 4738-4745, 2006.
 30. Verhaegen, M., Bauer, J. A., Martin de la Vega, C., Wang, G., Wolter, K. G., Brenner, J. C., Nikolovska-Coleska, Z., Bengtson, A., Nair, R., Elder, J. T., Van Brocklin, M., Carey, T. E., Bradford, C. R., Wang, S., and Soengas, M. S. A novel BH3 mimetic reveals a mitogen-activated protein kinase-

dependent mechanism of melanoma cell death controlled by p53 and reactive oxygen species. *Cancer Res*, 66: 11348-11359, 2006.

CHAPTER II

DIFFERENTIAL ONCOGENIC POTENTIAL OF ACTIVATED RAS ISOFORMS IN MELANOCYTES

This work appeared in *Oncogene* advance online publication, 5 February 2007.

Abstract

RAS genes are mutated in approximately 30% of all human cancers. Interestingly, there exists a strong bias in favor of mutation of only one of the three major *RAS* genes in tumors of different cellular origins. *NRAS* mutations occur in approximately 20% of human melanomas, while *HRAS* and *KRAS* mutations are rare in this disease. To define the mechanism(s) responsible for this preference in melanocytes, we compared the transformation efficiencies of mutant *NRAS* and *KRAS* in immortal, non-transformed *Ink4a/Arf*-deficient melanocytes. *NRAS* mutation leads to increased cellular proliferation and is potently tumorigenic. In contrast, *KRAS* mutation does not enhance melanocyte proliferation and is only weakly tumorigenic on its own. While both *NRAS* and *KRAS* activate MAPK signaling, only *NRAS* enhances MYC activity in these cells. Our data suggests that the activity of specific *RAS* isoforms is context dependent and provides a possible explanation for the prevalence of *NRAS* mutations in melanoma. In addition, understanding this mechanism will have important implications for cancer therapies targeting *RAS* pathways.

Introduction

Molecular analysis of melanoma has identified specific genomic loci implicated in the genesis and progression of melanoma. A significant percentage of both familial and sporadic melanomas have mutations that functionally inactivate the tumor suppressor genes *INK4a/ARF* (1). Activated *NRAS* oncogenes, which activate mitogen-activated protein kinase (MAPK) signaling, have been detected in approximately 20% of human melanomas (2). Moreover, expression of either an *NRAS* or *HRAS* oncogene in the melanocytes of *Ink4a/Arf*-deficient mice results in the formation of melanoma in 90% or 50% of the animals, respectively, by six months of age (3, 4). Recently, activating mutations in the *BRAF* gene, which also activates MAPK signaling, have been found in a high percentage (> 65%) of melanomas (5). With mutually exclusive mutations in *RAS* and *BRAF*, the MAPK signaling pathway is activated in over 85% of melanomas, indicating the importance of the RAS/MAPK pathway in melanomagenesis.

The RAS subfamily consists of Harvey(H)-RAS, neuroblastoma(N)-RAS, and two splice variants of Kirsten(K)-RAS (KRAS4A and KRAS4B). The RAS isoforms share a high degree of homology. The main differences between the isoforms are in the C-terminal hypervariable region, which contains the membrane targeting domain (6). HRAS and NRAS co-localize to lipid rafts, whereas KRAS is excluded from lipid rafts and localizes to the disordered plasma membrane (7). Differences in the hypervariable regions correlate with functional differences of the RAS isoforms in mammary epithelial cells (8), whereas sequences between amino acids 84 and 143 are responsible for the greater transforming capabilities of HRAS in fibroblasts.

Interestingly, NRAS shows greater activity in hemopoietic cells (9). Moreover, while *NRas* and *HRas* are dispensable for mouse development both alone and in combination (10, 11), mice that are completely devoid of *KRAS* expression are embryonic lethal (12). These data suggest that there are specific non-redundant functions of the RAS proteins in different cell types. However, the mechanism(s) underlying the biological differences between the RAS isoforms remain unclear.

In many tumors, oncogenic mutations have been identified at positions 12, 13, or 61, which cause RAS to remain constitutively active. With the exception of thyroid cancers, most tumors are associated with mutation of only one isoform of RAS and this association cannot be explained solely on differential regulation of *RAS* gene expression in different tissues (8). While approximately 20% of human melanomas have been found to harbor *NRAS* mutations, *HRAS* and *KRAS* mutations are rare (<1%) (2). Interestingly, several reports have demonstrated that transformation of certain cells by specific RAS isoforms requires cooperation by a second oncogene such as MYC (13, 14). However, the mechanism responsible for this cooperation has not been elucidated in melanocytes.

Here we report the isolation and characterization of a non-transformed, immortal *Ink4a/Arf*-deficient mouse melanocyte cell line, which was used to delineate the mechanism(s) responsible for the prevalence of NRAS mutations in melanocytes. We found that expression of mutant V12-NRAS increased the rate of proliferation of the melanocytes and was more potently transforming compared with melanocytes expressing V12-KRAS. The increased rate of proliferation was due to the ability of NRAS (but not KRAS) to prevent GSK-3-mediated phosphorylation of c-MYC.

Furthermore, coexpression of *c-MYC* with *KRAS* in the melanocytes resulted in an increased rate of proliferation and transformation comparable to the rate of proliferation and transformation of V12-NRAS alone.

Materials and Methods

Isolation of primary melanocytes and melanoma cells.

Melanocytes were isolated from 3.5 day postnatal *Ink4a/Arf*-null mice (15) by separating the dorsal lateral skin from the underlying muscular layers. The skin was washed in PBS, transferred to 0.25% trypsin, and digested overnight at 4 °C. The epidermal and dermal layers were then separated and placed in 0.02% EDTA in PBS. Single cells were obtained by mincing the tissue with a razor blade. After centrifugation for 10 min at $1000 \times g$, the cells were plated in 100-mm culture dishes at 37 °C with 5% CO₂ in Melanocyte Growth Medium (MGM; Clonetics, San Diego, CA) supplemented with 5% FBS and $1 \times$ penicillin/streptomycin (Invitrogen). The cells were incubated for 14 days and the FBS was excluded from the medium after the first two days to prevent the growth of keratinocytes and fibroblasts. The medium was changed every two days and the supernatant was stored at -20 °C as conditioned medium (CM). After 14 days, the cells were treated with 0.05% trypsin, split 1:3, and grown in 1/3 CM and 2/3 MGM for 2 weeks. The cells were maintained in MGM with 10% FBS. To obtain a pure melanocyte culture, 6.5×10^5 cells were serially diluted across and down a 96-well plate to obtain single cell clones. Single cells were identified in wells A8, B7, D6, E5, F4, H4, and H3. These clones were expanded and the cells from well D6 appeared to be pure melanocytes. To ensure

that the cells were of melanocyte origin, tyrosinase expression was detected within the cells immunohistochemically (see below). Mouse melanoma cells were established in culture from tumors that developed in *Ink4a/Arf*^{-/-};tyrosinase HRAS mice (Jackson Labs, Bar Harbor, ME) (4).

Cell culture.

Melanocyte/melanoma cultures were maintained in 254 medium containing human melanocyte growth supplement (HMGS) (Cascade Biologics, Portland, OR), 10% FBS, and 50 µg/ml gentamicin at 37 °C with 5% CO₂. Melan-A cells were maintained in MEM (Invitrogen, Carlsbad, CA) containing 5% FBS, 5 mM NaHCO₃, 25 µM β-mercaptoethanol, 200 nM 12-*O*-tetradecanoylphorbol-13-acetate (TPA; Sigma, St. Louis, MO), 1× non-essential amino acids (Invitrogen), 1× sodium pyruvate (Invitrogen), and 1× penicillin/streptomycin (Invitrogen) at 37 °C with 5% CO₂. DF-1 cells were grown in DMEM-high glucose supplemented with 10% FBS and 1× penicillin/streptomycin at 39 °C with 5% CO₂. Melanocytes were incubated with 20 mM LiCl or KCl for 30 min where indicated.

Immunohistochemistry.

To detect tyrosinase expression, melanocytes were cultured on Lab-Tek Chamber Slides (Nalge Nunc International, Rochester, NY) until confluent and then fixed with 100% methanol for 10 min at 4 °C. The cells were permeabilized with Tris-buffered saline (TBS) containing 0.1% Tween-20 (TBS-T) for 5 min at room temperature (r.t.), blocked in 10% goat serum, and then incubated in rabbit anti-PEP7 antibody (V. Hearing, NIH, Bethesda, MD), which recognizes the carboxyl terminus

of tyrosinase, diluted 1:20 in TBS-T (16). After washing three times in TBS-T, Oregon Green 488-conjugated anti-rabbit secondary antibody (Molecular Probes, Eugene, OR) in 2% goat serum diluted 1:50 in TBS-T was added to the sections for 30 min at r.t. in the dark. The slides were washed three times in TBS-T and stained sections were cover slipped with anti-fade Gel/Mount aqueous mounting medium. The signal was detected immunofluorescently using a Zeiss confocal microscope.

Microarray data generation and analysis.

Total RNA was isolated from mouse tissue and cell lines using TRIzol reagent (Invitrogen) according to the manufacturer's specifications. RNA was purified by precipitation with 7.0 M LiCl (Ambion, Austin TX), and concentrated by precipitation with 3.0 M sodium acetate (Ambion). Corning GAPS2 microarray slides (Lot 02705000B, Corning NY) spotted with 15,361 cDNA clones from the NIA Mouse 15K clone set (National Institute on Aging, Baltimore, MD) were fabricated at the Van Andel Research Institute, and microarray experiments were performed as follows. Briefly, 50 μ g of total RNA and an equal quantity of mouse embryo reference RNA were primed with oligo d(T)₂₀VN and reverse transcribed using Superscript II (Invitrogen) in the presence of Cy5-dCTP and Cy3-dCTP (Perkin Elmer, Boston MA). After direct labeling, template RNA was degraded using RNase One (Promega, Madison, WI) and purified using a PCR purification kit (Qiagen, Valencia, CA). The target was concentrated by vacuum centrifugation, combined with hybridization buffer and hybridized to a microarray slide for 19 h at 50 °C. The slides were then washed in buffers of 1 \times SSC with 0.1% SDS, 0.2 \times SSC with 0.1% SDS, 0.2 \times SSC, and 0.1 \times SSC (Ambion), immediately dried, and scanned at 532 nm

and 635 nm in an Agilent Microarray Scanner (Agilent Technologies, Palo Alto, CA). Images were analyzed using Genepix Pro 5.0 (Axon, Union City, CA). Prior to statistical analysis, spots with signal lower than three times the standard deviation of the global array background in either channel were excluded. Clustering analysis was performed using the SAS software version 9.1 in which euclidean distances and average linkage clustering were used to generate the dendrogram. Prior to clustering, missing values were imputed using the Multiple Imputation (PROC MI) method (17). The gene expression data described in this manuscript have been deposited in NCBI's Gene Expression Omnibus (GEO, <http://www.ncbi.nlm.nih.gov/geo/>) and are accessible through GEO Series accession number GSE6194 (18).

Vector constructs.

The RCASBP(M2C)797-8 retroviral vector has been described (19). The RCASBP(A)MYC virus (20), the RCASBP(A)AKT virus, which encodes the activated form of AKT designated AKT-Myr Δ 11-60 with a C-terminal HA tag, and pENTR3C-TRE-KRAS, which contains the mutant G12V activated form of human KRAS4B with an N-terminal FLAG epitope tag, have been described (21). The amphotropic RCASBP(M2C)797-8 vector was converted into a Gateway™ destination vector, RCASBP(M)-DV, using the Gateway™ Vector Conversion Reagent System (Invitrogen). RCASBP(M2C)797-8 was digested with *Cla*I, filled-in with Klenow to generate blunt ends, ligated to 50 ng of Reading Frame Cassette C.1, transformed into DB3.1 Competent Cells (Invitrogen), and plated on agar plates containing 100 μ g/ml ampicillin and 30 μ g/ml chloramphenicol. Orientation of the

Reading Frame Cassette was determined by *SalI* digest. Human *c-MYC* cDNA was PCR-amplified from the RCASBP(A)*MYC* virus, cloned into the pCR8/GW/TOPO TA cloning vector (Invitrogen), and sequence verified. pENTR3C-TRE-*KRAS* was digested with *XhoI* and *XbaI*, and the 676-bp *KRAS* fragment was gel isolated and ligated into pENTR3C digested with *SalI* and *XbaI* to generate pENTR3C-*KRAS*. RCASBP(A)*AKT* was digested with *KpnI* and *SalI* and the 1.5-kb fragment was gel isolated and ligated into pENTR3C digested with *KpnI* and *XhoI* to generate pENTR3C-*AKT*. Wild-type human *NRAS* cDNA was cloned from the M14-Mel human melanoma cell line by RT-PCR into the pCR8/GW/TOPO TA cloning vector (Invitrogen) and sequence verified. The QuickChange site-directed mutagenesis kit (Stratagene, Cedar Creek, TX) was used to generate G12V and Q61R *NRAS* mutants. RCASBP(M) expression clones were generated by mixing 150 ng of either pCR8-*MYC*, pENTR3C-*KRAS(G12V)*, pENTR3C-*AKT*, pCR8-*NRAS(G12V)*, or pCR8-*NRAS(Q61R)* with 150 ng of the RCASBP(M)-DV in the presence of the LR Clonase Enzyme Mix per the manufacturer's specifications (Invitrogen). LR reactions were performed for 2 h at room temperature and 1 μ l was transformed into 50 μ l TOP10-One Shot Competent Cells (Invitrogen). Transformations were plated on agar plates containing 100 μ g/ml ampicillin. Primer sequences are available upon request.

Virus propagation.

Virus propagation was initiated by calcium phosphate transfection of plasmid DNA that contained the retroviral vector in proviral form as previously described (21).

Viral infections.

Melanocytes were seeded in 6-well cluster dishes at a density of 5×10^4 cells/well 16 h prior to infection. Viral infections were performed as previously described (21).

Cell lysis and immunoprecipitation.

Infected melanocytes were lysed in either SDS-lysis buffer (50 mM Tris-HCl pH 6.8, 100 mM DTT, 2% SDS, 0.1% bromophenol blue, 10% glycerol) or Myc lysis buffer (0.1% Triton-X-100 in PBS) as indicated. Protein concentrations were determined using the Bio-Rad D_C Protein Assay (Bio-Rad, Hercules, CA). For immunoprecipitations, infected melanocytes were lysed in RIPA buffer (150 mM NaCl, 0.5% deoxycholate, 0.1% SDS, 1% IGEPAL, 150 mM Tris-HCl, pH 8.0) containing protease inhibitors (complete tablets, Roche, Indianapolis, IN). After centrifugation at 16,000 x g for 10 min at 4 °C, 0.5 ml was transferred to a new tube and incubated with 1 µg of anti-myc goat polyclonal IgG (789-G; Santa Cruz Biotechnology, Santa Cruz, CA). After incubation for 2 h at 4 °C, 50 µl rabbit anti-goat IgG conjugated agarose beads (Sigma) were added and incubated overnight at 4 °C with constant agitation. Immune precipitates were washed three times in 1 ml of cold RIPA buffer and resuspended in 50 µl SDS-lysis buffer. The samples were resolved on either 10%, 14%, or 4-20% Tris-glycine SDS polyacrylamide gels (Invitrogen), transferred to nitrocellulose, and incubated for 1 h at room temperature in TBS-T (0.05% Tween-20 in Tris-buffered saline) blocking solution (5% non-fat dry milk).

Western blotting.

Blots were immunostained for NRAS and KRAS using a mouse monoclonal anti-RAS antibody (RAS10; Upstate, Lake Placid, NY) at a 1:2000 dilution; for total Myc using a mouse monoclonal anti-c-Myc antibody (9E10; Covance, Berkley, CA or C-33; Santa Cruz Biotechnology) at a 1:250 dilution; for phospho T58 Myc using a rabbit polyclonal anti-phospho-T58-Myc antibody (Abcam, Cambridge, MA) at a 1:1000 dilution; for AKT using a mouse monoclonal antibody to the HA epitope (HA.11; Covance) at a 1:1000 dilution; for phospho ERK using a mouse monoclonal anti-phospho-p44/42 MAPK (Thr202/Tyr204) antibody (E10; Cell Signaling, Beverly, MA) at a 1:2000 dilution; for total ERK using a rabbit polyclonal anti-p44/42 MAPK antibody (Cell Signaling) at a 1:1000 dilution; for tubulin using a mouse monoclonal anti- α -tubulin (DM 1A; Sigma) at a 1:1000 dilution; and for glyceraldehyde-3-phosphate dehydrogenase (GAPDH) using a mouse monoclonal anti-GAPDH antibody (Chemicon, Temecula, CA) at a 1:1000 dilution. All antibodies were diluted in blocking solution. Western blots were incubated in the primary antibody overnight at 4 °C, washed in TBS-T, and then incubated with either an anti-mouse or anti-rabbit IgG-HRP secondary antibody, as appropriate, diluted 1:2000 (Amersham, Piscataway, NJ) for 1 h at room temperature. The blots were washed in TBS-T, incubated with ECL solutions per the manufacturer's specifications (Amersham), and exposed to film.

Growth in soft agar.

To assess anchorage-independent growth, 1.5×10^5 cells were suspended in 0.55% Difco agar noble (Becton Dickinson, Sparks, MD) in MGM/10% FBS and

layered over pre-solidified 0.65% Difco Noble Agar in MGM/10% FBS per well of a 6-well dish. Each cell line was assayed in triplicate.

Cell proliferation studies.

Each cell line was seeded into 24 wells of a 96-well dish at a density of 5,000 cells/well. The cells were cultured and assayed for proliferation in triplicate at the times indicated using the CellTiter 96[®] AQueous One Solution Cell Proliferation Assay (Promega) according to the manufacturer's specifications.

In vivo studies.

Four-week-old female athymic nude mice were injected subcutaneously with 1×10^7 cells/mouse in 100 μ l Hanks' balanced salt solution. Tumor size was evaluated by caliper measurements, and tumor volume was calculated by length \times width \times depth. All experiments were performed in compliance with the guiding principles of the *Guide for the Care and Use of Laboratory Animals* (available at <http://www.nap.edu/books/0309053773/html/>) and were approved by the VARI IACUC prior to experimentation.

Results

Ink4a/Arf-deficient melanocytes are immortal in culture.

To study the role of different oncogenes in melanoma formation, we generated mouse melanocyte cell lines from *Ink4a/Arf*-deficient mice (15). We established a pure melanocyte culture (lab designation D6-MEL) and confirmed the melanocyte origin of the cells by immunohistochemical staining for tyrosinase expression (16) (data not shown). It has been shown that *Arf*-deficiency confers immortality on fibroblasts (22) whereas *Ink4a*-deficiency confers immortality on melanocytes (23). Similarly, we observed that melanocytes isolated from *Ink4a/Arf*-deficient mice proliferated continuously and never experienced a detectable senescence crisis even after 30 population doublings, suggesting they are immortal in culture. To ensure that these cells were non-transformed, they were assayed for colony formation in soft agar as well as for tumor formation in nude mice. These cultures yielded no cells that were capable of anchorage-independent growth in soft agar and they were unable to produce tumors in nude mice (Table 1), consistent with immortality but not transformation.

Previous studies have demonstrated that cell lines isolated from a common tissue tend to have consistent similarities in gene expression patterns (24). Therefore, to further validate the melanocyte origin of the D6-MEL cells and to justify the use of this cell line for studying melanomagenesis, we compared the gene expression profile of the D6-MEL cell line to the gene expression profiles of several other tissues and *Ink4a/Arf*-deficient cell lines (Figure 1). In this analysis, the D6-MEL cell line

clusters near another melanocyte cell line, Melan-A (25), indicating that these cells have similar patterns of gene expression. As such, this data suggests these cells were likely derived from a common tissue type. In contrast, D6-MEL and Melan-A have distinct gene expression patterns from *Ink4a/Arf*-deficient fibroblast cell lines (3T3, VA-MEF), lymphoblast cells (VA-475), and a variety of other tissue types. Included in this plot is data generated from two derivatives of the D6-MEL cell line (NRAS-MEL and KRAS-MEL) as well as a mouse melanoma cell line established from *Ink4a Arf*^{-/-};tyrosinase V12-HRAS mice (HRAS-MEL). The melanocytes expressing

Table 1. Tumorigenicity of <i>Ink4a/Arf</i> ^{-/-} melanocytes expressing different combinations of oncogenes.		
Cells/gene(s) ¹	Soft-agar growth ²	Tumors in nude mice ³
D6-MEL	No	0/8
V12-NRAS	Yes	8/8
V12-KRAS	Yes	4/8
AKT	No	0/8
MYC	No	0/8
MYC + AKT	Yes	0/8
V12-KRAS + AKT	Yes	8/8
V12-KRAS + MYC	Yes	8/8
V12-KRAS + MYC + AKT	Yes	8/8
Tyrosinase-V12-HRAS	Yes	8/8
M14-MEL ⁴	Yes	8/8

¹D6-MEL cells were infected with viruses containing the genes indicated.

²Cells (1.5 x 10⁵ cells/well) were resuspended in 0.55% Noble agar in growth medium and layered over presolidified 0.65% agar in a 6-well plate. After eight weeks, colony formation was assessed.

³Athymic nude mice (n = 8) were injected subcutaneously with 1 x 10⁷ cells/mouse of each cell line and monitored for tumor formation for 12 weeks.

⁴M14-MEL human melanoma cells were used as a positive control.

KRAS show the highest degree of similarity to the D6-MEL and Melan-A cell lines. Taken together, analysis of the gene expression patterns supports the melanocyte origin of the D6-MEL cell line.

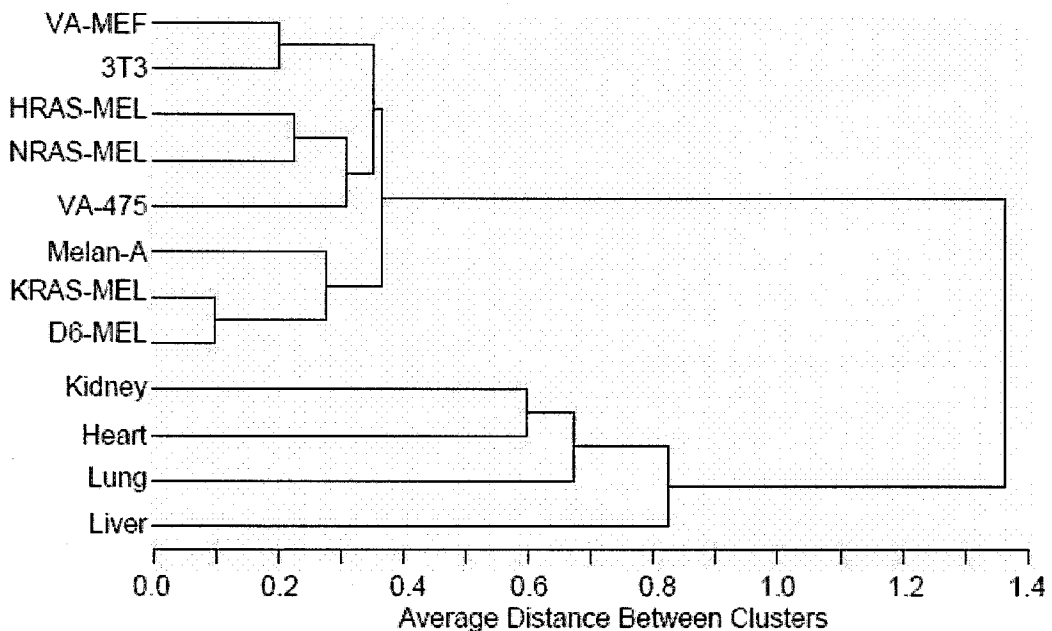


Figure 1. Gene expression-based evaluation of the melanocytic origin of the D6-MEL cell line. RNA was isolated from the indicated cell lines and tissues and applied to in-house generated cDNA microarrays. Dendrograms reflective of the overall similarities and differences of the cell line and tissue gene expression patterns were generated from about 6000 of the best measured and variable features using average-linkage hierarchical clustering (see Materials and Methods). In the dendrogram shown, a shorter arm indicates higher similarity while a longer arm indicates lower similarity. All of the cell lines analyzed are *Ink4a/Arf*-deficient. The samples used are as follows: VA-MEF, mouse embryonic fibroblasts; 3T3, NIH 3T3 fibroblasts; HRAS-MEL, melanoma cells isolated from an *Ink4a/Arf*^{-/-};tyrosinase-HRAS mouse; NRAS-MEL, D6-MEL melanocytes expressing V12-NRAS; VA-475, lymphoma cells isolated from *Ink4a/Arf*-deficient mice; Melan-A, a reported nontransformed melanocyte cell line; KRAS-MEL, D6-MEL melanocytes expressing V12-KRAS; D6-MEL, melanocytes isolated from an *Ink4a/Arf*-deficient mouse and established as a single cell clone; kidney, heart, lung, and liver represent samples isolated from normal mouse tissue.

RAS/MAPK activation induces anchorage-independent growth of melanocytes *in vitro*.

The RAS/MAPK signaling pathway is activated in the vast majority of characterized malignant melanomas. Interestingly, NRAS mutations are common while KRAS and HRAS mutations are rarely detected in melanoma (2). To determine the efficiency of melanocyte transformation by different isoforms of RAS, melanocytes were infected with retroviral vectors expressing either V12-NRAS or V12-KRAS. Although Q61R-NRAS is more common in melanoma and similar results were obtained with this mutant (data not shown), the V12 mutant was used in these studies such that a direct comparison could be made between the transforming capabilities of different RAS isoforms harboring the same mutation. Introduction of either V12-NRAS or V12-KRAS resulted in a significant increase in the total amount of RAS protein compared with uninfected melanocytes, as assessed using a pan-RAS antibody by Western blot (Figure 2a).

The ability of the mutant RAS isoforms to induce anchorage-independent growth of melanocytes was initially assayed *in vitro* by colony formation in soft agar. Whereas the parental, uninfected melanocytes were unable to grow in soft agar, melanocytes expressing activated V12-NRAS formed numerous colonies in soft agar, demonstrating that NRAS activation in melanocytes results in anchorage-independent growth, a characteristic of transformed cells. Although melanocytes expressing V12-KRAS formed colonies in soft agar, they were smaller and significantly fewer in number than melanocytes expressing V12-NRAS (Table 1).

NRAS activation in melanocytes is potently tumorigenic *in vivo*.

While anchorage-independent growth suggests that activated NRAS and KRAS are transforming in melanocytes, a more stringent assay of tumorigenic potential is the ability to form tumors *in vivo*. To determine the relative efficiency of tumor formation *in vivo* by different RAS isoforms, melanocytes expressing either V12-N, H, or KRAS were injected subcutaneously into nude mice. Whereas the mice injected with the parental, uninfected melanocytes did not produce tumors, all of the mice injected with melanocytes expressing V12-NRAS developed tumors (Table 1, Figure 3). These tumors reached 200 mm³ within five weeks. All of the mice injected with melanocytes expressing activated HRAS also developed tumors, but the growth of these tumors was slightly delayed compared with the NRAS tumors, taking an additional two weeks to reach 200 mm³. In contrast, only four of eight mice injected with melanocytes expressing activated KRAS developed tumors (Table 1, Figure 3), and these tumors progressed significantly more slowly than tumors expressing either activated NRAS or HRAS. The KRAS-expressing tumors reached a volume of 200 mm³ five weeks later than tumors expressing activated NRAS (Figure 3). The slightly slower tumor growth observed with melanocytes expressing V12-HRAS compared with melanocytes expressing V12-NRAS is most likely due to differences in RAS expression levels between the virally infected NRAS cells and the cells from the *Ink4a/Arf*-null-Tyrosinase-*HRAS* mice where expression of *HRAS* is driven from the tyrosinase promoter (4). NRAS and KRAS expression was similar in the D6-MEL cells (Figure 2a).

NRAS and KRAS both activate the classical MAPK pathway in melanocytes.

In further support of the *in vitro* and *in vivo* growth differences between the N-, H- and KRAS-expressing melanocytes, these cell lines also have differences in their corresponding gene expression patterns (Figure 1). Based on gene expression data, the melanocytes expressing activated KRAS show a high degree of similarity to the D6-MEL and Melan-A cell lines. In contrast, the H- and NRAS-transformed melanocytes show lesser similarity to the D6-MEL and Melan-A melanocytes and have the greatest degree of similarity to the highly transformed and highly proliferative VA-475 lymphoma cells. These data suggest that the altered patterns of gene expression in the N- and KRAS-expressing cell lines may be the result of differential activation of RAS signaling pathways and/or differences in overall cell proliferation.

To determine if the difference in *in vivo* tumorigenicity between KRAS and NRAS is due to differential activation of the classical MAPK signaling pathway (i.e., RAF/MEK/ERK; Figure 2b), cell lysates were collected from D6-MEL cells expressing either V12-NRAS or V12-KRAS. Expression of either activated NRAS or KRAS strongly activated ERK in these cells (Figure 2a). Since ERK phosphorylation mediated by both RAS isoforms is robust, the greater *in vivo* tumorigenic potential of NRAS appears not to be due to differential ERK activation.

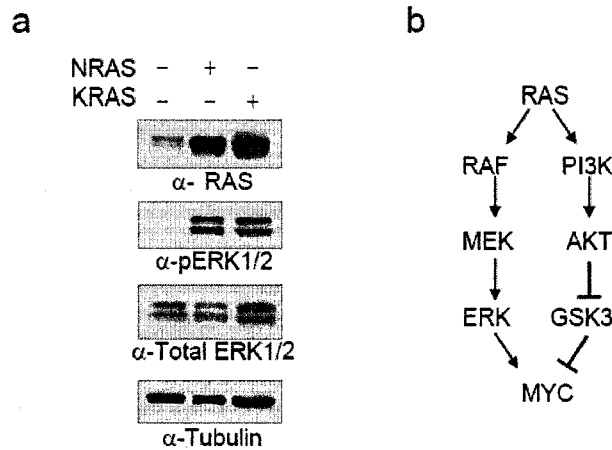


Figure 2. Proposed RAS signaling pathways. (a) Expression of RAS and ERK activation in D6-MEL cells. Cell lysates from uninfected D6-MEL melanocytes (-) or cells infected with retroviruses containing either V12-NRAS or V12-KRAS (+) were collected in SDS lysis buffer, separated on a 4-20% gradient gel and immunoblotted for total RAS expression (α -RAS), activated phosphorylated ERK p44/42 (α -pERK1/2), total ERK p44/42 expression (α -Total ERK1/2), and α -tubulin. (b) Schematic representation of RAS signaling pathways and their effect on Myc activity.

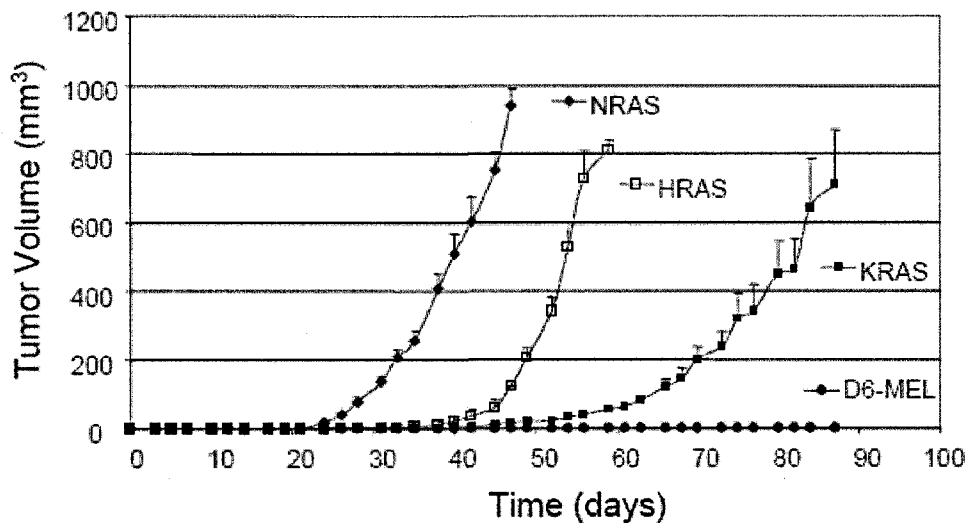


Figure 3. *In vivo* tumor formation. Nude mice were injected subcutaneously with 10^7 uninfected melanocytes (D6-MEL) or melanocytes expressing the indicated genes. Tumor volume was determined by caliper measurement on the days indicated (data are represented as mean \pm SEM; n = 8).

NRAS, but not KRAS, increases the rate of proliferation of melanocytes and prevents GSK3-mediated phosphorylation of Myc.

In culturing the melanocytes expressing V12-NRAS or KRAS, we observed that cells expressing V12-NRAS grew at a faster rate than either uninfected melanocytes or melanocytes expressing V12-KRAS. This observation was confirmed by measurement of the *in vitro* proliferation rates of the cells. Expression of V12-NRAS significantly increased the proliferation rate of the melanocytes (Figure 4). In contrast, the V12-KRAS melanocytes proliferated at the same rate as the uninfected melanocytes until day 8, at which point their growth was significantly reduced compared with that of all the other cell lines (Figure 4). To determine the mechanism responsible for the disparity in growth and tumorigenicity, differences in downstream RAS effectors known to play a role in proliferation were evaluated.

The c-Myc protein plays a role in multiple cellular processes, including proliferation, and is a downstream target of RAS signaling (26). We assessed endogenous *c-Myc* expression in cell lysates from uninfected melanocytes, and melanocytes expressing either V12-NRAS or V12-KRAS. When these samples were separated on a gradient polyacrylamide gel, a differential c-Myc banding pattern was observed. We suspected that the higher-molecular-weight bands were post-translationally modified forms of Myc, since Myc has been reported to be phosphorylated by ERK at serine 62 (S62) and by glycogen synthase kinase-3 (GSK3) at threonine 58 (T58) (27). These two phosphorylation sites exert opposing control on c-Myc stability; whereas S62 phosphorylation stabilizes c-Myc, T58 phosphorylation promotes S62 dephosphorylation and ubiquitin-mediated proteasome

degradation. Myc is normally turned over rapidly in cells, but RAS signaling stabilizes Myc by inducing phosphorylation of S62 through the MAPK/ERK pathway (26) and by inhibiting phosphorylation of Myc at T58 by GSK3 via phosphatidylinositol 3-kinase (PI3K) signaling (28) (Figure 2b).

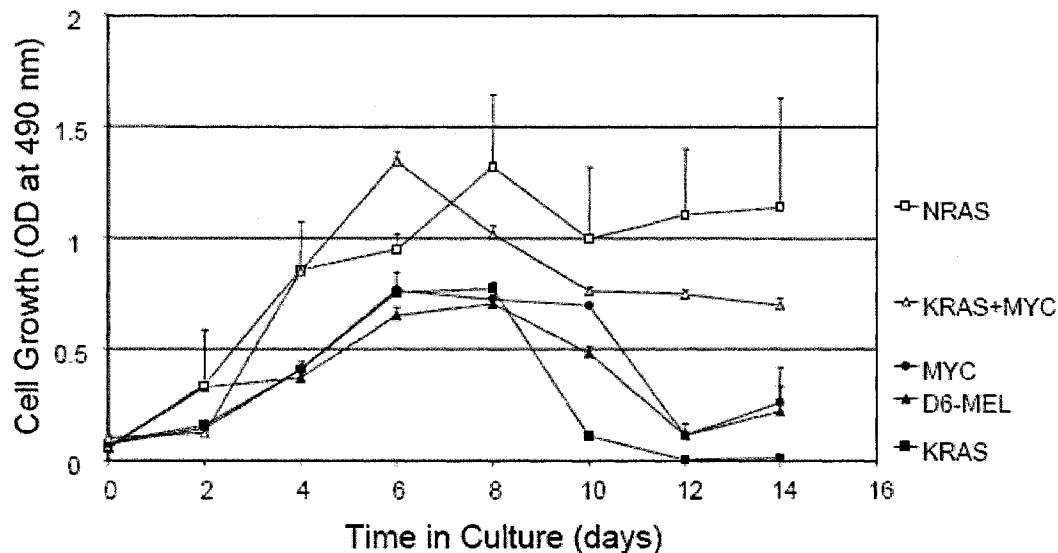


Figure 4. *In vitro* proliferation of melanocytes expressing different genes. Uninfected melanocytes (D6-MEL) or melanocytes infected with retroviruses containing V12-NRAS, V12-KRAS, MYC, or V12-KRAS coexpressed with MYC were seeded in microtiter wells and assayed at the indicated time points. Viable cells were quantitated using the CellTiter 96[®] AQueous One Solution Cell Proliferation Assay by optical density readings at 490 nm (data are represented as mean \pm SEM; $n = 3$).

Consistent with observations in other cell types, the S62 singly phosphorylated protein was more pronounced in the NRAS- and KRAS-expressing melanocytes than in uninfected melanocytes (Figure 5a, 56-kDa band). However, whereas the uninfected melanocytes and the KRAS-expressing melanocytes both showed T58/S62 dual phosphorylation (Figure 5a, 51-kDa band), NRAS-expressing

cells did not, suggesting that NRAS more effectively prevents GSK3-mediated phosphorylation of Myc at T58 than does KRAS in these cells.

To further verify the differential phosphorylation of Myc and to analyze the contribution of the PI3K/AKT/GSK3 pathway to Myc regulation, uninfected melanocytes and melanocytes expressing either V12-NRAS or V12-KRAS were incubated in the presence or absence of lithium to inhibit GSK3-mediated phosphorylation of Myc at T58 (29, 30). Following treatment, endogenous Myc protein was immunoprecipitated and phosphorylation was detected using a T58 phospho-specific Myc antibody. Prominent T58 Myc bands were detected in lysates from uninfected melanocytes and melanocytes expressing V12-KRAS, but not from those expressing V12-NRAS (Figure 5b, top panel). Upon inhibition of GSK3 activity by lithium treatment, T58 phosphorylation of Myc was no longer detectable (Figure 5B, top panel). Effective inhibition of GSK3 by lithium was verified by analysis of the same cell lysates prior to immunoprecipitation of Myc using a phospho-specific GSK3 antibody (Figure 5b). Inhibition of GSK3 correlates with an increase in the level of phosphorylated GSK3. These results suggest that phosphorylation of Myc at T58 is mediated by GSK3 in melanocytes, and further demonstrate that V12-NRAS effectively prevents GSK3-mediated phosphorylation of Myc whereas V12-KRAS does not.

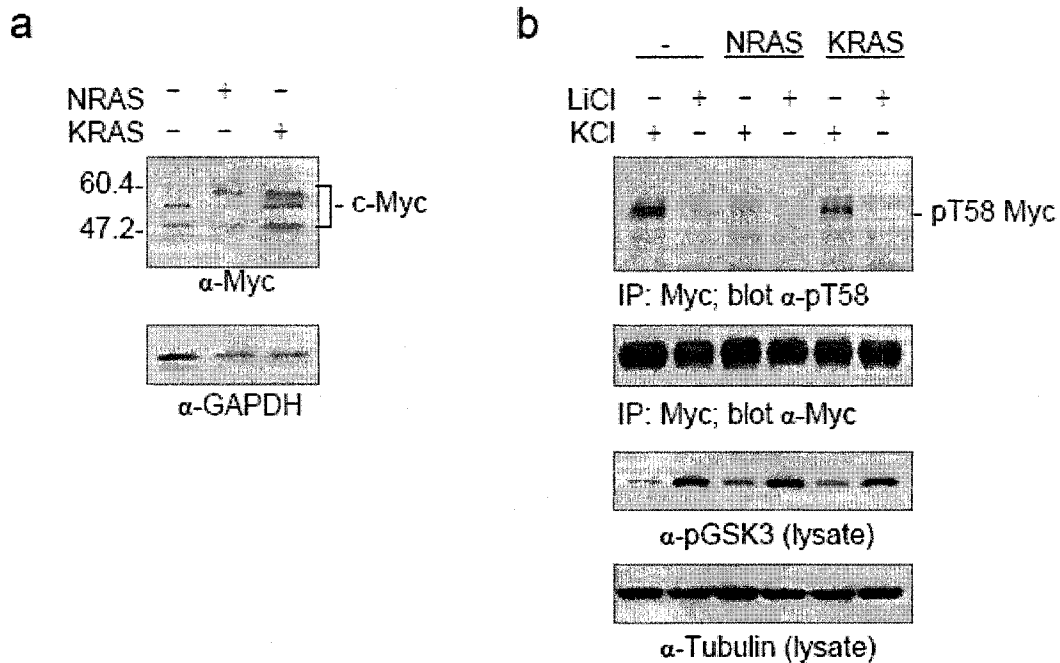


Figure 5. RAS-mediated regulation of c-Myc phosphorylation. (a) Cell lysates from uninfected melanocytes (-) or melanocytes infected with retroviruses containing V12-NRAS or V12-KRAS (+) were collected in Myc lysis buffer, separated on a 4-20% polyacrylamide tris-glycine gradient gel, and immunoblotted for endogenous Myc expression using an anti-Myc monoclonal antibody (9E10; α -MYC). The S62-Myc band (56 kDa) is predicted to be larger than the doubly phosphorylated S62/T58-Myc band (51 kDa) due to glycosylation of T58 in the absence of phosphorylation (30). The blot was re-probed for GAPDH to ensure equal loading (α -GAPDH). (b) Uninfected melanocytes (-) or melanocytes infected with retroviruses containing V12-NRAS (NRAS) or V12-KRAS (KRAS) were treated with either 20 mM LiCl or KCl (as a control) for 30 min. After treatment, cell lysates were collected in RIPA buffer and phosphorylated GSK3 (α -pGSK3) and tubulin (α -Tubulin) were detected from whole cell lysates, while T58 Myc phosphorylation (α -pT58) and total Myc (9E10; α -MYC) were detected from c-Myc immunoprecipitates with the antibodies indicated.

Coexpression of KRAS and either MYC or AKT increases the tumorigenicity of melanocytes.

To determine if coexpression of *KRAS* with either *AKT*, *MYC*, or both *AKT* and *MYC* would result in tumorigenicity comparable to that induced by expression of *NRAS* alone, melanocytes expressing *MYC* or *AKT* were infected with retroviruses containing V12-KRAS to generate melanocytes expressing *KRAS* and *MYC*, *KRAS*

and *AKT*, or *KRAS*, *AKT*, and *MYC*. Melanocytes expressing *AKT* alone, *MYC* alone, and the combination of *AKT* and *MYC* in the absence of *KRAS* were generated as controls. Expression of individual genes was confirmed by Western blot (Figure 6).

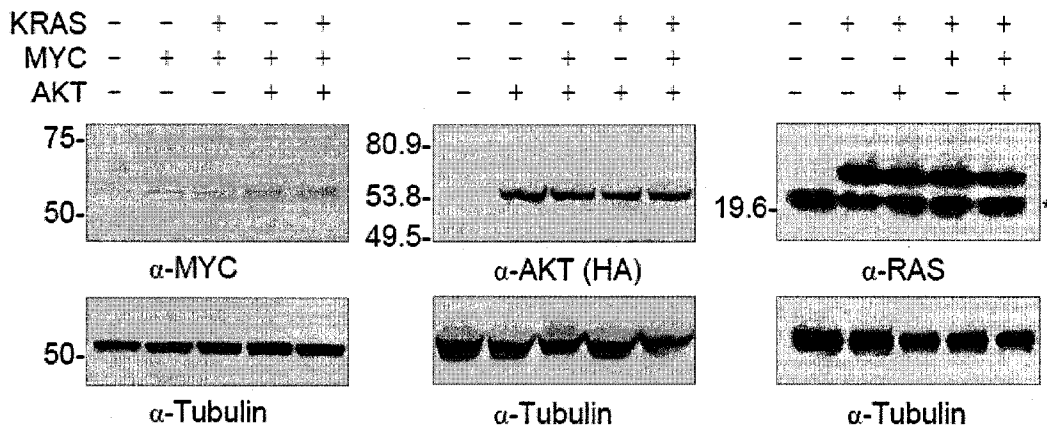


Figure 6. Expression of *KRAS*, *AKT* and *MYC* in melanocytes. *KRAS*, *AKT*, and/or *c-MYC* were stably introduced into D6 melanocytes by retroviral infection in the combinations indicated (+). Expression of each gene was assayed by immunoblotting cell lysates collected in SDS lysis buffer and separated on 10% (MYC and AKT) or 14% (RAS) polyacrylamide gels with antibodies to *c-MYC* (C-33; α -MYC), the HA epitope tag on AKT (HA.11; α -AKT-HA), RAS (RAS10; α -RAS), and tubulin (DM 1A; α -tubulin). * Indicates a nonspecific band.

Expression of either *MYC* or *AKT* alone is not sufficient to transform the melanocytes even in the context of *Ink4a/Arf* deficiency. Neither soft agar colonies nor *in vivo* tumors formed from melanocytes expressing only *MYC* or *AKT* (Table 1, Figure 7). However, coexpression of *KRAS* with either *AKT* or, more dramatically, *MYC* resulted in potent transformation. Whereas melanocytes expressing V12-*KRAS* alone only formed tumors in half of the injected mice with a long latency, tumors were detected in all of the mice injected with melanocytes coexpressing *KRAS* and *AKT* (Table 1). The kinetics of tumor growth outpaced that of *KRAS*-only tumors, but still lagged behind *NRAS* tumors (Figure 7). Coexpression of *KRAS* and *MYC* was even

more potently tumorigenic than *KRAS* with *AKT*. Tumors developed in all mice injected with *KRAS*- and *MYC*-expressing melanocytes (Table 1); the tumor growth kinetics were indistinguishable from the rate of *NRAS*-induced tumors. Additional expression of *AKT* did not significantly enhance the tumorigenicity of *KRAS*- and *MYC*-expressing melanocytes (Figure 7). These results further support the idea that either *MYC* or *AKT* is capable of cooperating with *KRAS* in this system. Furthermore, in the absence of V12-*KRAS* expression, coexpression of *MYC* and *AKT* resulted in the formation of soft agar colonies but not *in vivo* tumors (Table 1, Figure 7). These results further illustrate the importance of a *RAS* signal in this context.

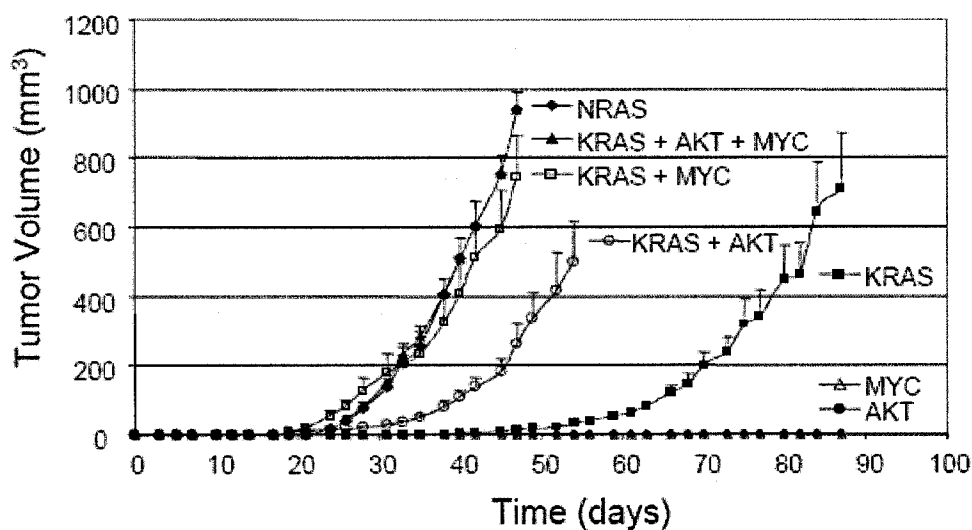


Figure 7. *In vivo* tumor formation. Nude mice were injected subcutaneously with 10^7 uninfected melanocytes (D6-MEL) or melanocytes expressing the indicated genes. Tumor volume (represented as mean \pm SEM; $n = 8$) was determined by caliper measurement on the days indicated.

The proliferation rate of KRAS-expressing melanocytes is increased by MYC expression.

To further explore the mechanisms that underlie the differences in tumorigenic potential of the RAS isoforms, and to further characterize how *MYC* coexpression increases the tumorigenicity of V12-KRAS melanocytes, the proliferation rates of melanocytes expressing V12-NRAS, V12-KRAS, and MYC, as well as the combination of V12-KRAS and MYC, were measured. While V12-KRAS or MYC expression alone did not affect the cellular proliferation rate, coexpression of MYC with V12-KRAS increased the proliferation rate of the melanocytes to a rate similar to that observed by V12-NRAS alone (Figure 4). This indicates that MYC expression cooperates with V12-KRAS by increasing the rate of cellular proliferation.

Discussion

Using a genetically defined system, we demonstrate that the combination of V12-NRAS expression and *Ink4a/Arf* loss is potently tumorigenic in melanocytes, whereas transformation by V12-KRAS requires the expression of a cooperating oncogene. V12-NRAS expression alone significantly increases the proliferation of *Ink4a/Arf*-deficient melanocytes. In contrast, V12-KRAS expression does not enhance cell proliferation, but rather induces growth arrest at higher cell densities. While tumors did develop in half of the mice injected with V12-KRAS-expressing *Ink4a/Arf*-deficient melanocytes, the long latency and incomplete penetrance of tumor formation in these mice suggests that additional genetic changes were acquired over time.

It has been established that RAS and MYC can cooperate in the transformation of rodent fibroblast and mammary epithelial cells (13, 14). However, the mechanism responsible for this cooperation has not been elucidated in melanocytes. Analysis of downstream RAS effector pathways revealed that while both V12-NRAS and V12-KRAS efficiently activate the classical MAPK pathway in melanocytes, only V12-NRAS effectively prevents GSK3-mediated phosphorylation of Myc via PI3K/AKT, which results in enhanced activity of endogenous Myc protein in these cells. These results are in agreement with observations in fibroblasts where HRAS more effectively activates PI3K than does KRAS (31). Since both HRAS and NRAS co-localize to lipid rafts, whereas KRAS is excluded from lipid rafts and localizes to the disordered plasma membrane (7), the more potent activation of PI3K/AKT by NRAS and HRAS may be due to differential membrane localization and therefore access to a defined subset of downstream effector proteins. Alternatively, recruitment of PI3K to distinct domains (e.g., lipid rafts) within the plasma membrane may result in activation that is more efficient than that of KRAS.

The importance of the PI3K/AKT/MYC pathway in melanoma genesis was further illustrated by the combination of V12-KRAS with either AKT or MYC, which results in transformation efficiencies similar to that of V12-NRAS alone. Inactivating PTEN mutations, which result in enhanced AKT activity, appear to be mutually exclusive with NRAS mutations in human melanoma tissues and cell lines, suggesting overlapping redundant functions. Furthermore, half of melanomas with BRAF mutations, which activate downstream MAPK signaling but not PI3K/AKT

signaling, also harbor PTEN mutations (32). Concurrent BRAF/PTEN mutations appear to function like an NRAS mutation in melanomagenesis.

While we have observed that *NRAS* is the most potent *RAS* protooncogene in melanocytes, *HRAS* and *KRAS* mutations are clearly selected for in tumors of different cellular origins. The differences that we and others have observed in the ability of the RAS proteins to activate different effector molecules may explain the selection pressure for specific *RAS* mutations in certain human tumors. The presence of additional mutations in other genes most likely contributes to this selection pressure, and the multistep process of oncogenesis varies significantly between cell types. For example, in colorectal cancer loss of the adenomatous polyposis coli (*APC*) gene is an early event that results in increased levels of β -catenin and subsequent increases in *MYC* gene expression (33). Since loss of *APC* typically precedes activation of *KRAS* in colorectal cancer progression, this may explain the selection pressure for *KRAS* mutation in those cells.

Our results demonstrate the importance of NRAS-mediated activation of both MAPK and PI3K/AKT/MYC signaling in melanoma genesis and identify distinct differences between the signaling capabilities of NRAS and KRAS in melanocytes. These differences offer a rationale explanation for the greater occurrence of *NRAS* mutations relative to *KRAS* mutations in melanoma. In addition, the relative resistance to MEK inhibition of melanomas harboring *NRAS* mutations (34) suggests that these tumors may be ideal candidates for combination therapies that also target the PI3K/AKT/MYC pathway.

Acknowledgements

We thank Dr. Vincent Hearing for providing the anti-PEP7 antibody, Dr. Stephen Hughes for the RCASBP(M2C)797-8 virus, and Dr. Brian Lewis for the RCASBP(A)MYC virus. We thank Bryn Eagleson, Elissa Boguslawski, Dawna Dylewski, and the vivarium staff for assistance with the animal experiments. We thank Dr. Kyle Furge and Karl Dykema (Laboratory of Computational Biology) for technical assistance and helpful comments. We also thank David Nadziejka for critical review of the manuscript. This work was supported by funds from the Melanoma Research Foundation, the James A. Schlipmann Melanoma Cancer Foundation, and the Van Andel Research Institute. Lastly, the authors wish to dedicate this work to the memory of Dr. Han-Mo Koo, who made significant contributions to the scientific community and especially to cancer research.

BIBLIOGRAPHY

1. Castellano, M. and Parmiani, G. Genes involved in melanoma: an overview of INK4a and other loci. *Melanoma Res*, *9*: 421-432, 1999.
2. Chin, L., Garraway, L. A., and Fisher, D. E. Malignant melanoma: genetics and therapeutics in the genomic era. *Genes Dev*, *20*: 2149-2182, 2006.
3. Ackermann, J., Frutschi, M., Kaloulis, K., McKee, T., Trumpp, A., and Beermann, F. Metastasizing melanoma formation caused by expression of activated N-RasQ61K on an INK4a-deficient background. *Cancer Res*, *65*: 4005-4011, 2005.
4. Chin, L., Pomerantz, J., Polsky, D., Jacobson, M., Cohen, C., Cordon-Cardo, C., Horner, J. W., 2nd, and DePinho, R. A. Cooperative effects of INK4a and ras in melanoma susceptibility in vivo. *Genes Dev*, *11*: 2822-2834, 1997.
5. Davies, H., Bignell, G. R., Cox, C., Stephens, P., Edkins, S., Clegg, S., Teague, J., Woffendin, H., Garnett, M. J., Bottomley, W., Davis, N., Dicks, E., Ewing, R., Floyd, Y., Gray, K., Hall, S., Hawes, R., Hughes, J., Kosmidou, V., Menzies, A., Mould, C., Parker, A., Stevens, C., Watt, S., Hooper, S., Wilson, R., Jayatilake, H., Gusterson, B. A., Cooper, C., Shipley, J., Hargrave, D., Pritchard-Jones, K., Maitland, N., Chenevix-Trench, G., Riggins, G. J., Bigner, D. D., Palmieri, G., Cossu, A., Flanagan, A., Nicholson, A., Ho, J. W., Leung, S. Y., Yuen, S. T., Weber, B. L., Seigler, H. F., Darrow, T. L., Paterson, H., Marais, R., Marshall, C. J., Wooster, R., Stratton, M. R., and Futreal, P. A. Mutations of the BRAF gene in human cancer. *Nature*, *417*: 949-954., 2002.
6. Giehl, K. Oncogenic Ras in tumour progression and metastasis. *Biol Chem*, *386*: 193-205, 2005.
7. Prior, I. A. and Hancock, J. F. Compartmentalization of Ras proteins. *J Cell Sci*, *114*: 1603-1608, 2001.
8. Kim, K., Lindstrom, M. J., and Gould, M. N. Regions of H- and K-ras that provide organ specificity/potency in mammary cancer induction. *Cancer Res*, *62*: 1241-1245, 2002.
9. Maher, J., Baker, D. A., Manning, M., Dibb, N. J., and Roberts, I. A. Evidence for cell-specific differences in transformation by N-, H- and K-ras. *Oncogene*, *11*: 1639-1647, 1995.

10. Umanoff, H., Edelman, W., Pellicer, A., and Kucherlapati, R. The murine N-ras gene is not essential for growth and development. *Proc Natl Acad Sci U S A*, *92*: 1709-1713, 1995.
11. Esteban, L. M., Vicario-Abejon, C., Fernandez-Salguero, P., Fernandez-Medarde, A., Swaminathan, N., Yienger, K., Lopez, E., Malumbres, M., McKay, R., Ward, J. M., Pellicer, A., and Santos, E. Targeted genomic disruption of H-ras and N-ras, individually or in combination, reveals the dispensability of both loci for mouse growth and development. *Mol Cell Biol*, *21*: 1444-1452, 2001.
12. Koera, K., Nakamura, K., Nakao, K., Miyoshi, J., Toyoshima, K., Hatta, T., Otani, H., Aiba, A., and Katsuki, M. K-ras is essential for the development of the mouse embryo. *Oncogene*, *15*: 1151-1159, 1997.
13. Land, H., Parada, L. F., and Weinberg, R. A. Tumorigenic conversion of primary embryo fibroblasts requires at least two cooperating oncogenes. *Nature*, *304*: 596-602, 1983.
14. Sinn, E., Muller, W., Pattengale, P., Tepler, I., Wallace, R., and Leder, P. Coexpression of MMTV/v-Ha-ras and MMTV/c-myc genes in transgenic mice: synergistic action of oncogenes in vivo. *Cell*, *49*: 465-475, 1987.
15. Serrano, M., Lee, H., Chin, L., Cordon-Cardo, C., Beach, D., and DePinho, R. A. Role of the INK4a locus in tumor suppression and cell mortality. *Cell*, *85*: 27-37, 1996.
16. Aroca, P., Urabe, K., Kobayashi, T., Tsukamoto, K., and Hearing, V. J. Melanin biosynthesis patterns following hormonal stimulation. *J Biol Chem*, *268*: 25650-25655, 1993.
17. Lavori, P. W., Dawson, R., and Shera, D. A multiple imputation strategy for clinical trials with truncation of patient data. *Stat Med*, *14*: 1913-1925, 1995.
18. Edgar, R., Domrachev, M., and Lash, A. E. Gene Expression Omnibus: NCBI gene expression and hybridization array data repository. *Nucleic Acids Res*, *30*: 207-210, 2002.
19. Barsov, E. V., Payne, W. S., and Hughes, S. H. Adaptation of chimeric retroviruses in vitro and in vivo: isolation of avian retroviral vectors with extended host range. *J Virol*, *75*: 4973-4983, 2001.
20. Lewis, B. C., Klimstra, D. S., and Varmus, H. E. The c-myc and PyMT oncogenes induce different tumor types in a somatic mouse model for pancreatic cancer. *Genes Dev*, *17*: 3127-3138, 2003.

21. Holmen, S. L. and Williams, B. O. Essential role for Ras signaling in glioblastoma maintenance. *Cancer Res*, 65: 8250-8255, 2005.
22. Kamijo, T., Zindy, F., Roussel, M. F., Quelle, D. E., Downing, J. R., Ashmun, R. A., Grosveld, G., and Sherr, C. J. Tumor suppression at the mouse INK4a locus mediated by the alternative reading frame product p19ARF. *Cell*, 91: 649-659, 1997.
23. Sviderskaya, E. V., Hill, S. P., Evans-Whipp, T. J., Chin, L., Orlow, S. J., Easty, D. J., Cheong, S. C., Beach, D., DePinho, R. A., and Bennett, D. C. p16(Ink4a) in melanocyte senescence and differentiation. *J Natl Cancer Inst*, 94: 446-454, 2002.
24. Scherf, U., Ross, D. T., Waltham, M., Smith, L. H., Lee, J. K., Tanabe, L., Kohn, K. W., Reinhold, W. C., Myers, T. G., Andrews, D. T., Scudiero, D. A., Eisen, M. B., Sausville, E. A., Pommier, Y., Botstein, D., Brown, P. O., and Weinstein, J. N. A gene expression database for the molecular pharmacology of cancer. *Nat Genet*, 24: 236-244, 2000.
25. Bennett, D. C., Cooper, P. J., and Hart, I. R. A line of non-tumorigenic mouse melanocytes, syngeneic with the B16 melanoma and requiring a tumour promoter for growth. *Int J Cancer*, 39: 414-418, 1987.
26. Sears, R. C. The life cycle of C-myc: from synthesis to degradation. *Cell Cycle*, 3: 1133-1137, 2004.
27. Henriksson, M., Bakardjiev, A., Klein, G., and Luscher, B. Phosphorylation sites mapping in the N-terminal domain of c-myc modulate its transforming potential. *Oncogene*, 8: 3199-3209, 1993.
28. Gregory, M. A., Qi, Y., and Hann, S. R. Phosphorylation by glycogen synthase kinase-3 controls c-myc proteolysis and subnuclear localization. *J Biol Chem*, 278: 51606-51612, 2003.
29. Klein, P. S. and Melton, D. A. A molecular mechanism for the effect of lithium on development. *Proc Natl Acad Sci U S A*, 93: 8455-8459, 1996.
30. Kamemura, K., Hayes, B. K., Comer, F. I., and Hart, G. W. Dynamic interplay between O-glycosylation and O-phosphorylation of nucleocytoplasmic proteins: alternative glycosylation/phosphorylation of THR-58, a known mutational hot spot of c-Myc in lymphomas, is regulated by mitogens. *J Biol Chem*, 277: 19229-19235, 2002.
31. Yan, J., Roy, S., Apolloni, A., Lane, A., and Hancock, J. F. Ras isoforms vary in their ability to activate Raf-1 and phosphoinositide 3-kinase. *J Biol Chem*, 273: 24052-24056, 1998.

32. Goel, V. K., Lazar, A. J., Warneke, C. L., Redston, M. S., and Haluska, F. G. Examination of mutations in BRAF, NRAS, and PTEN in primary cutaneous melanoma. *J Invest Dermatol*, 126: 154-160, 2006.
33. Vogelstein, B., Fearon, E. R., Hamilton, S. R., Kern, S. E., Preisinger, A. C., Leppert, M., Nakamura, Y., White, R., Smits, A. M., and Bos, J. L. Genetic alterations during colorectal-tumor development. *N Engl J Med*, 319: 525-532., 1988.
34. Solit, D. B., Garraway, L. A., Pratilas, C. A., Sawai, A., Getz, G., Basso, A., Ye, Q., Lobo, J. M., She, Y., Osman, I., Golub, T. R., Sebolt-Leopold, J., Sellers, W. R., and Rosen, N. BRAF mutation predicts sensitivity to MEK inhibition. *Nature*, 439: 358-362, 2006.

CHAPTER III

MALIGNANT TRANSFORMATION OF MELANOCYTES BY OVEREXPRESSION OF p90 RIBOSOMAL S6 KINASE

This work has been submitted for publication.

Abstract

While many genetic alterations have been identified in melanoma, the relevant molecular events that contribute to melanocyte tumorigenesis and metastasis are poorly understood. Most melanomas harbor activating mutations in NRAS or BRAF conferring constitutive activation of MAPK signaling that results in downstream activation of many effectors including p90 Ribosomal S6 Kinase (RSK). Although RSK promotes survival through inactivation of the pro-apoptotic protein BAD and also regulates cell cycle progression, it has not been implicated in melanomagenesis. We observed high levels of RSK activation in all human melanoma cell lines examined as well as overexpression in several of these cell lines. Expression of wild type and a constitutively active form of RSK enhanced mouse melanocyte proliferation. Using a CDKN2A deficient melanocyte cell line we show that overexpression of constitutively active or wild-type RSK can transform mouse melanocytes *in vitro* and *in vivo* in this context. However, RSK expressing tumors exhibited delayed tumor growth compared with NRAS expressing tumors suggestive of secondary genetic events required for progression. Upon investigation, high level intrachromosomal gene amplification of *Met*, a growth factor receptor tyrosine kinase implicated in melanoma progression, was identified in each independent RSK

expressing tumor. MET expression is rarely detected in primary human melanoma, but is frequently observed in advanced metastatic disease and therefore may be an attractive therapeutic target to prevent disease progression.

Introduction

The incidence of melanoma has increased by more than 600% over the last forty years; 59,940 new cases are expected in the United States this year (1). If detected early, the disease is treatable; however, following metastasis it is largely resistant to most conventional therapies and is associated with a high mortality rate (2). Several loci mutated in familial or sporadic melanoma have been identified, providing targets for study and potentially for therapeutic intervention (reviewed in (3)). The *CDKN2A* locus has been linked to numerous cancers, including melanoma and encodes two distinct tumor suppressor proteins: p16^{INK4A}, which inhibits CDK4/6 and cell cycle progression, and p14^{ARF} a key element involved in p53 regulation (4, 5). With less frequency, mutations in tumor suppressors such as *p53*, *PTEN*, and *Rb* have also been reported (3). With mutually exclusive mutations in *NRAS* and *BRAF*, the mitogen-activated protein kinase (MAPK) signaling pathway is constitutively activated in over 70% of sporadic malignant melanomas (6). *NRAS* and *BRAF* mutations are frequently found in benign nevi suggestive of an important initiating role in melanoma genesis whereas hyperactive receptor tyrosine kinase (RTK) signaling by the epidermal growth factor receptor (EGFR) or c-MET has been associated with melanoma progression and metastasis (7-9). MAPK signaling promotes survival in human melanoma cell lines as small molecule inhibitors of

MEK induce high levels of apoptosis, whereas normal melanocytes experience a cell cycle arrest (10-12).

The family of 90-kDa serine/threonine ribosomal S6 kinases (RSK or p90^{rsk}) was among the first MAPK substrates identified. In humans, there are four separate genes encoding the RSK isoforms (RSK1, 2, 3 and 4) and mutations in RSK-2 have been associated with the X-linked neurodegenerative disorder Coffin-Lowry syndrome, which is characterized by skeletal abnormalities and mental retardation (13, 14). RSK contains two distinct kinase domains: The N-terminal domain (NTD) is responsible for phosphorylation of all known RSK substrates while the C-terminal domain (CTD) is autoregulatory. RSK is activated through ERK and 3-phosphoinositide-dependent protein kinase 1 (PDK1) phosphorylation and subsequent autophosphorylation of the NTD by the CTD (10, 11, 15). In melanoma cell lines, RSK-1 has been shown to be the most activated isoform, but RSK-2 and RSK-3 are present and active as well (11). Once activated, the targets of RSK are diverse, regulating cell cycle progression, transcription, and survival. Transcription factors such as cAMP response element-binding (CREB), c-Fos, Myt-1, and Nuclear factor- κ B (NF- κ B) have been reported as RSK targets, as well as several proteins related to cell cycle progression and survival (16-18). RSK has been shown to promote survival through phosphorylation and subsequent inactivation of the pro-apoptotic Bcl-2 family member Bad (15, 16, 19). This activity can be MAPK independent (11, 15), but overexpression of active RAS and RAF increase Bad phosphorylation while MEK inhibitors reduce Bad phosphorylation (15, 16, 19). Phosphorylation of the inactivating Ser⁷⁵ residue in human Bad is dependent on

activation of ERK and RSK in melanoma cells but not in normal melanocytes (11). MEK inhibitors block Bad phosphorylation/inactivation and this coincides with the onset of melanoma cell apoptosis. Subsequent expression of constitutively active RSK circumvents MEK inhibition, resulting in increased Bad phosphorylation and increased survival of melanoma cells (11).

In this study, we examined the expression and activation of RSK in human melanoma cells and found that RSK is highly activated in several melanoma cell lines, compared with normal melanocytes. In some melanoma cell lines, RSK-1 was overexpressed. We observed that overexpression of wild-type (wt) RSK or a constitutively active mutant of RSK (RSK-CAII) increases the proliferation of melanocytes *in vitro*. In addition, RSK overexpression/activation induces transformation of melanocytes devoid of *Ink4a/Arf*, but *in vivo* tumor growth was significantly delayed compared with cells expressing activated NRAS. This delay in tumor growth in the RSK expressing cells suggested that additional genetic events were required. Cytogenetic analysis of RSK-induced tumors revealed high-level amplification of the RTK *Met*. This amplification was intrachromosomal and was found only in tumors driven by overexpression of wild-type RSK.

Materials and Methods

Cell culture.

Mouse melanocytes and neonatal human epidermal melanocytes (Cascade Biologics, Portland OR) were cultured in 254 media containing HMGS, 5% FBS, and 50 µg/ml gentamicin at 37 °C with 5% CO₂. Human melanoma cell lines were obtained from the Developmental Therapeutics Program, National Cancer Institute/NIH and cultured in RPMI 1640 (Invitrogen, Carlsbad, CA) supplemented with 5% FBS, 2 mM L-glutamine, and 50 µg/ml gentamicin at 37 °C with 5% CO₂. Single cells were obtained from subcutaneous tumors by mincing the tissue with a razor blade followed by incubation in 0.05% trypsin for 45 min at 37 °C. Cells were established in culture and maintained in 254 media supplemented with 10% fetal bovine serum. DF-1 cells were grown in DMEM-high glucose (Invitrogen) supplemented with 10% fetal bovine serum, 100 units of penicillin per ml, and 100 µg of streptomycin per ml, and maintained at 39 °C with 5% CO₂ (30, 31).

Inhibitors.

PD98059 (Cell Signaling, Beverly, MA) and PD184352 (Upstate Biotechnology, Lake Placid, New York) was dissolved in DMSO, and the cells were treated as previously described (10). Controls were treated with an equivalent volume of DMSO.

Immunohistochemistry.

M14-MEL and SK-MEL-28 cells that were treated with either DMSO or PD98059 were formalin-fixed and dehydrated through a graded alcohol series in a Ventana Renaissance processor (Ventana Medical Systems, Tucson, AZ). The cells were paraffin-embedded and 5 μm sections were adhered to glass slides. Following deparaffinization and rehydration, the slides were heated in DAKO Target Retrieval Solution (Dako, Carpinteria, CA) for 25 min for antigen retrieval. The slides were cooled, rinsed three times in cold water and then washed once in phosphate-buffered saline (PBS) with 0.05% Tween-20 (PBST). The slides were blocked in 1% BSA plus 5% goat serum in PBS for 30 min at room temperature. The blocking solution was rinsed away in PBS-T and the sections were incubated with a rabbit polyclonal anti-p90 RSK-1 antibody (Upstate Biotechnology) diluted 1:100 in antibody dilution buffer (Biomedex, Foster City, CA) overnight at 4°C. During this period, the sections were covered with coverslips for even distribution of the antibody and to prevent excessive evaporation. After washing in PBS-T three times for 5 min each, the sections were reacted with 1:100 dilution of Alexa-Fluor 488-conjugated goat anti-rabbit IgG antibody (Molecular Probes, Eugene, OR) and the DNA dye TO-PRO3 600 nM (Molecular Probes, Inc.) to mark the nuclei in antibody dilution buffer (Biomedex) for 1 hr at room temperature in the dark. After washing in PBS-T three times for 15 min each, the slides were mounted with coverslips. The stained sections were imaged on a confocal microscope and analyzed with the Image Pro-Plus v.4.1 software (Media Cybernetics, Bethesda, MD). Activation of RSK-1 was estimated with the relative nuclear/cytoplasmic staining ratio.

Vector constructs.

The pLPCX-RSK-IRES-GFP retroviral vectors (11), and the RCASBP(M)-NRAS (Q61R) retroviral vector (20) have been described.

Virus production.

RCASBP(M)-NRAS (Q61R) viral infection was initiated by calcium phosphate transfection of plasmid DNA that contained the retroviral vector in proviral form (32). In standard transfections, DF-1 cells were plated at 30% confluency, allowed to attach (2–3 h), and 5 µg of purified plasmid DNA was introduced using the mammalian transfection kit (Stratagene, Cedar Creek, TX) per the manufacturer's specifications, followed by a 5 min glycerol shock at 39 °C (15% glycerol in the medium). Viral spread was monitored by assaying culture supernatants for avian leukosis virus capsid protein by ELISA as previously described (33). Virus stocks were generated from the cell supernatants. The supernatants were cleared of cellular debris by centrifugation at 2000 × g for 10 min at 4 °C, filtered through a 0.45-µm filter, and stored in aliquots at –80 °C. Virus was determined to be replication-competent by a reading of 0.200 or greater on ELISA for the viral capsid protein (33). The pLPCX-RSK-IRES-GFP retroviral vectors were transfected into the 293-GPG helper cell line to produce VSV-G pseudotyped viral stocks and viral titers were determined on HEK293 cells as previously described (11).

Viral infections.

Melanocytes were seeded in 254 media containing human melanocyte growth supplement (HMGS) (Cascade Biologics, Portland, OR) and 10% FBS in 6-well

cluster dishes at a density of 5×10^4 cells/well 16 h prior to infection at 37 °C. The next day, the medium was removed and replaced with 1 ml of filtered viral stock in the presence of 8 µg/ml of polybrene (Sigma, St. Louis, MO) for 6 h at 37 °C. After the infection, the virus containing media was removed, replaced with fresh media, and the cells were expanded. For pLPCX-RSK-IRES-GFP infections, stable expressing cells were selected with 50 µg/ml puromycin and pooled.

Western blotting.

Melanocytes or melanoma cells were washed with PBS and 150 µl SDS-lysis buffer was added to each well of a 6-well dish. The cell lysates were boiled for 10 min and passed through a 26-gauge needle 5 times. Following centrifugation, the proteins were separated on a 14% Tris-glycine polyacrylamide gel, transferred to nitrocellulose, and incubated for 1 h at room temperature in blocking solution (0.05% Tween-20 in TBS with 5% non-fat dry milk). Blots were immunostained for NRas using an anti-NRas monoclonal antibody (Ab-1; Oncogene, San Diego, CA) at a 1:1000 dilution; for total RSK-1 using an anti-RSK-1 monoclonal antibody (Upstate Biotechnology); for phospho-RSK (T-573) using a rabbit polyclonal antibody (9346; Cell Signaling) at a 1:1000 dilution; for phospho ERK using a mouse monoclonal anti-Phospho MAPK antibody (E10; Cell Signaling) at a 1:1000 dilution; Total ERK using a rabbit polyclonal anti-MAPK antibody (Cell Signaling) at a 1:1000 dilution; and anti- α -tubulin (AB-1) at a 1:1000 dilution (Oncogene). All antibodies were diluted in blocking solution. Western blots were incubated in the primary antibody overnight at 4 °C with constant shaking and then washed three times in TBS-T wash

buffer (0.05% Tween-20 in Tris-buffered saline). The blots were then incubated with either an anti-mouse or anti-rabbit IgG-HRP secondary antibody diluted 1:3000 (Sigma, St. Louis, MO) for 1 h at room temperature. The blots were washed three times in TBS-T wash buffer, incubated with ECL solutions per the manufacturer's specifications (Amersham, Piscataway, NJ), and exposed to film.

Growth in soft agar.

To assess anchorage-independent growth, 1.5×10^5 cells were suspended in 0.55% Difco agar noble (Becton Dickinson, Sparks, MD) in MGM/10% FBS and layered over pre-solidified 0.65% Difco agar noble in MGM/10% FBS per well of a 6-well dish. Fresh medium was added twice per week for 4 weeks. Each cell line was assayed in triplicate.

Cell proliferation studies.

Each cell line was seeded into 24 wells of a 96-well dish at a density of 5×10^3 cells/well. The cells were cultured and assayed for viable cell count at the times indicated using the CellTiter 96[®] AQueous One Solution Cell Proliferation Assay (Promega, Madison, WI) according to the manufacturer's specifications.

In vivo studies.

Four-week old female athymic nude (NCr *nu/nu*) mice were injected subcutaneously (s.c.) on the right upper dorsal area with 1×10^7 cells/mouse in 100 μ l Hanks' balanced salt solution (HBSS). Tumor size was evaluated by caliper measurements, and tumor volume was calculated by length \times width \times depth. For histological examination, tumors were dissected, fixed in 10% neutral-buffered

formalin overnight, embedded in paraffin blocks, and cut into thin sections. All experiments were performed in compliance with the guiding principles of the “Care and Use of Animals” (available at <http://www.nap.edu/books/0309053773/html/>) and were approved by the IACUC prior to experimentation.

Metaphase spreads.

Melanocytes were incubated overnight with colcemid (12ng/ml; Invitrogen) to arrest cells in metaphase. Cells were detached by trypsin, washed twice in PBS and then gently resuspended in 5 ml 37 °C, 75 mM KCl for 10 min. to permeabilize the plasma membrane, and fixed in 10 ml ice cold fixative (75% methanol, 25% glacial acetic acid).

Reverse DAPI.

Metaphase spread slides were prepared from cell cultures that were harvested and fixed with methanol:acetic acid (3:1), as described above. Slides were aged overnight at 55 °C. Once slides were cooled to room temperature, DAPI was applied and covered with a glass cover slip. Image acquisition was performed with a COOL-1300 SpectraCube camera (Applied Spectral Imaging-ASI, Vista, CA) mounted on an Olympus BX51 epifluorescence microscope and analyzed using FISHView software (EXPO 4.0, ASI). Chromosomes were counted and obvious aberrations were noted for at least 20 metaphases per slide.

Spectral karyotyping (SKY).

Metaphase spreads were prepared from cell cultures as described above and SKY was performed according to the standard supplied protocol (ASI) on freshly prepared metaphase slides to investigate cytogenetic abnormalities. Image

acquisitions were performed using a SKY™ Spectracube™ system (ASI) with a high-resolution scientific digital camera (VDS Vosskühler GmbH) mounted on an Olympus BX51 microscope with a custom designed optical filter (SKY-1, Chroma Technology, Brattleboro, VT). Twenty metaphases were analyzed using the SKYView v1.6.2 software (ASI).

Fluorescent *in situ* hybridization (FISH).

FISH probes were prepared from purified BAC clones RP23-73G15 and RP24-462C10 (Children's Hospital Oakland Research Institute; <http://bacpac.chori.org>) and labeled with SpectrumOrange and SpectrumGreen (Abbott Molecular Inc, Des Plaines, IL), respectively, by nick translation. These probes were used to detect *Met* amplification within region 6A2 and region 6D3 as a control, respectively. Metaphase spread slides were prepared from cell cultures that were harvested and fixed with methanol:acetic acid (3:1), as described above. The slides were pretreated with 2× saline/sodium citrate at 37 °C for 10 min, 0.005% pepsin at 37 °C for 4 min, and 1× PBS for 5min. The slides were then placed in 1% formaldehyde for 10 min at room temperature, washed with 1× PBS for 5 min, and dehydrated in an ethanol series (70%, 85%, and 95%) for 2 min each. Samples were denatured in 70% formamide/2× saline/sodium citrate at 73 °C for 5 min, washed in a cold ethanol series (70%, 85%, 95%) for 2 min each, and air dried. FISH probes were denatured at 73° C for 5 min before applying to each dried slide and mounted with a glass cover slip. The slides were hybridized overnight at 37 °C, washed with 2× saline/sodium citrate at 73° C for 2 min, and rinsed briefly in H₂O. Slides were then air-dried, counterstained with anti-fade 4'-6-diamidino-2-phenylindole (DAPI), and

covered with cover slips. Image acquisition was performed with a COOL-1300 SpectraCube camera (ASI) mounted on an Olympus BX51 epifluorescence microscope and analyzed using FISHView 4.0 software (ASI). Hybridization signals were analyzed for at least 10 metaphases per slide.

Results

RSK is overexpressed and highly activated in human melanoma cells.

We examined RSK expression and activation in a subset of melanoma cell lines and normal melanocytes. We observed that RSK is overexpressed and highly activated in all of the melanoma cell lines tested compared with normal melanocytes (Figure 1). Inhibition of MEK activity with the small molecule MEK inhibitor PD184352 resulted in inactivation of the downstream protein kinase ERK and RSK in these melanoma cell lines (Figure 1). Localization by subcellular fractionation revealed that the majority of active, phosphorylated RSK was localized to the nucleus (Figure 1). To further examine the subcellular localization of both active and inactive RSK-1, we performed immunohistochemistry for RSK-1 on formalin-fixed, paraffin-embedded cell blocks generated from M14-MEL and SK-MEL-28 cells treated with DMSO (active RSK-1) or the MEK inhibitor PD98059 (inactive RSK-1). Consistent with the immunoblotting results (Figure 1), a higher level of RSK-1 expression was detected in the M14-MEL cells (mean staining intensity 118 ± 5) compared with SK-MEL-28 cells (84 ± 17) (Figure 2A). Increased nuclear RSK-1 staining was detected

in the DMSO-treated control cells compared with the PD98059-treated cells, indicating nuclear translocation of active RSK-1 (Figure 2A).

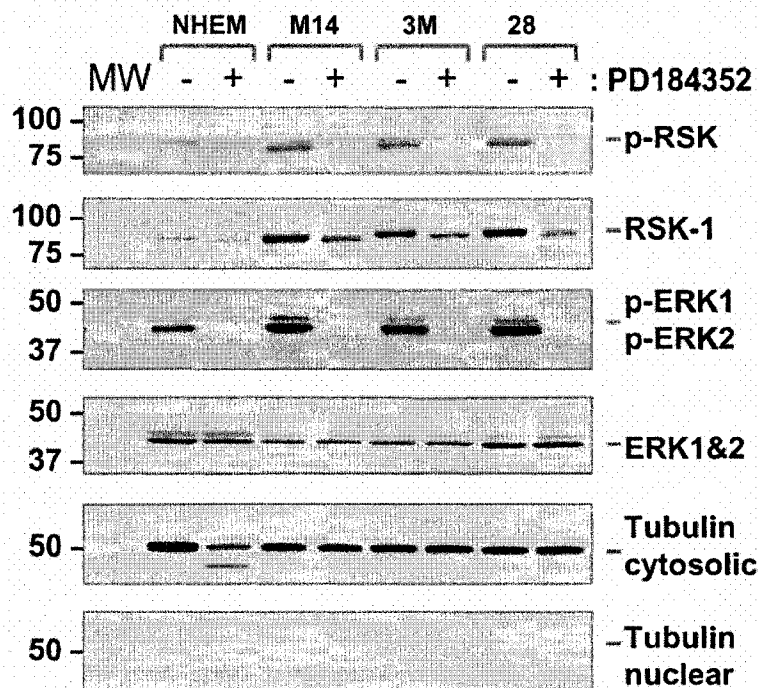


Figure 1. MAPK (ERK1&2) and RSK activation in melanoma cell lines. Cells were treated with PD184352 (+) or DMSO (-) for 72 hours. Lysates were subjected to nuclear and cytoplasmic fractionation. Active phospho-MAPK (ERK1P and ERK2P), total MAPK (ERK1 & 2), and tubulin immunoblots from the cytoplasmic fraction are shown. Active phospho-RSK (RSKP), total RSK-1, and tubulin immunoblots from the nuclear fraction are shown. For comparison, the actively growing normal human epidermal melanocytes (NHEM) were included.

RSK overexpression/activation increases the proliferation of melanocytes.

To determine the functional significance of RSK overexpression and/or activation, we introduced wt RSK and constitutively active mutants of RSK, RSK-CAI or CAII, into *Ink4a/Arf*-null immortalized melanocytes (20). RSK-CAI contains an N-terminal myristoylation sequence in addition to several activating mutations

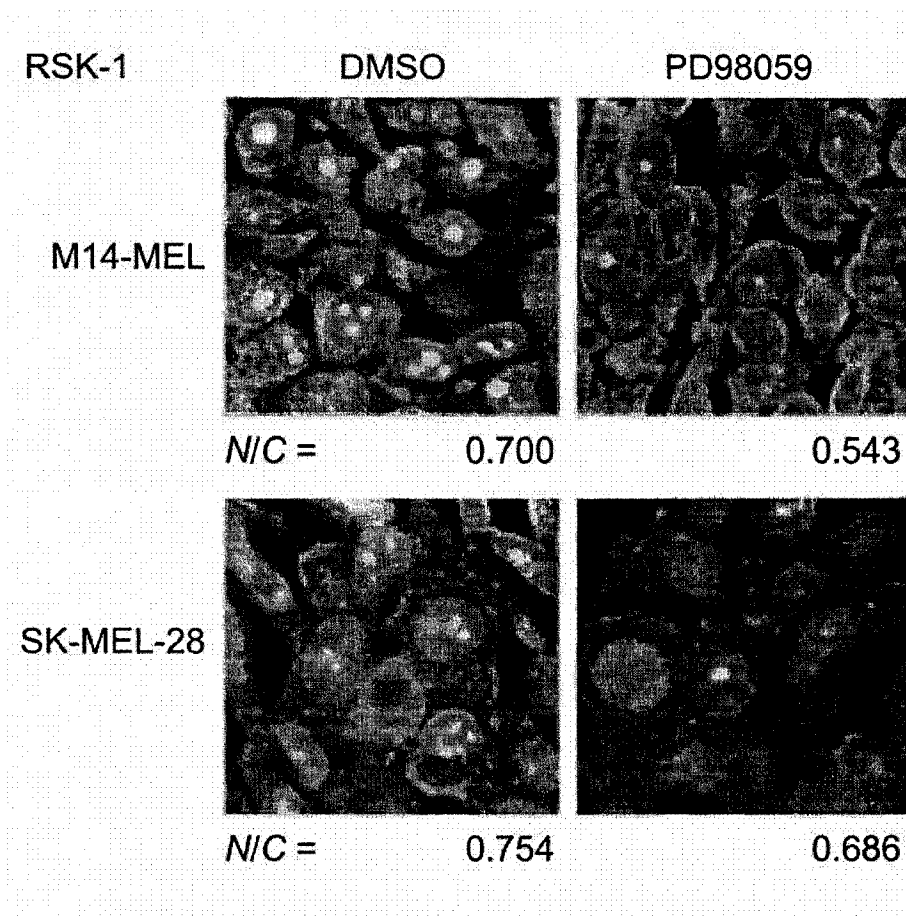


Figure 2. Indirect immunofluorescent staining of RSK-1 in human melanoma cells treated with DMSO or PD98059. M14-MEL and SK-MEL-28 cells were treated with DMSO or PD98059 for 24 hrs. The cells were fixed in formalin, embedded in paraffin, and 5 μ m sections were adhered to glass slides. Following antigen retrieval, RSK-1 expression (*green*) was detected immunohistochemically. Nuclei were marked by co-staining with the DNA dye TO-PRO3 (*red*; Molecular Probes, Inc.). Mean staining intensities calculated from six independent images for M14-MEL and SK-MEL-28 cells were 118 ± 5 and 84 ± 17 , respectively. A ratio (N/C) of the mean staining intensity within nuclear regions to cytoplasmic staining is also shown for each image.

(T357EED, S363EDD, Y702A) (Figure 3A). RSK-CAII lacks the first 43 N-terminal amino acids and also contains several activating mutations (T357EED, S363EDD, Y702A) (Figure 3A). The activity of these RSK constructs was previously demonstrated by an *in vitro* kinase assay using recombinant GST-mouse Bad as a substrate (11). The introduction of wt RSK or constitutively active RSK in *Ink4a/Arf*-null melanocytes led to an increase in RSK protein as assessed by Western

blot (Figure 3B, left panel). Since Ras is oncogenic in melanocytes (21), the cells were also infected with a retrovirus encoding constitutively active NRAS and expression was confirmed by Western blot (Figure 3B, middle panel).

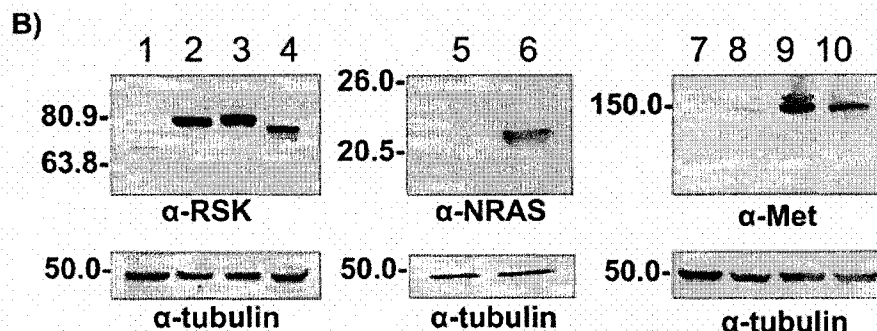
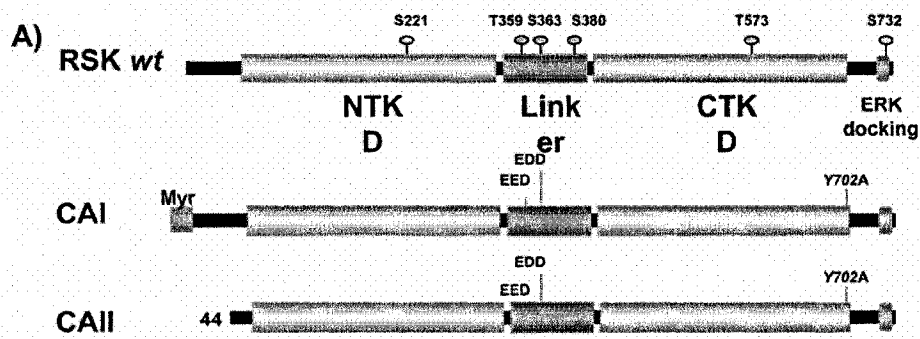


Figure 3. Oncogene expression in immortal melanocytes. (A) Diagram of p90RSK-1 wild-type (wt) and generated RSK-CAI and RSK-CAII mutants. NTKD: NH₂-terminal kinase domain, CTKD: COOH-terminal kinase domain, Myr: Myristoylation signal. (B) Western blots of lysates from uninfected melanocytes (Lanes 1, 5, and 7) or melanocytes infected with retroviruses containing wt RSK (Lanes 2, 8-10), RSK-CAI (Lane 3), RSK-CAII (Lane 4), or NRAS (Q61R) (Lane 6). Lanes 9 and 10 are lysates from wt RSK expressing tumors that were established in culture and passaged for either 3 or 10 passages, respectively. The blots were re-probed for tubulin to ensure equal loading.

To determine whether expression of these genes increases the rate of cellular proliferation, *in vitro* proliferation of melanocytes expressing wt RSK, RSK-CAI, RSK-CAII or NRAS (Q61R) was measured (Figure 4A). Wild-type RSK, RSK-CAII, and NRAS (Q61R) expression all increased the rate of cellular proliferation compared with the parental cells. Interestingly, cells expressing RSK-CAI decreased the rate of cellular proliferation compared with the parental cells.

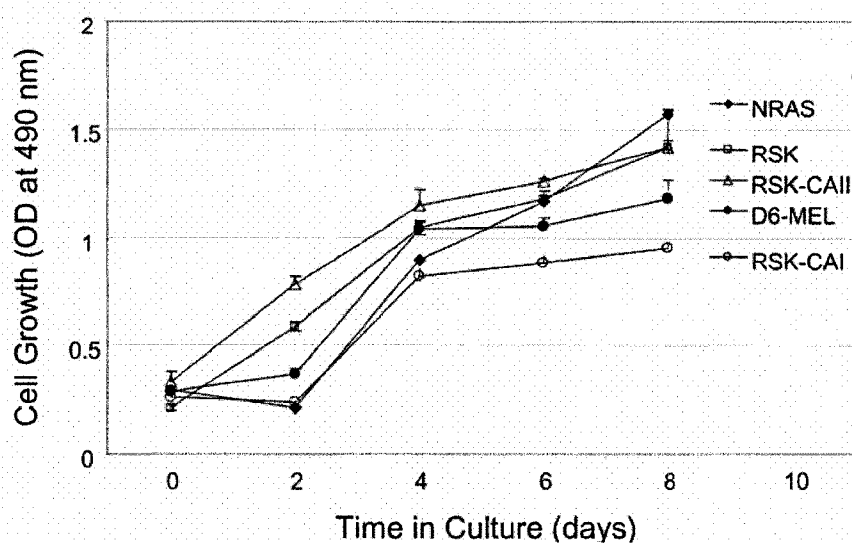


Figure 4. (A) *In vitro* proliferation of melanocytes expressing different genes. Uninfected melanocytes (D6-MEL) or melanocytes expressing NRAS (Q61R), wt RSK, RSK CAI, or RSK CAII were cultured in microtiter wells for the indicated time points and viable cells were quantitated using the CellTiter 96 AQueous One Solution Cell Proliferation Assay by optical density readings at 490 nm (data are represented as mean \pm s.e.m.; $n = 3$).

Melanocytes expressing wt RSK or RSK-CAII are tumorigenic.

To determine whether expression of these genes causes anchorage-independent growth, the cells were assayed for their ability to grow in soft agar. Whereas the parental melanocytes and the melanocytes expressing RSK-CAI failed to

grow in soft agar, melanocytes expressing NRAS (Q61R) formed numerous colonies in soft agar, demonstrating that NRAS activation in melanocytes results in anchorage-independent growth, a characteristic of transformed cells. While wt RSK and RSK-CAI also formed colonies in soft agar, they were smaller and significantly fewer in number than melanocytes expressing NRAS (Table 1).

Table 1. Tumorigenicity of melanocytes expressing different components of the MAPK pathway.			
Cell lines	Soft-agar growth*	Tumors in nude mice†	Maximal tumor volume§
D6-MEL	No	0/8	NA
NRAS	Yes	8/8	> 800 mm ³
RSK-wt	Yes	8/8	> 800 mm ³
RSK-CAI	No	0/8	NA
RSK-CAII	Yes	6/8	< 10 mm ³
M14‡	Yes	8/8	> 800 mm ³

*Cells (1.5×10^5 cells/well) were resuspended in 0.55% Noble agar in growth medium and layered over presolidified 0.65% agar in a 6-well plate. After 4-week culturing, colony formation was assessed.

†Athymic nude mice (n=8) were injected subcutaneously with 1×10^7 cells/mouse of each cell line and monitored for tumor formation for 12 weeks.

§Mean maximal tumor volume as measured by length \times width \times depth.

‡M14 human melanoma cells were used as a positive control.

Although anchorage-independent growth is indicative of transformation, a more stringent assay of tumorigenic potential is the ability to form tumors *in vivo*. To determine whether expression of these genes in melanocytes results in tumor formation *in vivo*, cells expressing NRAS (Q61R), wt RSK, RSK-CAI, or RSK-CAII were injected subcutaneously into nude mice. Melanocytes expressing NRAS (Q61R), wt RSK, and RSK-CAII all formed tumors in nude mice but with

significantly different efficiencies and latencies (Table 1, Figure 4B). As early as three weeks post-injection, tumors were visible in mice injected with melanocytes expressing constitutively active NRAS. In contrast, tumors were not visible in mice injected with melanocytes expressing wt RSK or RSK-CAII until eight weeks post-injection. In addition, whereas 8/8 mice injected with melanocytes expressing NRAS (Q61R) and wt RSK developed tumors, only 6/8 mice injected with melanocytes expressing RSK-CAII developed tumors (Table 1). Furthermore, while 8/8 tumors in the NRAS cohort reached 1,000 mm³, only 2/8 of the wt RSK tumors grew to that size. Interestingly, whereas 6/8 of the mice injected with melanocytes expressing RSK-CAII developed visible tumors eight weeks post-injection, none of these tumors grew larger than 10 mm³.

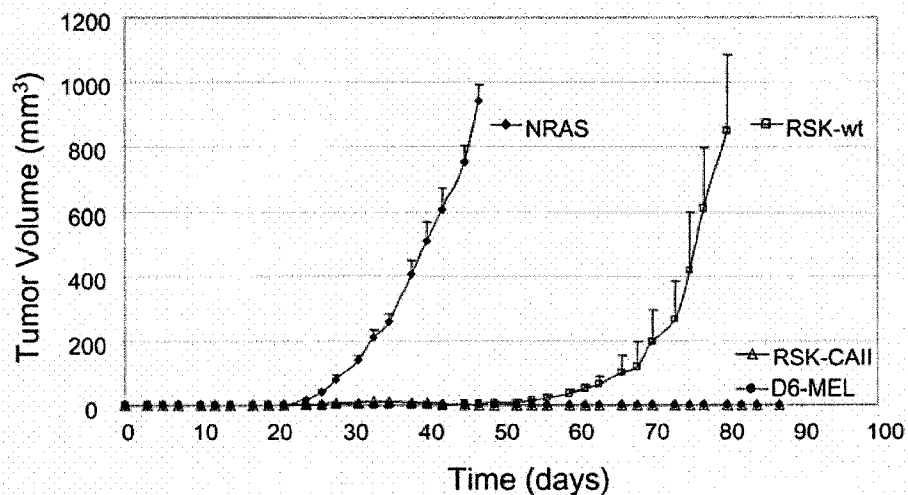


Figure 4. (B) *In vivo* tumor formation. Volumes are shown for tumors induced by subcutaneous inoculation of 1×10^7 cells/mouse for the cell lines indicated. Tumor size was evaluated by caliper measurements, and tumor volume was calculated by length \times width \times depth.

Tumor cells expressing wt RSK are aneuploid.

The slow kinetics of tumor formation in mice injected with melanocytes expressing wt RSK or RSK-CAII suggested that additional genetic alterations were required for tumor growth *in vivo*. To define the genetic alteration(s) that mediated the *in vivo* growth of melanocytes expressing wt RSK, subcutaneous tumors that grew to volumes greater than 500 mm³ were isolated and established in culture. As an initial quantification of nuclear DNA content, RSK tumor cell lines, melanocytes expressing wt RSK, and untreated D6-MEL melanocytes were stained with propidium iodide and analyzed by flow cytometry. Populations of RSK-expressing D6-MEL cells contained homogenous amounts of DNA, with two histogram peaks characteristic of diploid cells in G₀/G₁ and G₂/M phase (data not shown). The DNA content of cells expressing wt RSK (prior to injection into mice) was indistinguishable from untreated D6-MEL cells. In contrast, the DNA content of cell lines established from wt RSK expressing tumors indicated that between 55 and 65% of the cells were aneuploid (Table 2). To further evaluate the DNA content in these cells, reverse DAPI stained metaphase spreads from each cell line were analyzed cytogenetically. While only 1/20 metaphases from the parental D6-MEL cell line was 4n, 12/20 metaphases from the RSK-wt cells were 4n. Likewise, 17/20 and 18/20 of the metaphases from the RSK-wt tumor cells at passage 3 and 10, respectively, were 4n indicating significant aneuploidy in cells expressing wt RSK. The genomic integrity of the D6-MEL melanocyte cell line was also evaluated using spectral karyotyping (SKY). Twenty metaphases were analyzed and 17/20 metaphases had an additional chromosome 6 and 15, 18/20 metaphases had an extra derivative

chromosome 4 translocated with chromosome X, and 1/20 was near-tetraploid, an insignificant finding (Figure 5A, B, and C).

Cell line	Flow cytometry*		Cytogenetics†	
	2n	4n	2n	4n
D6-MEL	100%	0%	95%	5%
D6-RSK-wt	100%	0%	40%	60%
Tumor cells (p.3)	33.65%	65.18%	15%	85%
Tumor cells (p.10)	43.87%	56.13%	10%	90%

*Quantification of DNA content by propidium iodide staining of nuclear DNA.
† Analysis of 20 reverse DAPI-stained metaphase chromosome spreads.

Increased Met protein levels result from gene amplification.

Since amplification and/or overexpression of the receptor tyrosine kinases (RTK) *EGFR* (7, 9) and *MET* have been implicated in melanoma progression (8), we evaluated the expression of EGFR and Met in the tumor cells expressing wt RSK. While no difference in EGFR expression was observed (data not shown), a significant increase in Met protein levels was detected by western blot (Figure 3B, right panel). To determine if the mechanism of increased Met protein levels was the result of gene amplification, we analyzed both interphase and metaphase cells by fluorescent in-situ hybridization (FISH) using a probe specific for the *Met* locus. FISH analysis showed 3 copies of both the Met specific probe and the control probe in the D6-MEL parental melanocytes and the melanocytes expressing wt RSK (Figure 5D). The 3 copies of chromosome 6 correspond with the additional chromosome 6 detected by SKY in the D6-MEL cells (Figure 5C). In contrast, a high level of intrachromosomal *Met* gene amplification was detected in the RSK-wt expressing tumor cells; 46 copies were detected in the 2n tumor cells and 92 copies were detected in the 4n cells. Reduced

Met expression was observed with increased passage of the tumor cells in culture (Figure 3B, right panel).

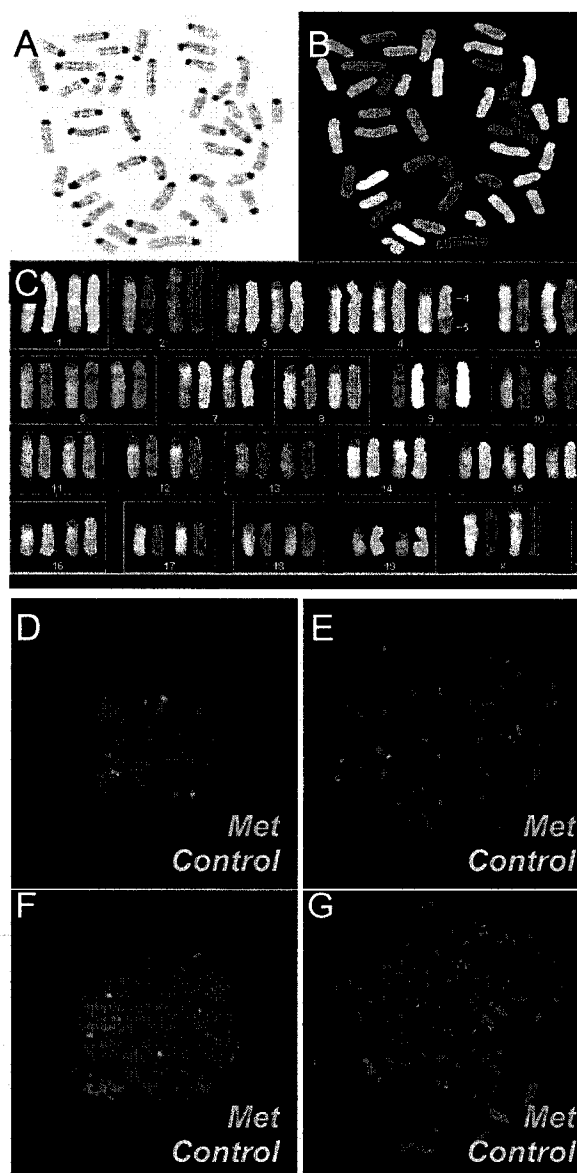


Figure 5. Spectral karyotyping and *Met* FISH of melanocytes and tumor cells. A-C SKY analysis of D6-MEL melanocytes. A. G-banding. B. Pseudocolored chromosomes. C. Chromosomal pattern adjacent to the corresponding pseudocolored chromosome. D-G *Met* FISH analysis. D. Interphase RSK-wt cell pre-implantation. E. Metaphase RSK-wt cell pre-implantation. F. Interphase RSK-wt tumor cell. G. Metaphase RSK-wt tumor cell. Ten metaphases were analyzed per cell line. A representative image is shown for each. Orange, probe detecting the *Met* locus on chromosome 6; green, chromosome 6 control probe.

Discussion

We observed that RSK is highly activated in several human melanoma cell lines compared with normal melanocytes. Expression of wild-type (wt) RSK or a constitutively active mutant of RSK (RSK-CAII) increases the proliferation of *Ink4a/Arf*-null melanocytes *in vitro* and induces transformation *in vivo*. However, tumor growth was significantly delayed compared with cells expressing activated NRAS. The delayed tumor growth in the RSK expressing cells suggested that additional genetic events were required. We compared tumors that grew to volumes greater than 500 mm³ with the RSK expressing pre-injected cells and observed overexpression of Met protein in the tumor cells. Cytogenetic analysis of RSK-induced tumors revealed high-level amplification of the RTK *Met* in all cases. This amplification was intrachromosomal and was found only in tumors driven by overexpression of wild-type RSK. Each explant had significant Met expression which diminished over several passages.

It is interesting that only the melanocytes expressing wt RSK went on to form tumors *in vivo*. While CA RSK mutants have activity in the absence of MAPK signaling, they have sub-maximal activity relative to wt RSK when MAPK is active (22). Previously, we demonstrated that overexpression of wt RSK prevented apoptosis equally as well as either CA-RSK in the presence of a MEK inhibitor in human melanoma cell lines (11). The duration of RSK activity may be relevant as RSK activity has been detected as long as two hours post stimulation (23). Therefore, in an *in vivo* setting with transient MAPK activation, overexpression of wt RSK is sufficient to promote proliferation while partially active CA RSK mutants may be

limited. Our data also show that the majority of active RSK-1 localizes to the nucleus (Figure 2A) and suggest that a ratio of the nuclear vs. cytoplasmic (N/C) staining intensity can be used as a correlate with activation status of RSK-1 in tissues. This is consistent with previous findings that upon activation, RSK translocates to the nucleus, where it phosphorylates nuclear substrates (24-26). Although CAI and CAII are equally able to phosphorylate a cytosolic substrate (11), the difference between CAI and CAII may lie in the inability of myristoylated CAI to translocate to the nucleus and phosphorylate nuclear substrates, suggesting that the effects mediated by RSK are nuclear. This idea is supported by the data in Figures 1 and 2, which demonstrate that active RSK is in the nucleus.

The c-MET proto-oncogene encodes the receptor for Hepatocyte Growth Factor/Scatter Factor (HGF/SF), which is known to mediate mitogenic, motogenic, and invasive responses. Gene amplification of the RTK MET can be found in 10-20% of primary human gastric cancers (27). In a Brca1/Trp53 mouse model, high level Met gene amplification was observed in 73% of the mammary tumors (28) providing further support for the relevance of secondary genetic events in tumorigenesis. While infrequent in nevi and primary melanomas, 38% of metastatic lesions have significant MET expression suggesting a role in tumor progression (8). Through its ability to promote tumor progression and enhance invasiveness, MET is being developed as a therapeutic target for drug intervention in many metastatic tumors including melanoma. Recently, a MET-specific RTK inhibitor displayed promising antitumor activity against melanoma cell lines expressing MET (29).

Acknowledgements

We thank Dr. Nita Maihle for the EGFR antibody. We also thank Bryn Eagleson, Elissa Boguslawski, Dawna Dylewski, and the vivarium staff for excellent animal husbandry and Bree Berghuis and Dr. James Resau of the Analytical Cellular and Molecular Microscopy Laboratory for technical assistance. This work was supported by funds from the Melanoma Research Foundation, the James A. Schlipmann Melanoma Cancer Foundation, the Van Andel Research Institute, and the Nevada Cancer Institute.

BIBLIOGRAPHY

1. Jemal, A., Siegel, R., Ward, E., Murray, T., Xu, J., and Thun, M. J. Cancer statistics, 2007. *CA Cancer J Clin*, 57: 43-66, 2007.
2. Ahmed, I. Malignant melanoma: prognostic indicators. *Mayo Clin Proc*, 72: 356-361, 1997.
3. Chin, L., Garraway, L. A., and Fisher, D. E. Malignant melanoma: genetics and therapeutics in the genomic era. *Genes Dev*, 20: 2149-2182, 2006.
4. Chin, L., Pomerantz, J., and DePinho, R. A. The INK4a/ARF tumor suppressor: one gene--two products--two pathways. *Trends Biochem Sci*, 23: 291-296, 1998.
5. Quelle, D. E., Zindy, F., Ashmun, R. A., and Sherr, C. J. Alternative reading frames of the INK4a tumor suppressor gene encode two unrelated proteins capable of inducing cell cycle arrest. *Cell*, 83: 993-1000, 1995.
6. Davies, H., Bignell, G. R., Cox, C., Stephens, P., Edkins, S., Clegg, S., Teague, J., Woffendin, H., Garnett, M. J., Bottomley, W., Davis, N., Dicks, E., Ewing, R., Floyd, Y., Gray, K., Hall, S., Hawes, R., Hughes, J., Kosmidou, V., Menzies, A., Mould, C., Parker, A., Stevens, C., Watt, S., Hooper, S., Wilson, R., Jayatilake, H., Gusterson, B. A., Cooper, C., Shipley, J., Hargrave, D., Pritchard-Jones, K., Maitland, N., Chenevix-Trench, G., Riggins, G. J., Bigner, D. D., Palmieri, G., Cossu, A., Flanagan, A., Nicholson, A., Ho, J. W., Leung, S. Y., Yuen, S. T., Weber, B. L., Seigler, H. F., Darrow, T. L., Paterson, H., Marais, R., Marshall, C. J., Wooster, R., Stratton, M. R., and Futreal, P. A. Mutations of the BRAF gene in human cancer. *Nature*, 417: 949-954., 2002.
7. Koprowski, H., Herlyn, M., Balaban, G., Parmiter, A., Ross, A., and Nowell, P. Expression of the receptor for epidermal growth factor correlates with increased dosage of chromosome 7 in malignant melanoma. *Somat Cell Mol Genet*, 11: 297-302, 1985.
8. Natali, P. G., Nicotra, M. R., Di Renzo, M. F., Prat, M., Bigotti, A., Cavaliere, R., and Comoglio, P. M. Expression of the c-Met/HGF receptor in human melanocytic neoplasms: demonstration of the relationship to malignant melanoma tumour progression. *Br J Cancer*, 68: 746-750, 1993.

9. Udart, M., Utikal, J., Krahn, G. M., and Peter, R. U. Chromosome 7 aneusomy. A marker for metastatic melanoma? Expression of the epidermal growth factor receptor gene and chromosome 7 aneusomy in nevi, primary malignant melanomas and metastases. *Neoplasia*, 3: 245-254, 2001.
10. Koo, H. M., VanBrocklin, M., McWilliams, M. J., Leppla, S. H., Duesbery, N. S., and Woude, G. F. Apoptosis and melanogenesis in human melanoma cells induced by anthrax lethal factor inactivation of mitogen-activated protein kinase kinase. *Proc Natl Acad Sci U S A*, 99: 3052-3057., 2002.
11. Eisenmann, K. M., VanBrocklin, M. W., Staffend, N. A., Kitchen, S. M., and Koo, H. M. Mitogen-activated protein kinase pathway-dependent tumor-specific survival signaling in melanoma cells through inactivation of the proapoptotic protein bad. *Cancer Res*, 63: 8330-8337., 2003.
12. Collisson, E. A., De, A., Suzuki, H., Gambhir, S. S., and Kolodney, M. S. Treatment of metastatic melanoma with an orally available inhibitor of the Ras-Raf-MAPK cascade. *Cancer Res*, 63: 5669-5673, 2003.
13. Bjorbaek, C., Zhao, Y., and Moller, D. E. Divergent functional roles for p90rsk kinase domains. *J Biol Chem*, 270: 18848-18852, 1995.
14. Trivier, E., De Cesare, D., Jacquot, S., Pannetier, S., Zackai, E., Young, I., Mandel, J. L., Sassone-Corsi, P., and Hanauer, A. Mutations in the kinase Rsk-2 associated with Coffin-Lowry syndrome. *Nature*, 384: 567-570, 1996.
15. Tan, Y., Ruan, H., Demeter, M. R., and Comb, M. J. p90(RSK) blocks bad-mediated cell death via a protein kinase C-dependent pathway. *J Biol Chem*, 274: 34859-34867, 1999.
16. Bonni, A., Brunet, A., West, A. E., Datta, S. R., Takasu, M. A., and Greenberg, M. E. Cell survival promoted by the Ras-MAPK signaling pathway by transcription-dependent and -independent mechanisms. *Science*, 286: 1358-1362, 1999.
17. Chen, R. H., Abate, C., and Blenis, J. Phosphorylation of the c-Fos transrepression domain by mitogen-activated protein kinase and 90-kDa ribosomal S6 kinase. *Proc Natl Acad Sci U S A*, 90: 10952-10956, 1993.
18. Xing, J., Ginty, D. D., and Greenberg, M. E. Coupling of the RAS-MAPK pathway to gene activation by RSK2, a growth factor-regulated CREB kinase. *Science*, 273: 959-963, 1996.
19. Fang, X., Yu, S., Eder, A., Mao, M., Bast, R. C., Jr., Boyd, D., and Mills, G. B. Regulation of BAD phosphorylation at serine 112 by the Ras-mitogen-activated protein kinase pathway. *Oncogene*, 18: 6635-6640, 1999.

20. Whitwam, T., Vanbrocklin, M. W., Russo, M. E., Haak, P. T., Bilgili, D., Resau, J. H., Koo, H. M., and Holmen, S. L. Differential oncogenic potential of activated RAS isoforms in melanocytes. *Oncogene*, 2007.
21. Chin, L., Pomerantz, J., Polsky, D., Jacobson, M., Cohen, C., Cordon-Cardo, C., Horner, J. W., 2nd, and DePinho, R. A. Cooperative effects of INK4a and ras in melanoma susceptibility in vivo. *Genes Dev*, *11*: 2822-2834, 1997.
22. Gross, S. D., Schwab, M. S., Lewellyn, A. L., and Maller, J. L. Induction of metaphase arrest in cleaving *Xenopus* embryos by the protein kinase p90Rsk. *Science*, *286*: 1365-1367, 1999.
23. Roux, P. P., Richards, S. A., and Blenis, J. Phosphorylation of p90 ribosomal S6 kinase (RSK) regulates extracellular signal-regulated kinase docking and RSK activity. *Mol Cell Biol*, *23*: 4796-4804, 2003.
24. English, J., Pearson, G., Wilsbacher, J., Swantek, J., Karandikar, M., Xu, S., and Cobb, M. H. New insights into the control of MAP kinase pathways. *Exp Cell Res*, *253*: 255-270., 1999.
25. Gioeli, D., Zecevic, M., and Weber, M. J. Immunostaining for activated extracellular signal-regulated kinases in cells and tissues. *Methods Enzymol*, *332*: 343-353, 2001.
26. Lewis, T. S., Shapiro, P. S., and Ahn, N. G. Signal transduction through MAP kinase cascades. *In*: G. F. Vande Woude and G. Klein (eds.), *Advances in Cancer Research*, Vol. 74, pp. 49-139. San Diego: Academic Press, 1998.
27. Smolen, G. A., Sordella, R., Muir, B., Mohapatra, G., Barmettler, A., Archibald, H., Kim, W. J., Okimoto, R. A., Bell, D. W., Sgroi, D. C., Christensen, J. G., Settleman, J., and Haber, D. A. Amplification of MET may identify a subset of cancers with extreme sensitivity to the selective tyrosine kinase inhibitor PHA-665752. *Proc Natl Acad Sci U S A*, *103*: 2316-2321, 2006.
28. Smolen, G. A., Muir, B., Mohapatra, G., Barmettler, A., Kim, W. J., Rivera, M. N., Haserlat, S. M., Okimoto, R. A., Kwak, E., Dahiya, S., Garber, J. E., Bell, D. W., Sgroi, D. C., Chin, L., Deng, C. X., and Haber, D. A. Frequent met oncogene amplification in a *Brcal/Trp53* mouse model of mammary tumorigenesis. *Cancer Res*, *66*: 3452-3455, 2006.
29. Puri, N., Ahmed, S., Janamanchi, V., Tretiakova, M., Zumba, O., Krausz, T., Jagadeeswaran, R., and Salgia, R. c-Met is a potentially new therapeutic target for treatment of human melanoma. *Clin Cancer Res*, *13*: 2246-2253, 2007.

30. Himly, M., Foster, D. N., Bottoli, I., Iacovoni, J. S., and Vogt, P. K. The DF-1 chicken fibroblast cell line: transformation induced by diverse oncogenes and cell death resulting from infection by avian leukosis viruses. *Virology*, 248: 295-304, 1998.
31. Schaefer-Klein, J., Givol, I., Barsov, E. V., Whitcomb, J. M., VanBrocklin, M., Foster, D. N., Federspiel, M. J., and Hughes, S. H. The EV-O-derived cell line DF-1 supports the efficient replication of avian leukosis-sarcoma viruses and vectors. *Virology*, 248: 305-311, 1998.
32. Federspiel, M. and Hughes, S. Retroviral gene delivery. *In*: C. Emerson and H. Sweeney (eds.), *Methods in Cell Biology: Methods in Muscle Biology*, pp. 179-214. San Diego: Academic Press, 1997.
33. Smith, E. J., Fadly, A., and Okazaki, W. An enzyme-linked immunosorbent assay for detecting avian leukosis-sarcoma viruses. *Avian Dis*, 23: 698-707, 1979.
34. Vindelov, L. L. Flow microfluorometric analysis of nuclear DNA in cells from solid tumors and cell suspensions. A new method for rapid isolation and straining of nuclei. *Virchows Arch B Cell Pathol*, 24: 227-242, 1977.

CHAPTER IV

A NOVEL BH3 MIMETIC REVEALS A MAPK-DEPENDENT MECHANISM OF MELANOMA CELL DEATH CONTROLLED BY P53 AND REACTIVE OXYGEN SPECIES

This work appeared in *Cancer Research* 2006; 66: (23). December 1, 2006.

Abstract

The RAS/BRAF/MEK/ERK mitogen activated protein kinase (MAPK) pathway is emerging as a key modulator of melanoma initiation and progression. However, a variety of clinical studies indicate that inhibiting the MAPK pathway is insufficient *per se* to effectively kill melanoma cells. Here we report on a genetic and pharmacological approach to identify survival factors responsible for the resistance of melanoma cells to MEK/ERK antagonists. In addition, we describe a new tumor-cell selective means to bypass this resistance *in vitro* and *in vivo*. By generating a panel of isogenic cell lines with specific defects in the apoptotic machinery, we found that the ability of melanoma cells to survive in the absence of functional MEK relies on an ERK-independent expression of the anti-apoptotic factor Mcl-1 (and to a lesser extent, Bcl-x_L and Bcl-2). Using computer-based modeling, we developed a novel Bcl-2 homology domain 3 (BH3) mimetic. This compound, named TW-37, is the first rationally designed small molecule with high affinity for Mcl-1, Bcl-x_L and Bcl-2. Mechanistic analyses of the mode of action of TW-37 showed a synergistic tumor cell killing in the presence of MEK inhibitors. Importantly, TW-37 unveiled an unexpected role of the MAPK pathway in the control of reactive oxygen species

(ROS). This function was critical to prevent the activation of pro-apoptotic functions of p53 in melanoma cells, but surprisingly, it was dispensable for normal melanocytes. Our results suggest that this MAPK-dependent ROS/p53 feedback loop is a point of vulnerability of melanoma cells that can be exploited for rational drug design.

Introduction

The identification of tumor-associated genetic and epigenetic hallmarks is providing a rational platform for molecularly targeted cancer therapies (1, 2). In particular, the concept that tumor cells may remain dependent on the oncogenes that promote cell transformation is being exploited for the design of more selective anticancer agents (3). However, the identification of targets for drug development is frequently challenged by the complex and heterogeneous background of neoplastic cells. Malignant melanoma is a prime example of an aggressive tumor type containing aneuploid cells which undergo a plethora of changes in gene expression during malignant transformation (4). The extreme resistance of melanoma cells to standard chemotherapeutic agents, either as single agents or in combination, has hampered the identification of prognostic factors or predictors of treatment response (5, 6).

Further complicating drug design, the activation of the apoptotic machinery, particularly the intrinsic or mitochondrial pathway, is defective in aggressive melanoma cells (5, 7). For example, the activation of p53, a main modulators of this pathway, can be compromised by upregulation of negative regulators (e.g. HDM-2)

(8) or by defective positive effectors (e.g. 14-3-3 or p14^{ARF}) (9, 10). Moreover, multiple anti-apoptotic members of the Bcl-2 family (primarily Bcl-x_L and Mcl-1) can act downstream of p53 to prevent the release from the mitochondria of Cytochrome *c*, Smac, AIF and other death inducers (5, 7). Additionally, inhibition of caspases can result from the increased expression of several members of the IAP (inhibitors of apoptosis proteins) family (11) and/or by downregulation of APAF-1, a cofactor of caspase-9 (12, 13). Overexpression of proteins such as survivin, that act at the interface between cell cycle progression and death, can also contribute to the aggressive phenotype of melanoma cells (7).

It is conceivable that key determinants of melanoma cell survival are acquired in a progressive and independent manner at different stages of tumor development. However, multiple alterations affecting the core of the apoptotic machinery rely on simultaneous transcriptional or post-translational events (affecting for example members of the Bcl-2 and IAP families) (5, 7). Therefore, it is possible that at least some antiapoptotic events are collectively regulated. The identification of such master regulator(s) could provide an ideal target for therapeutic intervention. In this context, the RAS/BRAF/MEK/ERK (MAPK) pathway is raising high expectations for the rational design of more effective anti-melanoma therapies (14-16). This pathway is invariably activated in early, intermediate and late stage melanomas (see Ref (17) for review), and dysregulated MAPK signaling contributes to the resistance of melanoma cells to a variety of chemotherapeutic agents (15, 18, 19). However, the precise contribution of downstream targets of ERK to melanoma cell survival is not well understood.

In a variety of tumor cell types, ERK can block apoptosis by favoring the transcription and activation of anti-apoptotic Bcl-2 proteins (Bcl-2, Bcl-x_L and Mcl-1), or by inhibiting pro-apoptotic factors such as Bim_{EL} or Bad (20-22). BRAF and ERK have also been reported to interfere with events acting downstream of the mitochondria, ultimately preventing the activation of caspase-9 and the execution of cell death (19, 23). However, while BRAF, MEK or ERK inhibitors can efficiently block melanoma cell proliferation (14, 15, 24), the killing activity of these compounds may be limited to selective groups of melanoma cells (25-27). Thus, the inhibition of MEK may be ineffective as a death inducer in melanoma cells lacking BRAF mutations (which constitute the majority of acral or mucosal melanomas and to more than 30% of cutaneous melanomas) (4). Moreover, melanoma clinical trials with farnesyltransferase inhibitors (to block RAS signaling), sorafenib (which inhibits CRAF and BRAF) or the MEK inhibitor PD-0325901 have demonstrated only modest clinical impact as single agents (see Ref (28) for review). Therefore, identifying new compounds that can bypass the resistance to MAPK inhibition can have a major impact in melanoma therapy.

In order to investigate the interplay between the MAPK pathway and the apoptotic machinery of melanoma cells, here we used lentiviral-driven short interfering RNAs (shRNA) to generate isogenic lines with specific defects in the apoptotic machinery. This strategy allowed for the identification of Mcl-1, Bcl-x_L and Bcl-2 as main mediators of the resistance to MEK inhibition. Since no synthetic inhibitor of Mcl-1 has been described, we used a computational approach to generate TW-37, the first rationally designed BH3 mimetic able to block Mcl-1, Bcl-x_L and

Bcl-2. TW-37 and MEK inhibition synergistically killed aggressive melanoma cell lines, with minimal secondary toxicity for normal skin cells (melanocytes, keratinocytes and fibroblasts). We present a comprehensive characterization of the molecular basis underlying the synergistic interaction between TW-37 and inactive MEK/ERK. Our studies revealed an unexpected tumor-cell selective role of the MAPK pathway upstream of the mitochondria, controlling ROS production and the activation of proapoptotic functions of p53. Our findings demonstrate the power of RNA interference and rational pharmacologic approaches to overcome melanoma chemoresistance.

Materials and Methods

Cell culture.

The non-metastatic WM-1366 cell line and the metastatic melanoma lines Malme-3M, UACC-62, G361, UACC-257 and the SK-Mel series (SK-Mel-19, -28, -29, -94, -103, -147, -173) were cultured in Dulbecco's modified Eagles's medium (DMEM) (Life Technologies, Rockville, MD) supplemented with 10% fetal bovine serum (Nova-Tech, Inc., Grand Island, NY). Human melanocytes were isolated from human neonatal foreskins as described (29) and maintained in Medium 254 supplemented with 10 nM TPA and melanocyte growth factors (Cascade Biologics, Portland, OR). Melanocytes were also incubated in DMEM-10% fetal bovine serum for direct comparison to melanoma cells. Keratinocytes and fibroblasts were also freshly isolated from foreskins. Keratinocytes were maintained in media 154 supplemented with keratinocyte growth factors (Cascade Biologics). Fibroblasts were

grown in DMEM supplemented with 10% fetal bovine serum. Specific details regarding the sequencing of *BRAF* and *NRAS* is indicated in the Supplementary Information section.

Reagents.

The MEK inhibitor 4-diamino-2,3-dicyano-1,4-bis(2-aminophenylthio)butadiene (U0126) was purchased from Calbiochem (La Jolla, CA). The MEK inhibitor CI-1040 was from Pfizer (Ann Arbor, MI), and doxorubicin hydrochloride (adriamycin) was from Fisher Scientific (Fair Lawn, NJ). The cell permeable pan-caspase inhibitor zVAD-FMK (Z-Val-Asp(OMe)-FMK) was from MP Biomedicals (Aurora, OH). The antioxidant 4,5-dihydroxyl-1,3-benzenedisulfonic acid disodium salt monohydrate (Tiron) and (+)-6-hydroxy-2,5,7,8-tetramethylchromane-2-carboxylic acid (Trolox) from Sigma-Aldrich (St. Louis, MO). The ROS indicator 5-(and -6)-chloromethyl-2', 7'-dichlorohydrofluorescein diacetate, acetyl ester (CM-H₂DCFDA) was purchased from Molecular Probes (Eugene, OR).

Design and binding assays for TW-37.

The detailed design and synthesis of TW-37 have been described elsewhere (G. W., Z. N-C., C. Yang, R. Wang, G. Tang, J. Gao, S. Shangary, S. Qiu, W. Gao, J. Meagher, J. Stuckey, K. Krajewski, S. Jiang, P. Roller, H.O. Abaan, Y. Tomita. S.W., in press). Binding affinities of TW-37 and TW-37i to purified Bcl-2, Bcl-x_L and Mcl-1 were determined by competitive fluorescence-polarization-based binding assays. In short, a Bid BH3-containing peptide (residues 79-99) was labeled at the N-terminus with 6-carboxyfluorescein succinimidyl ester (FAM). 1-2.5 nM FAM-Bid peptide were preincubated with 40 nM Bcl-2, 30 nM Bcl-x_L or 5 nM Mcl-1 in assay buffer

(100 mM potassium phosphate pH 7.5; 100 μ g/ml bovine gamma globulin; 0.02% sodium azide). Polarization values in milipolarization units (mP) were measured in Dynex 96-well, black, round-bottom plates (Fisher Scientific) in the absence or in the presence of increasing concentrations of TW-37 (excitation wavelength=485 nm and emission wavelength=530 nm) using a Ultra plate reader (Tecan U.S. Inc., Research Triangle Park, NC). Purified protein or fluorescent probes were also included as reference controls. K_i values were calculated with GraphPad Prizm 4 software (GraphPad Software, San Diego, CA) using previously described equations (http://sw16.im.med.umich.edu/software/calc_ki/) (30).

Drug treatments and cell viability.

Cell viability assays in response to drug treatments were performed after seeding human melanocytes or melanoma cells at least 18 h prior to drug treatment. Drug assays routinely used the small molecule inhibitor TW-37 at a final concentration of 5 μ M and the MEK inhibitor U0126 at a final concentration of 10 μ M. Drug combination assays included a pre-treatment step with TW-37 for 12 h prior to the addition of U0126. For simplicity, vehicle control treated cells are indicated as “non treated” (NT). Time dependent studies were considered to begin upon the addition of U0126 (t=0 h). Controls for DNA damage included adriamycin at a final concentration of 0.5 μ g/ml. Cell death resulting from drug treatments with single agents, combination agents or vehicle alone was estimated by MTT (3-(4,5-dimethylthiazol-2-yl)-2,5-diphenyltetrazolium bromide) or standard Trypan Blue

exclusion assays as previously described (12, 31, 32). Experiments were performed in triplicate and data are presented as the average \pm SEM.

Cell cycle analyses.

Cells were harvested following appropriate drug treatments and fixed with 1 mL of ice-cold 70% ethanol. Cells were washed twice with PBS, followed by incubation in a labeling solution of 50 μ g/mL propidium iodide (PI) (Sigma Chemical, St. Louis, MO), in PBS containing 0.2% Triton and 10 μ g/mL RNase A. PI fluorescence was analyzed using a FACS Calibur flow cytometer and cell cycle distribution was determined using Cell Quest software (Becton Dickinson, San Jose, CA).

Protein immunoblots.

Adherent and non-adherent cells were collected by either scraping or trypsinization and pelleted by centrifugation at 800g for 3 min. Total cell lysates were obtained by Laemmli extraction (31, 32). Protein samples were separated on 12% or 4-20% gradient SDS polyacrylamide gels and transferred to Immobilon-P membranes (Millipore, Bedford, MA). Alternatively, mitochondrial and cytosolic cell fractions were prepared by digitonin extraction as previously described (32). Sixty μ g of the cytosolic fractions were used for immunoblot analysis of the release of proapoptotic proteins from the mitochondria. α -tubulin or β -actin were included as loading controls.

Stable short hairpin interfering RNA constructs (shRNA).

Published references were used as a guide to generate short 19 bp hairpins for RNA interference: Bcl-2, nt 500-518, GenBank M13995 (33); Bcl-x_L, nt 714-732, GenBank BC019307 (34); p53, nt 611-629, GenBank NM000546 (35); BAK, nt 535-553, GenBank NM001188 (36). Oligos against Mcl-1 (nt 2343-2361, GenBank NM021960), BAX (nt 239-257, GenBank NM138761), were generated using the OligoRetriever database (http://katahdin.cshl.org:9331/RNAi_web/scripts/main2.pl). BLAST search was performed to ensure at least 4-nt differences with annotated human genes. The corresponding oligonucleotides were annealed and cloned under the control of the H1 promoter into a self-inactivating lentiviral vector (37). The vector was also designed to carry the GFP reporter gene under control of the human ubiquitin-C promoter to monitor infection efficiency. A scrambled shRNA construct was also designed to be used as a control. Lentiviral infections were performed essentially as described elsewhere (37) and the potency and specificity of each construct was determined by protein immunoblotting (see text). Primer sequences, cloning strategies, as well as transfection and infection strategies are available from the authors upon request.

Immunofluorescent visualization of activation-dependent conformational changes of BAX.

Cells of interest were seeded onto glass culture slides and treated with TW-37 (5 μ M) in the presence or absence of U0126 (10 μ M). Antioxidants were added as indicated. Cells were fixed with 4% formaldehyde at different time points after treatment, permeabilized with 0.2% Triton-X in PBS for 5 min and washed three

times with PBS. Following a 30 min blocking step in 1% BSA, the rabbit polyclonal Bax-NT antibody from Upstate Biotechnology (Lake Placid, NY) was used to visualize conformational changes in BAX following previously described protocols (38, 39). Melanoma cells rounded up and floated immediately after Cyt *c* release (not shown). To avoid for indirect effects on BAX conformation as byproducts of cell death, only adherent cells (corresponding to early apoptotic cells) were analyzed. The percent of cells with positive staining was estimated using vehicle-treated cells as a reference.

Detection of ROS production by fluorescent microscopy.

Melanoma cell lines and melanocytes were seeded onto glass culture slides (BD Biosciences, Bedford, MA) and treated with the indicated drugs. At various time points, media was aspirated and cells were loaded with 1 μ M CM-H₂DCFDA in PBS for 10 min at 37°C in the dark, followed by a PBS wash step essentially as previously reported (31). 0.03% H₂O₂ was used as a reference control for an active ROS inducer. DCF-dependent fluorescence was scored with ImageJ software and expressed with respect to untreated control cells.

Indirect measurement of oxidized proteins.

Following drug treatments both adherent and non-adherent cells were collected and subjected to Laemmli extraction. Oxidized proteins were visualized by derivatization of carbonyl groups with dinitrophenylhydrazine (DNPH) using the OxyBlot Oxidized Protein Detection Kit (Chemicon International, Temecula, CA) according to the manufacturer's instructions. Following SDS-PAGE separation and

standard Western blotting, the resulting DNP-hydrazone side chains were detected with a specific antibody to the DNP moiety of the protein.

Melanoma growth *in vivo* (Mouse xenographs).

Athymic NCr-nu/nu mice (NCI) were kept in pathogen-free conditions and used at 8-12 weeks of age. Animal care was provided in accordance with the procedures outlined in the Guide for the Care and Use of Laboratory Animals of the University of Michigan. To analyze localized melanoma growth *in vivo*, 0.5×10^6 GFP-expressing SK-Mel-147 melanoma cells were injected subcutaneously (s.c) in both rear flanks (n=12 tumors per experimental condition). Treatment was initiated on the third day following cell implantation (when tumors were palpable) and continued until day 20 with a one day resting period every 5 days. TW-37 was resuspended in 1:1 Tween 80:ethanol (diluted 10-fold in 0.9% saline prior to use) and administered daily at 40 mg/kg alternating intravenous or intraperitoneal injections. CI-1040 was resuspended in 8:1:1 H₂O:ethanol:Cremophor and administered by oral gavage twice per day at 75 mg/kg, as described (32). Control and single agent animal groups received vehicle treatments. Imaging of tumor cells *in vivo* was performed with an Illumatool TLS LT-9500 fluorescence light system (Lighttools Research, Encinitas, CA) and the emitted fluorescence from tumor cells was captured with a Hamamatsu Orca 100 CCD camera. Volume of the s.c xenografts was estimated as $V=L \times W^2/2$, where L and W stand for tumor length and width, respectively.

Statistics.

Statistical analyses of drug response in mouse xenograft models were performed using the SAS statistical software (SAS Institute, Inc. Cary, NC). The Tukey's HSD test was used for pairwise comparisons among groups, and the Dunnett test for individual comparisons to untreated controls. The type I error rate was set at 0.05.

Mutational status of BRAS and NRAS.

BRAF and *NRAS* mutations were identified by PCR amplification of genomic DNA followed by sequencing. Briefly, PCR products generated by standard methods were cleaned up by treatment with shrimp alkaline phosphatase (Roche Applied Sciences) and exonuclease I (Epicentre Technologies, Madison, WI), and sequenced with the BigDye Terminator sequencing protocol (Applied Biosystems, Foster City, CA). For *BRAF*, primers TCATAATGCTTGCTCTGATAGGA (forward) and GGCCAAAATTTAATCAGTGGA (reverse) were used for both PCR and sequencing. For *NRAS*, PCR was performed with forward primer AAGGGGGATTCCATTGCTTAG and reverse primer TGGGTAAAGATGATCCGACAAGTG, followed by sequencing using nested primers CCAAATGGAAGGTCACACTAGGG and AGTGAGAGACAGGATCAGGTCAGC. Sequences were assembled and examined using the Seqman component of DNASTar sequence analysis package (DNASTar, Madison, WI).

Primary antibodies.

Antibodies for Caspase-9 and Survivin were from Novus Biologicals (Littleton, CO); Caspase-3, Caspase-7, PUMA (Ab2), phospho-histone H2A.X (Ser 139), phospho-p53-Ser¹⁵, phospho-extracellular signal-regulated protein kinase (ERK) 1/2 (Thr2002/Tyr204) and total ERK1/2 from Cell Signaling Technology (Beverly, MA); Bim/BOD from Imgenex™ (San Diego, CA); BAX and BAK from Upstate Biotechnology (Lake Placid, NY); Cyt *c* (7H8.2C12) and Bcl-x_L (clone pAb) from BD Biosciences (Franklin Lakes, NJ); AIF (E-1) from Santa Cruz Biotechnology (Santa Cruz, CA); Bcl-2 from Dako Diagnostics (Glostrup, Denmark); Smac/DIABLO (222-237), Noxa and Caspase-8 (Ab-3) from Calbiochem (San Diego, CA); p53 (CM-1) from Novocastra Laboratories (Newcastle upon Tyne, UK); PUMA (Ab1) from eBioscience (San Diego, CA); and tubulin and β -actin (AC-74) from Sigma Chemical (St Louis, MO). The corresponding antibody signal was revealed with the ECL system from Amersham Biosciences (Amersham, Arlington Heights, IL).

Results

Identification of melanoma cell lines resistant to inhibition of the MAPK pathway.

It has been recently reported that NRAS and BRAF-expressing melanoma cells have a different sensitivity to inhibitors of the MAPK pathway (25). Thus, metastatic melanoma cells with NRAS mutations have an increased resistance to RAF and MEK inhibitors (25). To identify poorly responsive cells and address the molecular basis underlying the resistance to MAPK inhibition, a panel of 11

melanoma cell lines was sequenced for the most frequent mutational hotspots in the *NRAS* and *BRAF* genes (i.e. exons 3 and 15, respectively; see Figure 1A, B). The individual cell lines were subsequently compared in their response to the MEK inhibitor U0126 (40), which blocks ERK activation downstream of NRAS or BRAF (Figure 1C). U0126 was able to inhibit cell proliferation (Figure 1A) by a G1/S mediated cell cycle arrest in NRAS and BRAF mutated cells (Figure 1D). However, the killing activity of U0126 was even less efficient than expected. Thus, at concentrations required to maintain the viability of normal melanocytes, the NRAS-mutated cells and 3 out of 5 BRAF^{V600E}-expressing melanoma lines responded poorly to U0126 (Figure 1B). In fact, the overall killing activity by this MEK inhibitor was not significantly different from standard chemotherapeutic drugs such as Adriamycin (Figure 1B). Two of the most resistant lines (SK-Mel-103 and -147) were chosen as representative examples to identify survival mechanisms acting in the absence of ERK activation, and to test new compounds able to overcome melanoma chemoresistance.

Anti-apoptotic factors retained after ERK inhibition.

Despite the ability of U0126 to block ERK phosphorylation, it was possible that downstream apoptotic targets (e.g. Bim_{EL}, Bcl-x_L, Bcl-2 or Mcl-1) were not affected by treatment, and consistently, did not favor cell death. To address this possibility, protein extracts were prepared from melanoma cells at different points after incubation with U0126. As shown in Figure 1E, although Bim_{EL} was induced by U0126, Bcl-2 and Bcl-x_L were still detectable at late times after treatment and Mcl-1 levels did not significantly change (Figure 1E). With respect to other apoptotic

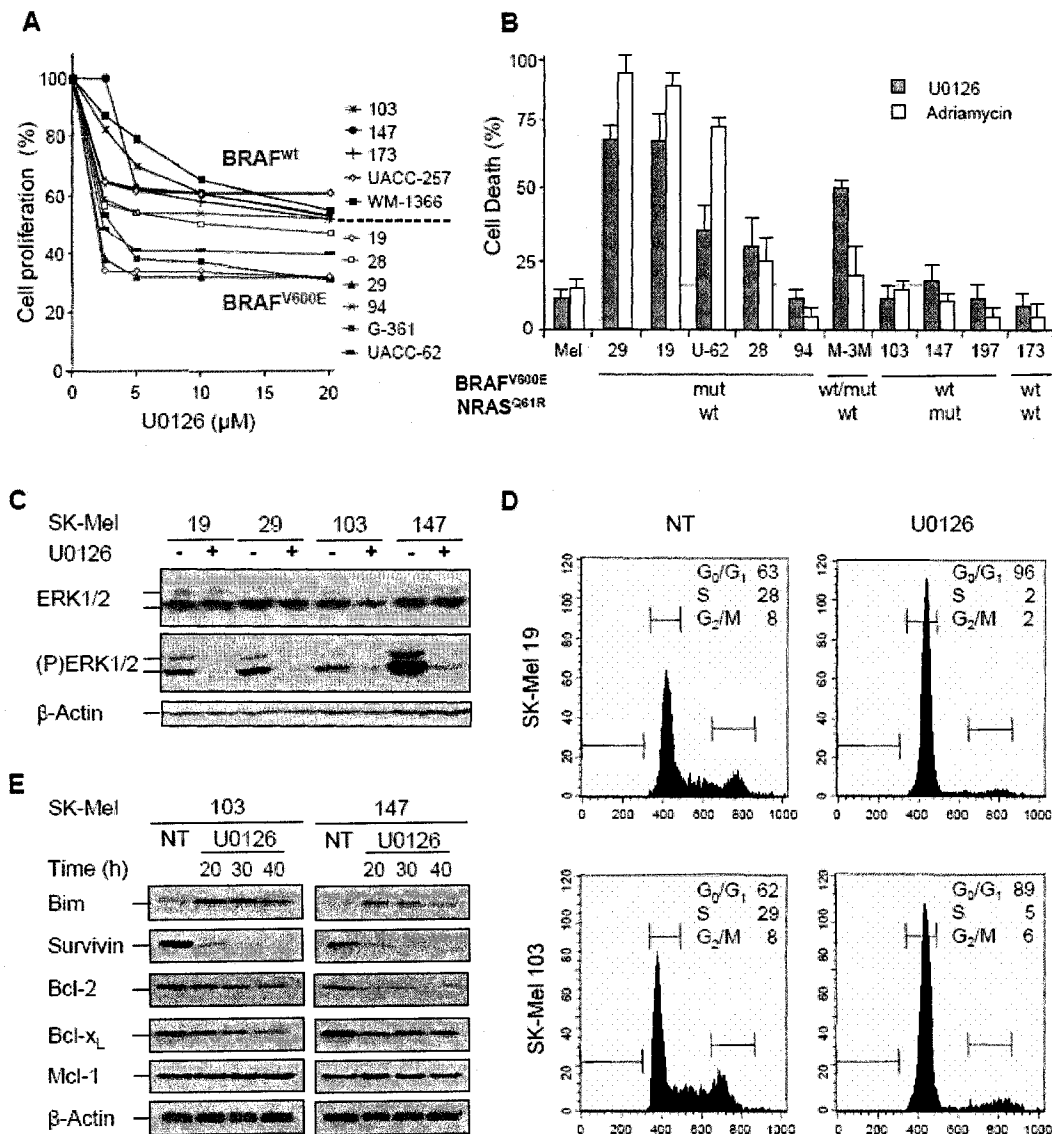


Figure 1. Cytostatic effect of the MEK inhibitor U0126 on metastatic melanoma lines. (A) Dose-response curves of the indicated melanoma cell lines estimated by MTT assay 48h after treatment. Cell code is indicated in materials and methods. Cells were grouped according to wild type (blue) or mutant V600E (red) BRAF status. (B) Cytotoxicity of U0126 (10 μM) or adriamycin (0.5 $\mu\text{g}/\text{mL}$) on normal melanocytes (Mel) and a panel of metastatic melanoma lines of either wild type (wt) or mutant (mut) BRAF and NRAS. U-62 and M-3M stand for lines UACC-62 and Malmme-3M, respectively. The rest of the cell lines correspond to SK-Mel-series. Cell death was assayed by Trypan Blue exclusion 48 h after treatment. (C) Visualization by protein immunoblotting of the inhibitory effect of U0126 (10 μM , 24 h) on phosphorylated ERK1/2 (p-ERK1/2). Total ERK1/2 and β -actin are shown as controls for protein loading. (D) Cell cycle distribution determined by flow cytometry of control (no treatment, NT) and U0126 (10 μM) treated melanoma cells. Shown are the percentage of viable cells at the G₀/G₁, S and G₂/M phases. (E) Impact of U0126 (10 μM) on apoptotic modulators as a function of time. Shown are representative SDS-PAGE gels.

Stable RNA interference for target validation.

To determine the relative contribution of Mcl-1, Bcl-2 and Bcl-x_L to U0126-mediated resistance, a lentiviral-mediated approach was used to stably express specific short interfering RNAs (shRNA) in melanoma cells. To allow for imaging of infected cells, the lentivirus used (KH1-LV) co-expressed eGFP under an independent UbC promoter (Figure 2A, B). Constructs able to promote a reduction of more than 80% of the intended protein expression without affecting the level of other Bcl-2 family members are shown in Figure 2C.

Acute inactivation of Bcl-2, Bcl-x_L or Mcl-1 by shRNA, significantly enhanced the response of melanoma cells to U0126 (Figure 3A). Interestingly, the most effective cytotoxic effect was found after inactivating Mcl-1 (Figure 3A), consistent with this protein remaining highly expressed in melanoma cells after treatment with U0126 (Figure 1E).

Altogether, these results indicate that despite the multiple genetic defects that melanoma cells harbor, the resistance to MEK/ERK inhibition is primarily dependent on Mcl-1, and to a lesser extent Bcl-x_L and Bcl-2.

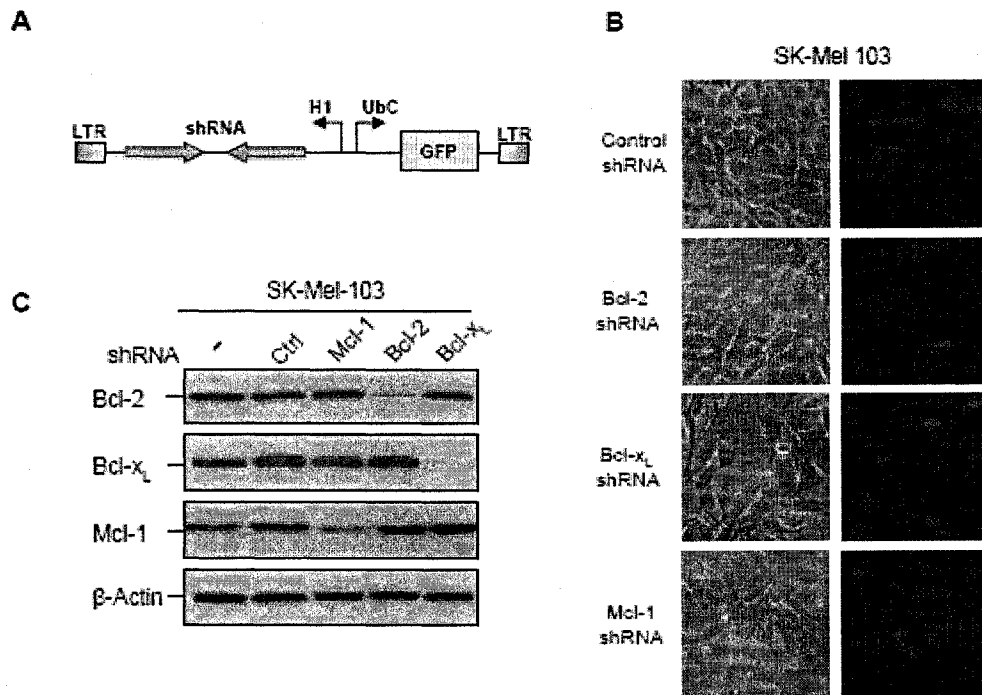


Figure 2. Tumor-cell selectivity of TW-37/U0126. (A) Long-term assays of the impact of acute TW-37/U0126 on normal melanocytes and SK-Mel 103. Cells were left untreated or treated with 5 μ M TW-57 and 10 μ M U0126 for 40 h. Drug was removed (red arrow) and cell number was estimated at the indicated time points and plotted with respect to the initial amount of seeded cells. (B) Comparative analysis of the sensitivity of normal skin melanocytes, keratinocytes and fibroblasts with respect to a representative metastatic melanoma cell line (SK-Mel-103). The three normal cell populations maintained their viability under conditions that promote the killing of tumor cells. Note that cell killing was not substantially affected by the growth media MGM, KGM and DMEM stand for melanocyte growth medium, keratinocyte growth medium (Epilife) and Dulbecco's Modified Eagle medium, respectively. See Materials and Methods for additional information about culture conditions of normal skin cells and malignant melanoma cells.

Pharmacological enhancement of the response of melanoma cells to U0126: Design and validation of new BH3 mimetics.

Small molecule inhibitors that interfere with anti-apoptotic members of the Bcl-2 family are emerging as a powerful anticancer strategy (43). Nevertheless, published synthetic BH3 mimetics either do not recognize or bind poorly to Mcl-1 (44-46). Therefore, we utilized a structure-based methodology to generate novel non-peptide small molecules able to bind Mcl-1 as well as Bcl-2 and Bcl-x_L (to improve efficacy). Our approach was based on the reported ability of the BH3 domain of the pro-apoptotic Bim protein to bind in a promiscuous manner to Mcl-1, Bcl-x_L and Bcl-2 (43, 47). Using the structure of Bim for computational docking and molecular dynamics a series of putative BH3 mimetics were designed, of which the compound TW-37 (Figure 3B) was chosen for displaying a high cell permeability (not shown).

Fluorescence polarization-based competitive binding assays were performed to address the ability of TW-37 to displace short peptides containing the BH3 domain of Bim or Bid from Bcl-2, Bcl-x_L or Mcl-1. Representative examples of binding curves are shown in Figure 3B. TW-37 was found to bind Mcl-1, Bcl-x_L and Bcl-2 with K_i values of 260 nM, 1100 nM, and 120 nM, respectively (Figure 3C and results not shown). Based upon computer modeling of X-ray structures of BH3-binding domains, the three hydroxyl groups in TW-37 were expected to play a crucial role in its interaction with BH3 domains. Consequently, to control for unspecific effects of the TW-37 backbone, a derivative (TW-37i), was generated in which the three hydroxyl groups were methylated (Figure 3B). As shown in Figure 3C, the K_i of TW-

37i for Bcl-2 was two orders of magnitude higher than TW-37 (Figure 3B).

Therefore, TW-37i was used as an inactive control.

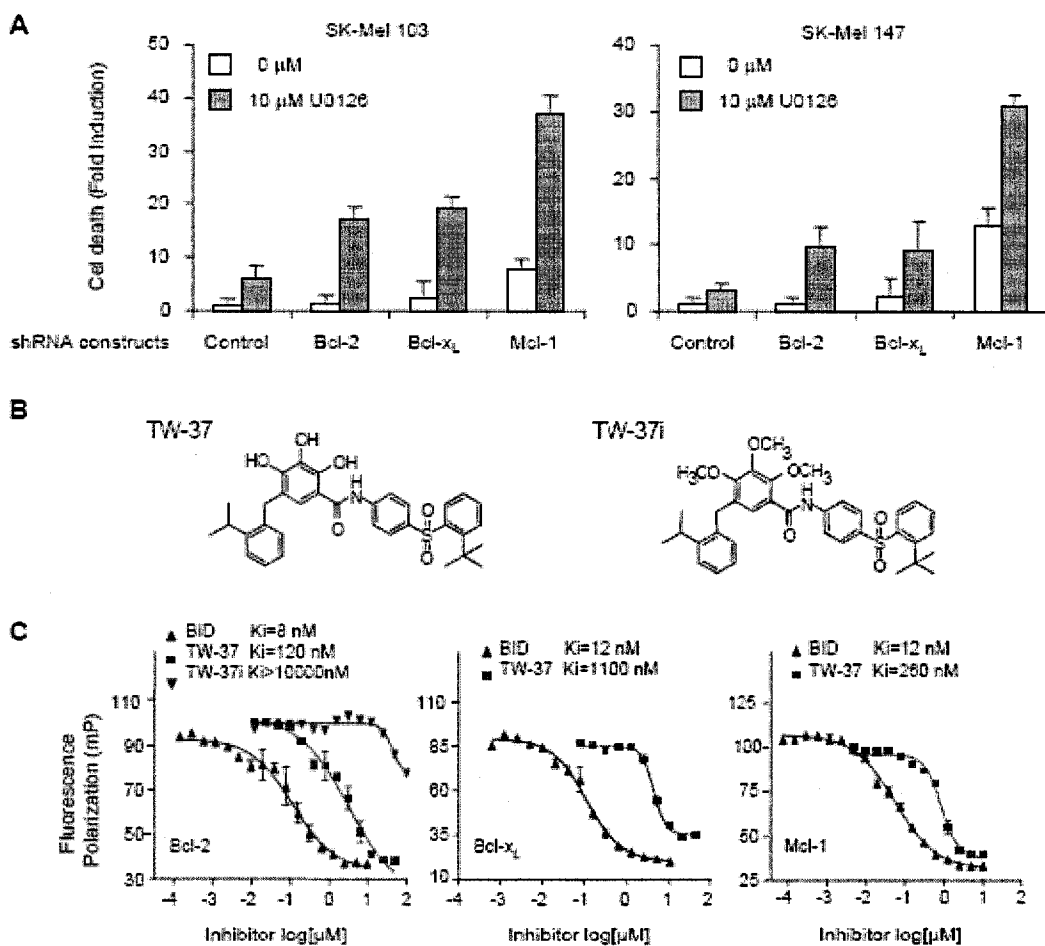


Figure 3. TW-37 as a novel class of BH3 mimetics. Tumor-cell selective enhancement of the cytotoxic effect of U0126. (A) Molecular structure of the small molecule inhibitor TW-37 and the inactive TW-37i derivative. (B) Binding kinetics of TW-37 to the anti-apoptotic Bcl-2, Bcl-x_L and Mcl-1 proteins estimated by fluorescence polarization-based spectroscopy (see Materials and Methods). (C) Isobolograms for a graphical visualization of the synergistic effect of the TW-37/U0126 combination. Values on the axes represent the EC₅₀ (upper panel) or EC₈₀ (lower panel) obtained from indicated drug administered as a single agent and tested in MTT assays (see Materials and Methods). Note that the data points corresponding to combination treatments fall below the line of additivity (broken line), indicating a supra-additive (synergistic) interaction.

Selective and synergistic killing of melanoma cells by U0126 and TW-37.

Aggressive melanoma lines such as SK-Mel-103 and SK-Mel-147 could be killed with TW-37 at concentrations of 10 μM (not shown). Interestingly, lower drug concentrations, although inducing minimal toxicity, were found to be highly synergistic with U0126 (see isobolograms at EC_{50} and EC_{80} in Figure 3D, and representative microphotographs of treated cells in Figure 3E). Confirming the BH3-binding features of TW-37, the inactive TW-37i was unable to synergize with U0126 (Figure 3E).

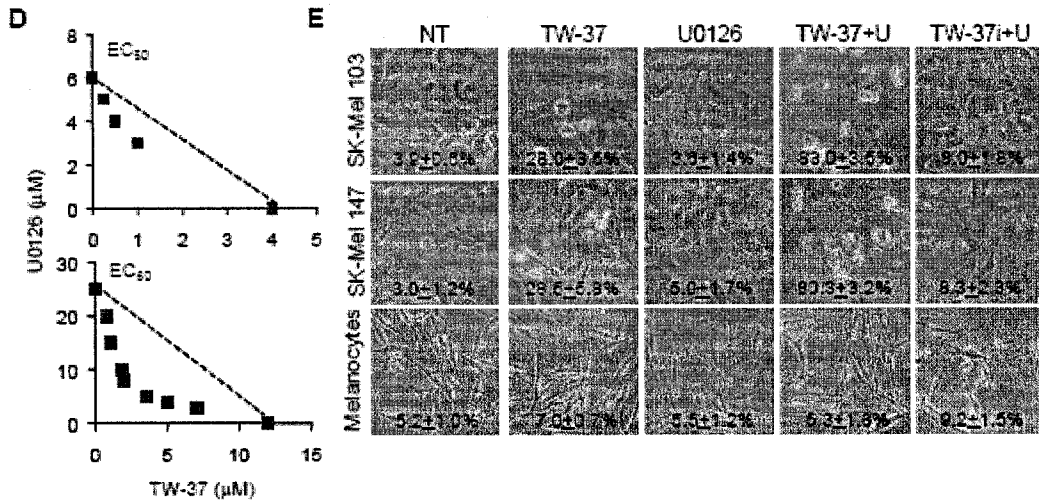


Figure 3 continued. TW-37 as a novel class of BH3 mimetics. (D) Cytotoxicity of TW-37 or the inactive TW-37i variant (5 μM each) in the absence or presence of U0126 (10 μM). Shown are microphotographs of the indicated melanoma cell lines or normal control melanocytes 40 h after treatment. Note the preferential toxicity of TW-37/U0126 towards the tumor cells (see Figure 2 for long-term effects of the different treatments). (E) Genetic inactivation of Bcl-2, Bcl-x_L or Mcl-1 by RNA interference synergizes with U0126. Shown are the death responses of the indicated melanoma cell populations in the absence (white bars) or presence (grey bars) of U0126 (10 μM , 48 h). Cell death was assayed in triplicate by Trypan Blue exclusion. Shown is the extent of cell death relative to shRNA scramble control-infected cells.

Notably, the U0126/TW-37 combination was well tolerated by melanocytes in after short-term treatments (Figure 3E) and long-term clonogenic assays (Figure 4A). Normal skin fibroblasts and keratinocytes were also resistant to U0126/TW-37, further illustrating the selectivity of this drug combination towards tumor cells (Figure 4B).

Importantly, in melanoma cells, the combination of TW-37/U0126 induced hallmarks of apoptosis, including a synergistic processing of regulatory and effector caspases and (Figure 5A) and classical chromatin condensation and formation of apoptotic bodies (Figure 6). It should be noted, however, that an important fraction of cells could still die in the presence of the pan-caspase inhibitor zVAD-fmk (Figure 5B). This feature of the TW-37/U0126 combination may be advantageous to kill melanoma cells even under conditions of defective caspase activation -which has been proposed as a main contributor to the resistance to standard chemotherapeutic agents (5, 7).

Mechanistic analyses of the TW-37/U0126 combination. Release of pro-apoptotic factors from the mitochondria.

The enhanced activity of TW-37 in the presence of U0126 prompted us to address the interplay between BH3-containing proteins and the MAPK pathway. An attractive feature of BH3 mimetics as anti-cancer agents is their potential ability to promote cell death by favoring the release of Cytochrome c (Cyt c) and other mitochondrial death inducers by directly activating BAX and BAK (47).

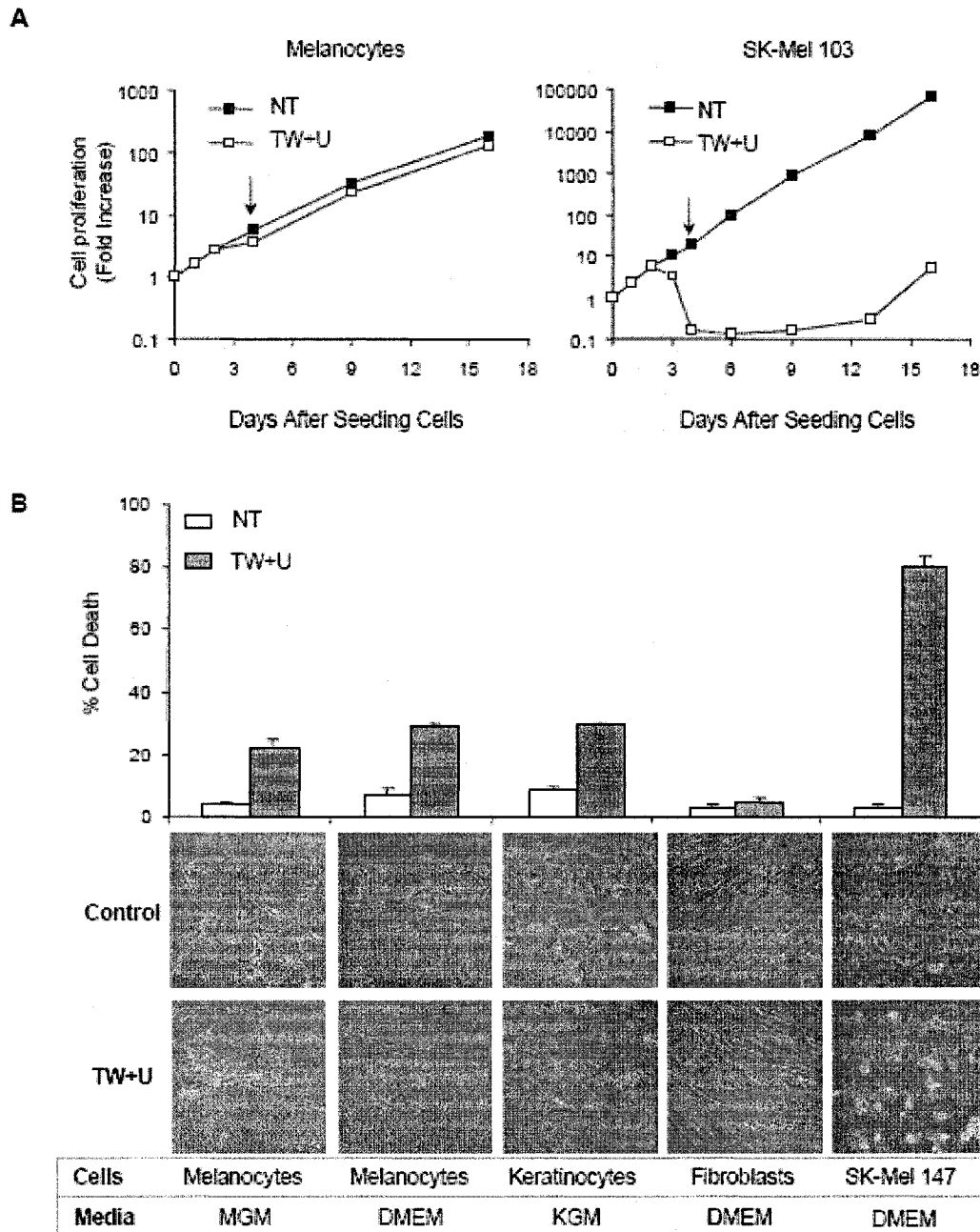


Figure 4. Synergistic caspase activation by the TW-37/U0126 combination. (A) Comparative ability of TW-37 (5 μ M) or U0126 (10 μ M) as single agents in combination (TW+U) to process regulatory and effector caspases. Total cell lysates were collected at the indicated times post-treatment and separated in a 12% SDS-PAGE for subsequent staining with specific antibodies. (B) Reduction of cell death by the pan-caspase inhibitor zVAD-fmk at 20 μ M, a dose we have previously shown that it effectively blocks caspase processing and activation by standard chemotherapeutic agents (1). Data correspond to the mean \pm SEM of three independent experiments.

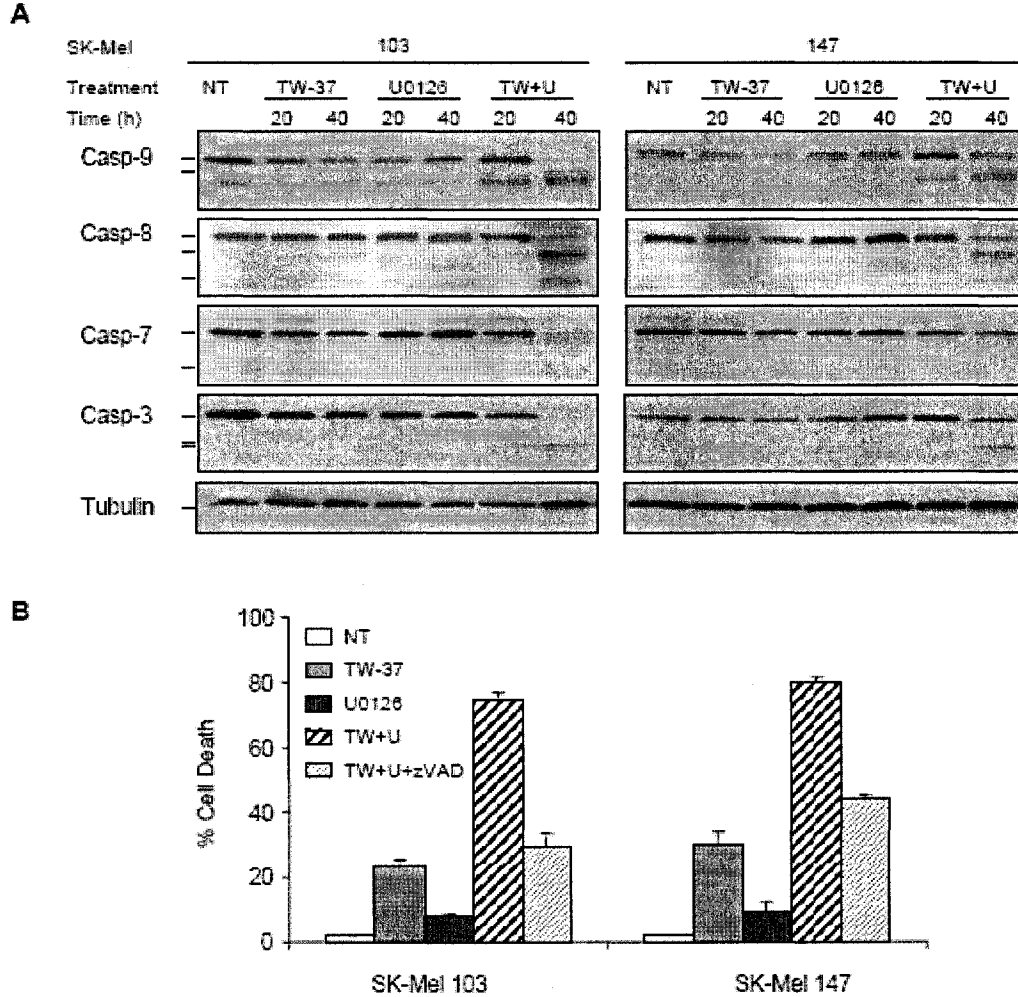


Figure 5. Genetic inactivation of anti-apoptotic Bcl-2 proteins by lentiviral-mediated RNA interference. (A) Brief schematic of the lentiviral construct used in this study to stably transduce short hairpin RNA (shRNA) in melanocytes and melanoma cells. In addition to the H1 promoter to drive the shRNA, the lentiviral vectors coexpress the GFP gene under control of the constitutively active UbC promoter to allow for visualization of infection efficiency. (B) High infection efficiency with lentiviral constructs expressing scrambled shRNA, or shRNA against Bcl-2, Bcl-x_L or Mcl-1. Shown are representative microphotographs of line SK-Mel-103 acquired by brightfield or fluorescence imaging (left and right, respectively). (C) Specific downregulation of Bcl-2, Bcl-x_L or Mcl-1 following infection with the corresponding shRNA lentiviruses. Total cell extracts were processed for protein immunoblotting 3 days after lentiviral infection.

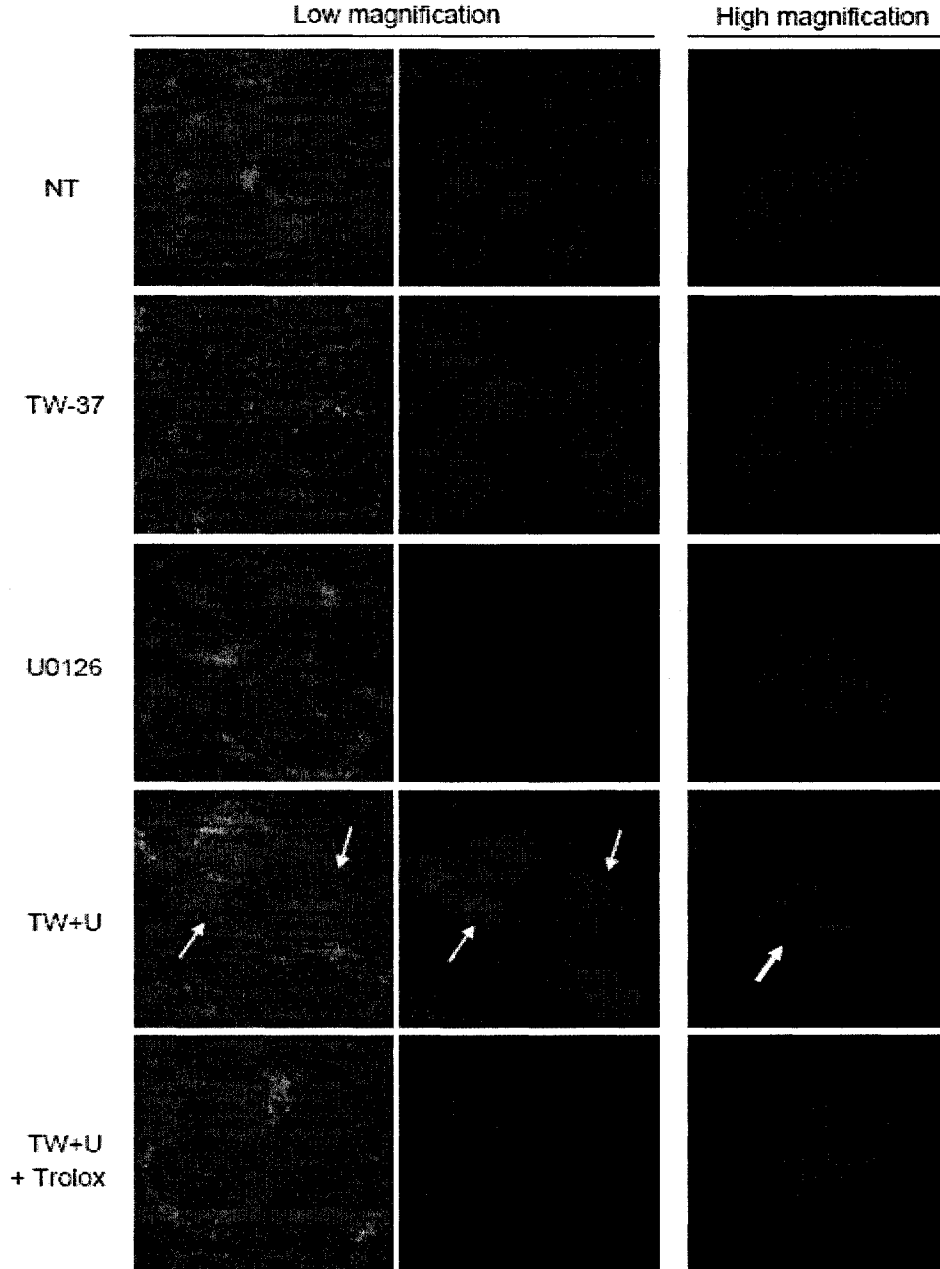


Figure 6. Inhibitory effect of antioxidants on BAX activation. Conformational changes of BAX determined by immunostaining with the BAX-NT antibody in the presence or absence of TW-37, U0126 or the TW-37+U0126 combination. The antioxidants Trolox (20 μ M, red line) or Tiron (1 mM, blue line) significantly reduced the amount of cells with active BAX expression. Data corresponds to percentage of adherent cells (early apoptotic) with positive staining. Note that these results underestimate the difference between cells treated in the absence or the presence of antioxidants. Floating cells (which constitute the largest fraction of cells at later time points after incubation with TW-37 and U0126; see Figure 8B) collapse and are not scored to avoid for secondary events that could affect indirectly BAX conformation and localization after cell death.

the mitochondria, shifting the detection of cytosolic Cyt *c* by immunoblotting from 40 h to as early as 6 h post-treatment (Figure 7A, see also Figure 7B and Figure 6 for representative analysis of the visualization of Cyt *c* release by immunofluorescence). Subsequent activation of BAX/BAK was important for TW-26/U0126 mediated cell death, since downmodulation of these apoptotic factors favored melanoma cell survival. Thus, shRNA-expressing lentiviruses were generated to block BAX or BAK expression by RNA interference (Figure 7C,D). shRNA of BAX reduced by 50% the killing activity of TW-37/U0126 in line SK-Mel-103, (Figure 7E, left panel). SK-Mel-147 required BAX and BAK for the induction of cell death, since shRNA against each of these proteins reduced TW-37/U0126-driven cell killing (Figure 7E, right panel).

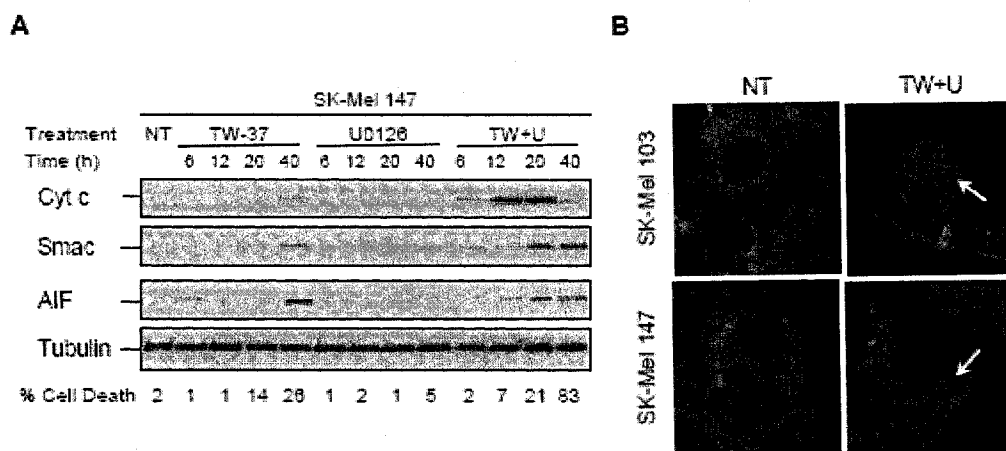


Figure 7. Classical BH3-mimetic features of TW-37. BAX/BAK-dependent activation of the mitochondrial apoptotic pathway. (A) Time course illustrating the release of mitochondrial apoptotic effectors Cyt *c*, Smac and AIF in response to the indicated treatments. Shown are representative SDS-PAGE gels of cytosolic extracts isolated by digitonin fractionation. (B) Visualization of Cyt *c* release from the mitochondria (white arrows) by immunofluorescence.

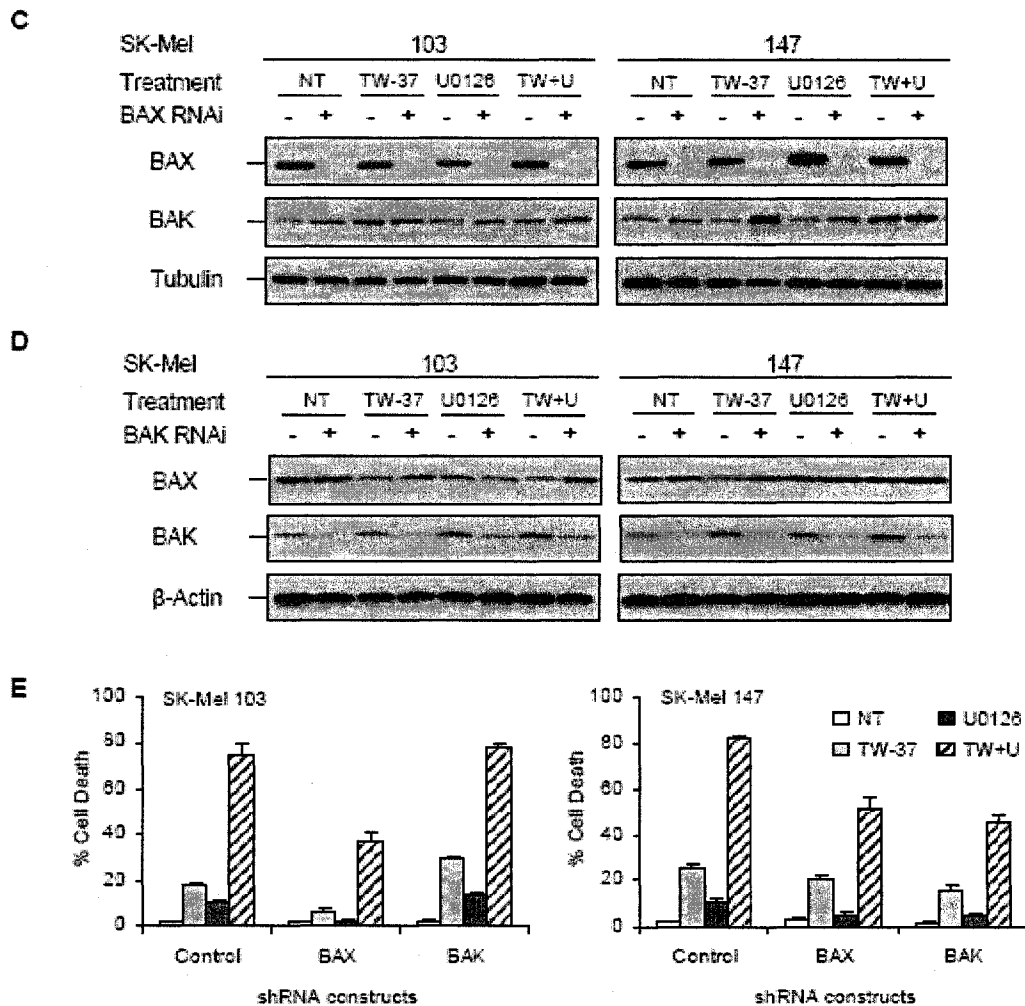


Figure 7 continued. Classical BH3-mimetic features of TW-37. BAX/BAK-dependent activation of the mitochondrial apoptotic pathway. (C-D) Requirement of BAX (C) and BAK (D) for TW-37/U0126-driven melanoma cell death. Shown are immunoblots illustrating the efficacy and selectivity of the shRNA-lentiviral approach used (see Materials and Methods for additional information of the sequences targeted). (E) The amount of cell death (%) was determined by Trypan Blue exclusion assay 40 h post drug treatment. Data correspond to the mean \pm SEM of three independent experiments.

Impact of MEK/ERK inhibition upstream of BAX.

BRAF and ERK have been reported to act downstream of Cyt c or Smac to control caspase activation (19, 23). However, the synergistic effect of U0126 on Cyt c

release suggest an additional role of the MAPK upstream of the mitochondria, controlling BAX/BAK activation. To this end, we used antibodies that can specifically recognize conformational changes associated to pro-apoptotic activation of BAX by immunofluorescence staining (38, 39). We specifically focused on BAX as it contributed to the death of SK-Mel-103 and -147. Interestingly, at the dose and treatment regimen in this study, no significant activation of BAX by TW37 was detected unless in the presence U0126 (Figure 8). Thus, the TW-37/U0126 increased by 7 to 10-fold the percentage expressing conformationally active BAX in SK-Mel-147 and SK-Mel-103, respectively. These results suggest a new role of MEK/ERK in the control of BAX and the mitochondrial pathway in melanoma cells.

Reactive oxygen species (ROS) modulating the cytotoxic effect of TW-37/U0126.

Dysregulation of cellular redox mechanisms can be potent activators of caspase-dependent and independent forms of cell death (48). Therefore, we tested the possibility that MEK inhibition was cooperating with TW-37 in allowing for ROS accumulation. Towards this end, drug treatments were performed in the presence potent antioxidants. Two structurally unrelated antioxidant were used: Tiron, a spin trap, and Trolox, a water-soluble Vitamin E analog (31). When added simultaneously with TW-37 both of these antioxidants blocked TW-37/U0126 drug synergy, preventing BAX activation (Figure 8A) and significantly reducing the kinetics and extent of cell death by TW-37/U0126 (Figure 8B and results not shown). Note that the inhibition of cell death by Tiron or Trolox was stronger than the blockage of caspases by zVAD (Figure 4) or BAX and BAK, suggesting a key role of ROS in TW-37/U0126 mediated cell death.

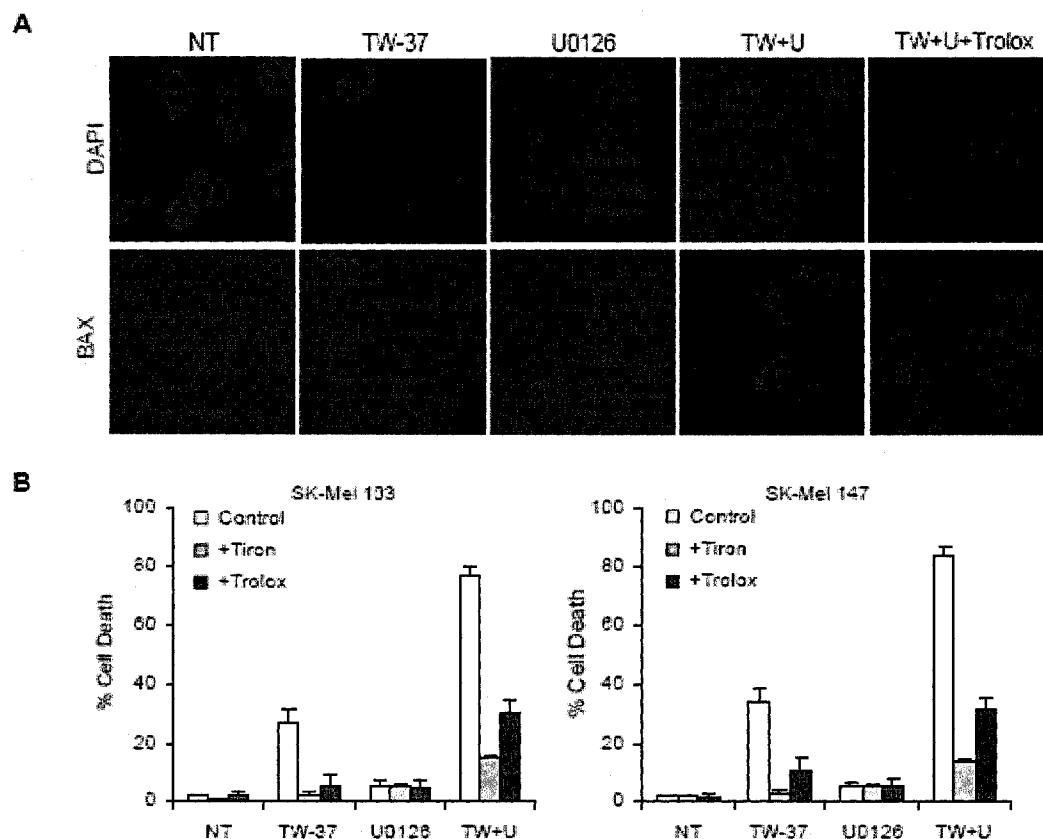


Figure 8. ROS production modulates the cytotoxic effect of TW-37/U0126. (A) Immunofluorescent staining with NT-Bax antibody (red fluorescence) as described in Materials and Methods to visualize conformational change (activation) after treatment. Cells were left untreated (NT), or were incubated in the presence of TW-37 (5 μ M) or U0126 (10 μ M), as single agents or in combination (TW+U). The antioxidant Trolox (200 μ M) was added simultaneously with TW-37. Nuclear staining is shown by DAPI. (B) Effect of antioxidants on cell death induced by TW-37 +/- U0126 in the presence or absence of Tiron (1 mM) or Trolox (200 μ M). Cell death (%) was determined by Trypan Blue exclusion 40 h after treatment.

The protective effect of Tiron or Trolox was compromised if they were added 12 h after treatment (not shown), suggesting an early contribution of ROS to melanoma cell death by TW-37/U0126. Production of ROS by TW-37 and further enhancement by U0126 was visualized in cultured cells with the oxidation-sensitive fluorescent probe CMH₂DCF-DA (see below in Figure 10B). These data are intriguing because they implicate a MAPK-dependent control of ROS production that

cooperates with anti-apoptotic Bcl-2 family proteins in the maintenance of melanoma cell viability.

ROS-dependent activation of p53 by TW-37/U0126.

ROS are notorious for the pleiotropic effects that can elicit in mammalian cells. To identify direct mediators of ROS-driven cell death among a plethora of byproducts of changes in cellular redox, we focused on pro-apoptotic factors whose expression is induced at early time points after TW37/U0126 treatment, but can be blocked by antioxidants. A protein that followed this expression pattern was p53. As shown in Figure 8C and 8D, TW-37 was able to induce sustained expression of p53 in SK-Mel-103 and -147. Interestingly, the addition of U-0126 to TW-37 enhanced 12 to 15-fold by the addition of U0126 (Figure 8C, D). Notably, this induction of p53 was reduced by 80% in the presence of Trolox (Figure 8C, D). Therefore, our results are consistent with the BH3 mimetic TW-37 and the MEK inhibitor U0126 activating p53 via ROS production.

To confirm the requirement of p53 for TW-37/U0126 mediated melanoma cell death, p53 protein expression was downmodulated by highly effective lentiviral vectors (Figure 9A). Of note, p53 knockdown provided a protection from melanoma cell death by about 75% (Figure 9B), and significantly reduced the activation and translocation of BAX by TW-37/U0126 (Figure 9C). This is in contrast to standard

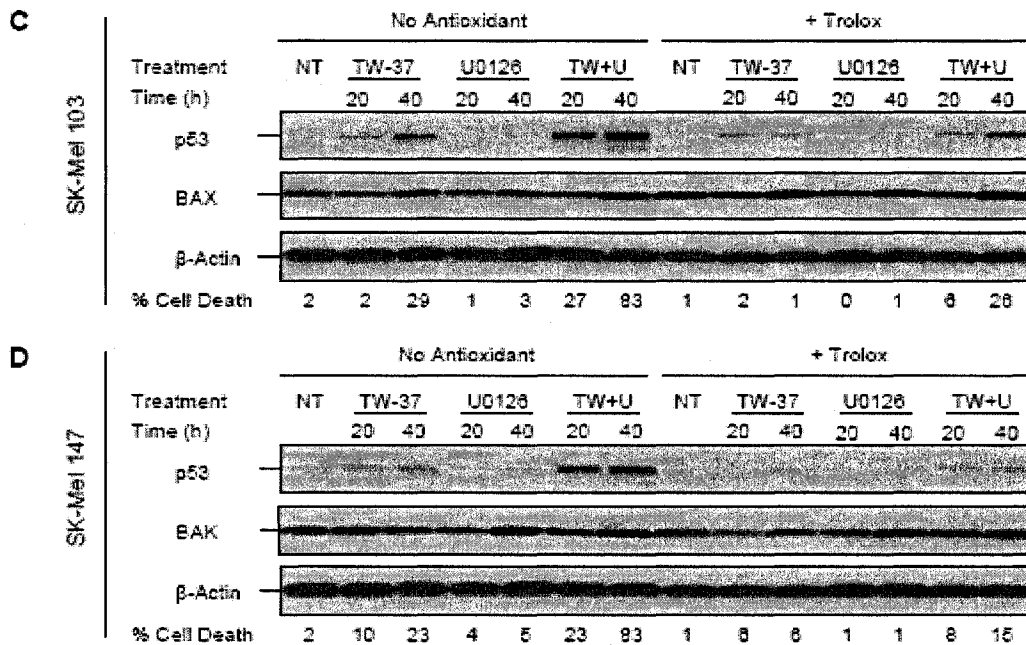


Figure 8 continued. ROS production modulates the cytotoxic effect of TW-37/U0126. (C) Induction of p53 by TW-37/U0126 and inhibition by the antioxidant Trolox (200 μ M). Shown are protein immunoblots for SK-Mel cell line 103 (C) and SK-Mel-147 (D), untreated (NT) or treated with TW-37 (5 μ M), U0126 (10 μ M) or a combination of both agents (TW+U). Note the effective inhibitory effect of Trolox on the ability of TW and TW+U to induce p53. No changes in the total expression of BAX were observed. β -actin was included as a loading control.

chemotherapeutic agents such as Adriamycin, etoposide or cisplatin which can induce p53 but cannot effectively engage the apoptotic machinery in aggressive melanoma cells (5, 7, 32).

p53 and ROS define the tumor cell-selective toxicity of TW-37/U0126.

As melanocytes do not die in response to TW-37/U0126 (Figure 3D), a corollary of our results is that the activation of the ROS/p53 apoptotic loop is restricted to tumor cells. To evaluate this possibility, normal melanocytes were compared in their response to melanoma cells. While a significant accumulation and activation (by phosphorylation) of p53 could be easily detectable in melanoma cells,

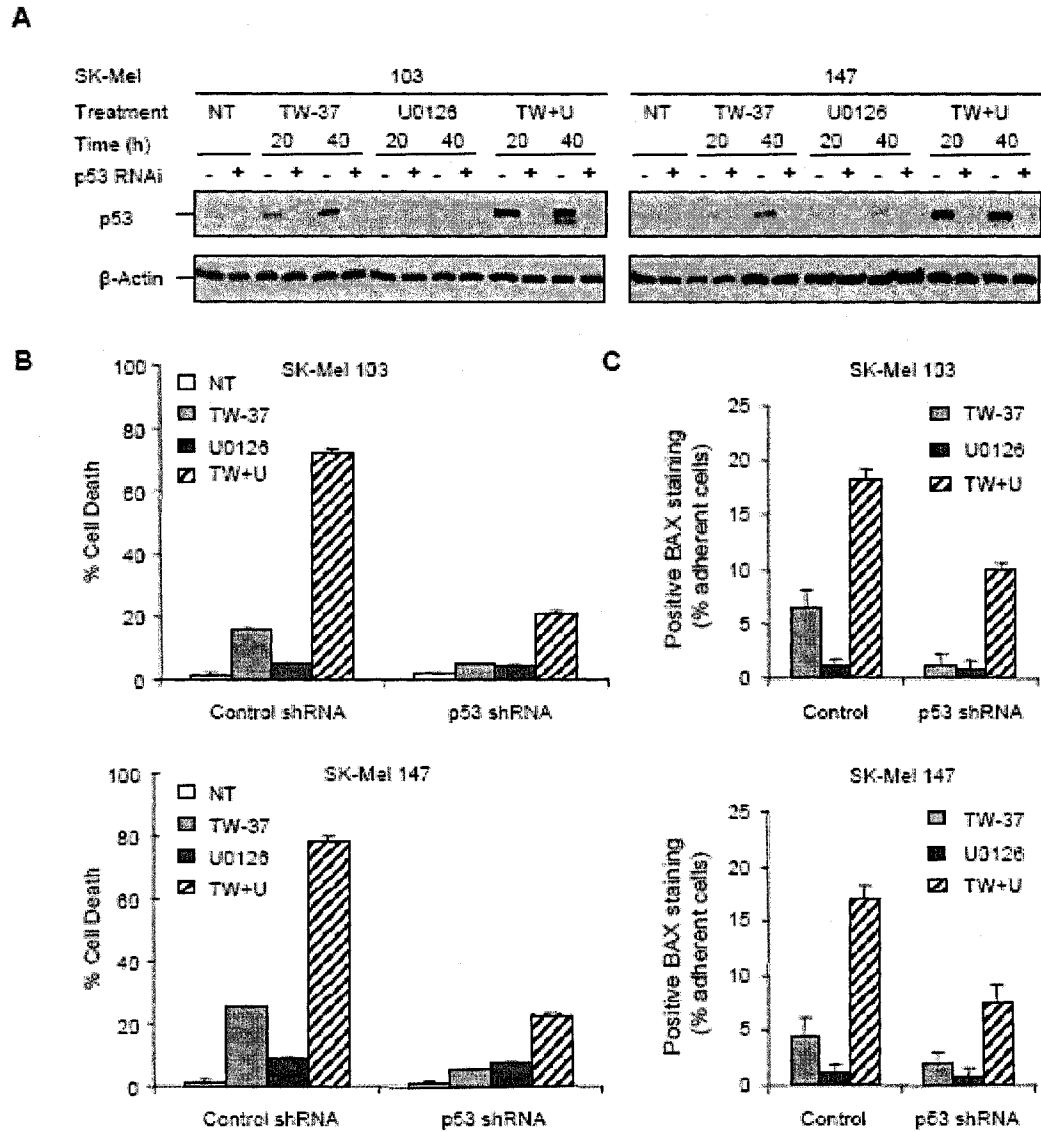


Figure 9. BH3 Mimetics and MEK inhibition cooperate in the activation of p53. (A) Contribution of p53 induction to melanoma cell death determined by RNA interference. The indicated melanoma lines were infected with lentiviral vectors coding scrambled control (-) or a validated shRNA against p53 (+) (35). Three days after infection, were treated with TW-37, U0126 or TW-37 + U0126. Total cell lysates were collected at the indicated times and probed for expression levels of p53. The impact of p53-shRNA on cell viability (Trypan Blue exclusion) is shown in (B). (C) Activation of BAX in adherent, early apoptotic cells visualized by immunofluorescence with a conformational-dependent anti-BAX specific antibody (see Materials and Methods). Note the efficacy of the shRNA approach used in the downregulation of p53 and inactivation of its pro-apoptotic functions.

normal melanocytes remained unaffected by TW-37, U0126 or the combination of both agents (Figure 10A, B). Furthermore, the redox indicator CM-H₂DCF-DA revealed a striking difference in the production of ROS by melanoma cells and normal melanocytes. Thus melanocytes remained negative for the production of oxidized DCF-dependent fluorescence even at late times post treatment with TW-37/U0126 (Figure 10C and results not shown). Yet, melanocytes could respond to strong ROS inducers such as H₂O₂ (not shown). With respect to mock-treated controls, melanoma cells incubated with TW-37 showed a 3-fold increase in the DCF-dependent signal, which was doubled in combination with U0126 (Figure 10C, right graph).

To further validate the differential ability of melanocytes and melanoma cells to produce and respond to ROS induction, global expression of oxidized proteins was monitored by protein immunoblotting. Specifically, the presence of carbonyl groups (generated by oxygen free radicals and other reactive species) was visualized after derivatization reactions with 2,4 dinitrophenylhydrazine (DNPH) and staining with anti-DNP antibodies. Interestingly, the basal levels of DNP-dependent staining were found to be already higher in untreated melanoma cells than in melanocytes (Figure 10D). Treatment of melanoma cells with TW-37, but not the inactive TW-37i led to a noticeable increase in oxidized proteins that was further exacerbated by U0126 (Figure 10D). Importantly, no such changes were observed in normal melanocytes. Together, our results identify a new BH3 mimetic (TW-37) as a novel strategy to exploit the differential redox metabolism of melanocytes and melanoma cells and subsequent activation of p53-mediated death programs.

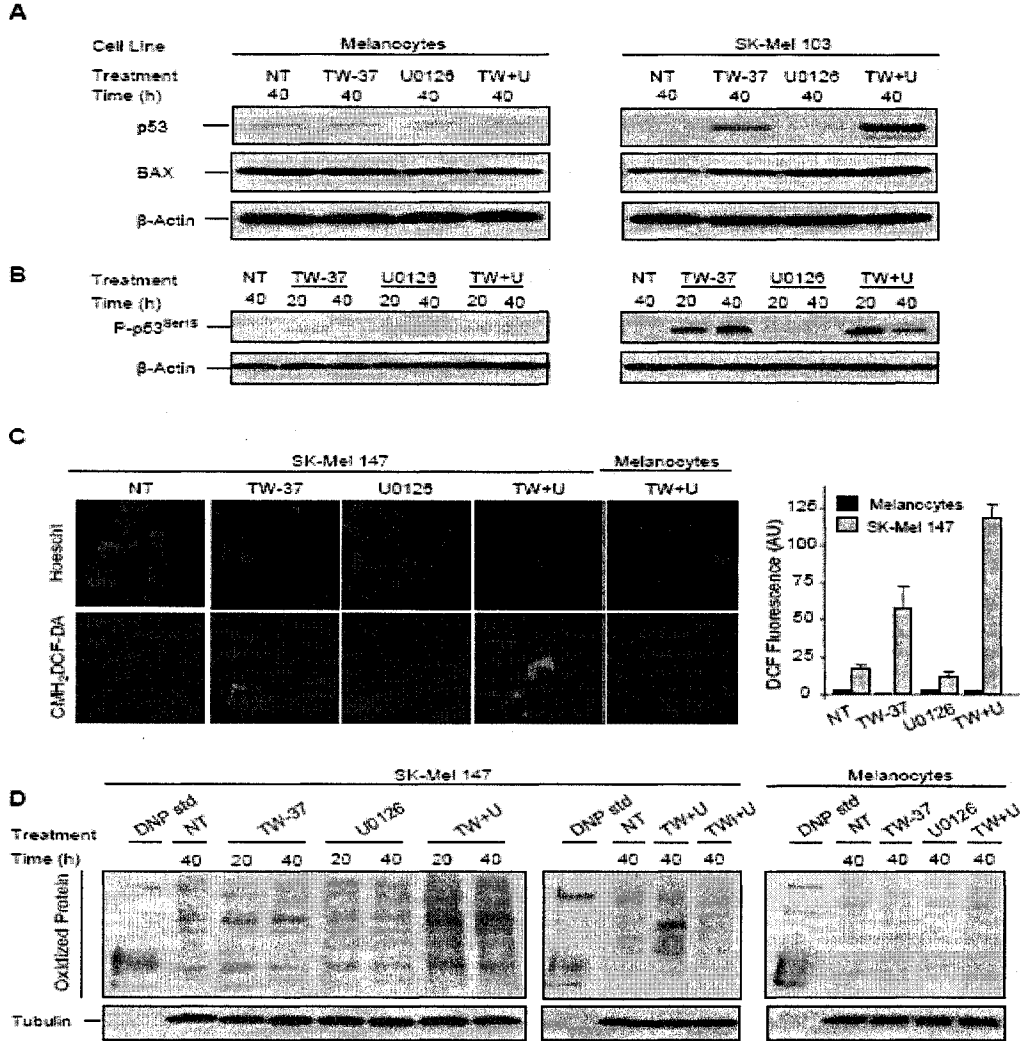


Figure 10. p53 and ROS define the tumor cell-selective toxicity of TW-37/U0126. (A) Comparative effect of TW-37, U0126 and their combination on p53 and BAX expression in normal melanocytes and melanoma cell line SK-Mel-103 shown by protein immunoblotting. No induction of p53 expression was detected in melanocytes. (B) Effect of the indicated treatments on the activation of p53 visualized with specific antibodies against p53 phosphorylated at Ser¹⁵. Note the absence of signal in treated melanocytes. (C) Early induction of ROS production in melanoma cells but not melanocytes. Shown are fluorescence micrographs of cells stained (green) with the ROS indicator CM-H₂DCFDA (1 μM) collected 6 h after incubation with the indicated treatments. The percentage of the total cells with positive staining is indicated (three independent fields were scored). Quantification of mean fluorescence intensity for melanocytes and the melanoma cells treated with the indicated agents is indicated in the right graph. Note that no significant signal could be visualized for normal melanocytes (at any treatment conditions). (D) Immunoblot analysis of cell lysates from melanoma line SK-Mel-147 and normal melanocytes for the presence of oxidized proteins. Cell pellets were collected following drug treatments at the indicated times and lysates were derivatized with DNP using the OxyBlot Kit (Chemicon) with resulting DNP-sidechains detected with a specific antibody to the DNP moiety. DNP protein standards allow for equivalent interblot comparisons and tubulin is used as a loading control.

General impact of MEK inhibitors on TW-37 mediated cell death. Anti-cancer activity *in vivo*.

U-0126 has been broadly used as a MEK inhibitor. However, to discard putative unspecific effects of this compound, additional viability studies were performed with CI-1040, a structurally different MEK inhibitor (49). Notably, and as the case of U-0126, CI-1040 was able to promote a tumor-cell selective killing of melanoma cells in the presence of TW-37 (Figure 11A, B). Thus, CI-1040 enhanced by 5 fold the death of TW-treated melanoma cells without affecting the viability of normal melanocytes (Figure 11A). Moreover, confirming the results with U0126, the synergistic effect of CI-1040 and TW-37 was strictly dependent on the production of ROS. Thus, both, Tiron and Trolox completely blocked the cytotoxic activity of the TW-37/CI-1040 combination in melanoma cells (Figure 11B).

CI-1040 has been previously used as the proof of principle for blocking MEK in human melanoma cells grown as mouse xenografts (50). Therefore, we used this compound to validate our hypothesis that BH3 mimetics targeting Mcl-1, Bcl-x_L and Bcl-2 can significantly improve the therapeutic impact of MEK inhibition *in vivo*, even in otherwise chemoresistant melanoma cells expressing NRAS mutations. Towards this end, SK-Mel-103 were transduced with GFP (to aid in non-invasive imaging of tumor growth) and injected s.c. in immunosuppressed mice (Figure 11C-F). Animals were treated with suboptimal concentrations of TW-37 and/or CI-1040 (to mimic unfavorable situations that may be encountered in human tumors) and

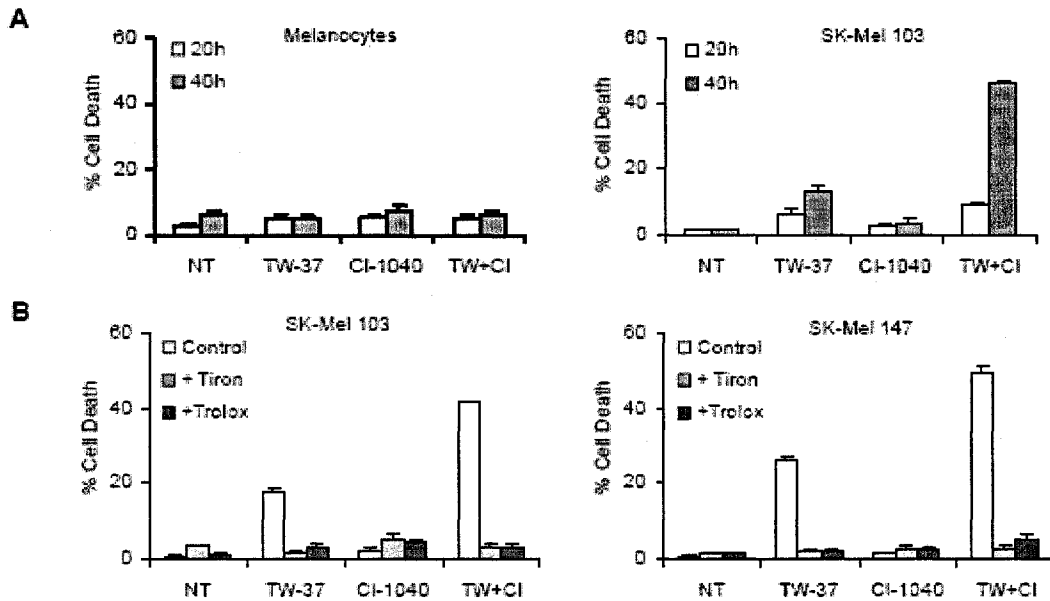


Figure 11. Synergy between TW-37 and MEK inhibitors is not restricted to U0126 and can be visualized *in vivo*. A, comparative analysis of the response of melanocytes (left) and the melanoma cell line SK-Mel-103 (right) to TW-37 in the absence or presence of the MEK inhibitor CI-1040. Columns, mean at 20 and 40 hours posttreatment (white and gray columns, respectively); bars, SE. Note the preferential killing of melanoma cells (but not melanocytes) by TW-37/CI-1040. B, inhibition of the synergistic effect of TW-37/CI-1040 by treatment with the antioxidants Tiron and Trolox, supporting a critical role of ROS in the killing of melanoma cells by the combination of BH3 mimetics and MEK inhibitors.

monitored for tumor growth at different times post-implantation. Consistent with the synergistic tumor-cell killing culture, the MEK inhibitor/TW-37 combination was found to block melanoma cell growth in mice as shown by a significant reduction in tumor volume and tumor mass (Figure 11C,D; see representative examples of placebo and drug-treated animals in Figure 11E, F). In summary, our results identify a new BH3 mimetic (namely, TW-37) as a potent strategy to overcome melanoma chemoresistance. Thus, rationally designed BH3 mimetics may broaden the spectrum of patients that could benefit from available inhibitors of the MAPK pathway.

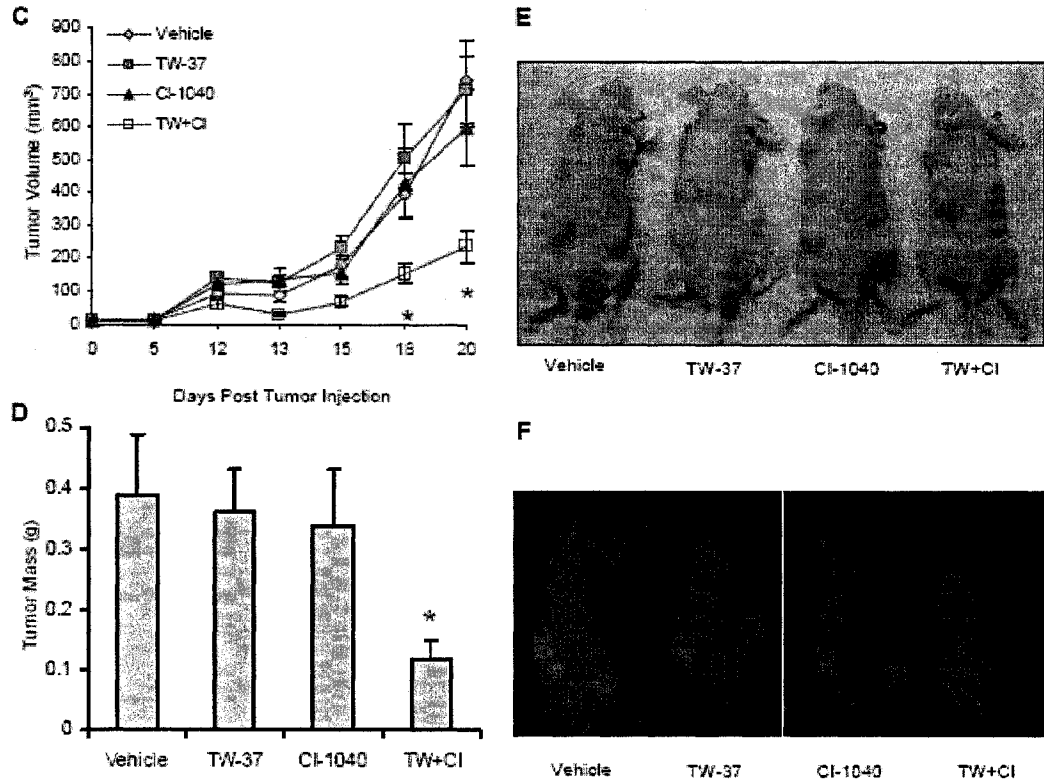


Figure 11 continued. Synergy between TW-37 and MEK inhibitors is not restricted to U0126 and can be visualized *in vivo*. C to F, effect of TW-37 and MEK inhibition on melanoma growth (mouse xenografts). C, comparative analysis of the localized growth of melanoma cells (line SK-Mel-147) implanted s.c. in immunosuppressed mice. Points, mean tumor volume in animals treated with placebo control (gray diamonds), TW-37 (gray squares), the MEK inhibitor CI-1040 (black triangles), or a combination of both agents (white squares); bars, SE. Pairwise comparisons among groups were analyzed with the Tukey's HSD test. *, $P < 0.05$, statistical significance with respect to untreated controls or the indicated drugs as single agents. D, tumor weight estimated for the indicated treatment groups at day 20 after implantation. The Dunnett test was used for individual comparisons to untreated controls. *, $P < 0.05$. E, representative photographs captured with visible light of animals corresponding to each treatment group at day 20 after tumor cell injection. F, noninvasive visualization of GFP-tagged tumor cells by whole-body fluorescence imaging showing a significant reduction in tumor size by the TW-37/MEK inhibition combination.

Discussion

Here, we describe an unexpected interplay between the MAPK pathway and anti-apoptotic factors in the control of melanoma cell viability. Moreover, we report a new strategy to activate the intrinsic expression of p53 in melanoma cells by exploiting their intrinsic sensitivity to ROS. This study capitalizes on stable RNA interference to define the specific role of single proteins in an otherwise intrinsically complex genetic background of tumor cells. By combining pharmacological approaches with selective downmodulation of Bcl-2, Bcl-x_L, Mcl-1, BAX, BAK and p53, we were able to (i) identify mechanisms of resistance to MEK inhibitors, (ii) provide the rationale for a pleiotropic BH3 mimetic (TW-37), (iii) address the mode of action of this compound and (iv) define a differential regulation of ROS production in melanocytes and melanoma cells.

Dissecting the molecular basis underlying the regulation of the MAPK pathway and Bcl-2 family members has important translational implications. The potentially “druggable” nature of both signaling cascades (14, 15, 43) and the fact that they are invariably dysregulated in melanoma cells, have inspired efforts aimed at the development of molecularly targeted therapies. Unfortunately, improved antitumor efficacy and reduced secondary toxicity from novel therapies has not yet been demonstrated in clinical settings (28). Certainly, multiple factors may contribute to marginal effects of current therapeutic agents. Limited solubility and stability of the compound(s) as well as increased drug efflux pumps or detoxification enzymes are some examples of factors that may compromise the bioavailability of anticancer drugs in melanoma cells (5, 7). Our results support the notion that melanoma cells

may be more resistant than other tumor cells by virtue of diversifying the regulation of death mediators, for example by reducing the number of anti-apoptotic proteins controlled by the same transcription factor. Thus, ERK-independent expression of Mcl-1, Bcl-x_L and Bcl-2 (Figure 1E) can provide a potent fail-safe mechanism for the maintenance of melanoma cell viability after RAS, BRAF or MEK inhibition. Conversely, ERK-dependent downregulation of apoptotic activators of BAX/BAK (e.g. Bim_{EL}), and the expression of survivin can prevent the induction of cell death by BH3 mimetics.

In the context of mechanistic analyses of cell death, TW-37 also sheds light on the requirements for the activation of the apoptotic machinery in melanoma cells. The molecular basis of the resistance to standard chemotherapeutic agents remains unclear (5, 7, 28). Extrapolating from other tumor types has been complicated because of a debated controversy on the hierarchical organization of Bcl-2 family members. Specifically, a major point of contention has revolved around the activation of BAX and BAK (47, 51). Two models have been described depending on how BAX and BAK become activated once they are released from anti-apoptotic Bcl-2 members. According to the so-called “displacement model”, the default state of BAX and/or BAK is an active conformation able to directly cause release of proapoptogenic factors from the mitochondria (52, 53). In this setting, BH3 mimetics are expected to be highly effective since they would bypass the requirement for additional upstream activators of the mitochondrial pathways (i.e. Bim, Bid or p53), which are frequently compromised in tumor cells.

The “direct binding model” argues that removal of anti-apoptotic proteins is not sufficient to promote cell death and that additional pro-apoptotic inducers are required for full activation of BAX and BAK (51, 54). Our data are consistent with this second model since low doses of TW-37 or inactivation of Bcl-2, Bcl-x_L or Mcl-1 by RNA interference were unable *per se* to engage the apoptotic machinery in melanoma cells. These results may account, at least in part, for the failure of Bcl-2 antisense strategies as monotherapy in melanoma (55). Taken at face value, our results would not even support the use of pleiotropic BH3 mimetics as single anti-melanoma agents. However, it should be emphasized that the very need for cooperative signals provides the basis for tumor cell selectivity. We propose MEK/ERK inhibition as an effective strategy to accelerate the kinetics and efficacy of BH3 mimetics. Thus, the induction of Bim_{EL} and reduction of survivin by U0126 together with the synergistic effect of U0126 and TW-37 on p53, could provide the required signals for the activation of BAX/BAK and the subsequent induction cell death in otherwise chemoresistant melanoma cells.

Perhaps one of the most intriguing results of this study is that the synergy between TW-37 and the inactivation of MEK/ERK relies on a tumor-cell restricted induction of p53 via ROS. Functional interactions between p53 and MAPK pathways have been described in a variety of systems. Thus, the MAP kinases, ERK, JNK and p38 can play an active role in the phosphorylation and induction of p53 (56). However, in melanoma cells treated with a BH3 mimetic, we found the opposite situation: inhibition of MEK/ERK favored an efficient accumulation and activation of

p53. Future studies will determine the specific impact of ROS on p53 function, but it may correspond to direct activation by oxidation (57).

Importantly, the TW-37/U0126 combination offers several advantages. First, the induction of p53 by TW-37/U0126 is tumor-cell selective. This is in contrast to stimuli such as UV and γ -radiation, as well as various DNA-damaging drugs including Adriamycin, etoposide or cisplatin among others, which affect p53 levels both in normal and tumor cells (12, 32). By avoiding the activation of p53 in normal cell compartments TW-37/U0126 could reduce the secondary toxicity characteristic of standard anti-tumor therapies. A second attractive feature of TW-37/U0126 is that it may exploit transcription-independent functions of p53 and thus bypass defects required for DNA binding (51). Thus, BAX and BAK activation were observed independently of significant increases in total protein expression (Figure 8C,D).

Furthermore, TW-37/U0126 can efficiently bypass defects downstream of the mitochondria. Of note, the melanoma lines used in this study express low levels of Apaf-1 and high levels of caspase inhibitors (e.g. XIAP, ML-IAP) (31, 58). These genetic defects, which can reduce the sensitivity to adriamycin, paclitaxel or high doses of etoposide (58-61), did not prevent cell death by TW-37/U0126.

Finally, the TW-37/U0126 treatment revealed an intrinsically different threshold for the accumulation and control of changes in ROS between normal melanocytes and melanoma cells. Melanocytes are specialized pigment-producing cells. They produce melanin, which is inherently adapted to scavenge ROS and thus prevent DNA damage, recruitment of stress-associated transcription factors, and the initiation of apoptosis (62). Paradoxically, this protective function of melanin is

frequently lost during tumor progression (63). Consequently, melanoma cells may be more sensitive than melanocytes to ROS-induced cell death (64). The accumulation of ROS following U0126 in melanoma cells treated with TW-37 indicate that the MEK/ERK MAPK pathway may play an additional mechanism of control of melanoma viability under ROS-inducing stress stimuli.

In conclusion, here we have shown a potential therapy for melanoma based on the capacity of a novel, pleiotropic BH3 mimetic (TW-37) to synergize with MEK inhibition (U0126). We have shown that melanoma cell death is dependent not only on the activation of BAX/BAK as expected from a BH3 mimetic, but a tumor-cell selective induction of a ROS-p53 feedback loop upstream of the mitochondria. Therefore, this combination therapy may prove especially beneficial for melanoma, since p53 is rarely mutated in this tumor type (5). The TW-37/U0126 combination takes full advantage of intrinsic dysregulated redox capacity of melanoma cells and highlights ROS as a point of vulnerability of melanoma cells that can be exploited for drug development.

Acknowledgements

Grant support.

Elsa U. Pardee Career Development Award (M.S.S.) and grants NIH R01 CA107237 (M.S.S), U19CA113317 (S.W), DE13346 (T.E.C), CA83087 (C.R.B), AR042742 and AR050511 (J.T.E and R.N), and University of Michigan Cancer Center Core Grant 5 P30 CA46592. J.A.B. was supported by T32 GM07767 and DC00011. M.S.S. is a V Foundation for Cancer Research Scholar.


We thank Wen-Hua Tang, Tom Miller and Ryan Stork for technical assistance, Yolanda Fernández and Christophe Denoyelle for advice at early stages of this study, and Judith Sebolt-Leopold (Pfizer) for help and advice with CI-1040. We also thank José Esteban, Mikhail Nikiforov and Gabriel Núñez for critical reading of this manuscript.

Appendix



Van Andel Institute
Founded by Jay and Betty VanAndel

333 Bostwick NE Grand Rapids, MI 49503 616.234.5000 Fax 616.234.5001

TO: Dr. Han-Mo Koo
CC: Dr. Matt Van Brocklin
FROM: Dr. Pamela Swiatek, Chair 
VARI Institutional Animal Care and Use Committee (IACUC)
DATE: 4/2/04
RE: Notice of Approval of Protocol #04-04-009

PROTOCOL DETAILS

Protocol #: 04-04-009
Protocol Title: *Evaluation and test of novel anti-cancer agents using human tumor xenografts in experimental mice*
IACUC Approval Date: 4/2/04
IACUC Expiration Date: 4/2/07
Funding Source: Internal only
Species: *Mus musculus*

The attached protocol for animal use (04-04-009) was reviewed and approved by the IACUC. Please ensure that all investigators and technicians using animals under this protocol are familiar with its contents and follow the procedures as outlined. **Any new procedures not described in this protocol will require IACUC review and cannot be undertaken until approved as either a protocol amendment or as a separate protocol.** Your protocol number must be included on all animal purchase requests.

When applying for external funding, the VARI Office of Grants and Contracts requires that the approval is current and the protocol reflects the proposed animal use procedures described in the grant application. The Committee should be notified by memorandum when additional project title(s) and sponsor(s) are added to an approved protocol. **This protocol will remain in effect until April 2, 2007.** Federal laws and guidelines require that the IACUC conduct an annual review of ongoing projects; therefore, you will be asked to submit an annual update form, provided by my office, describing any changes in procedures or personnel. Approval may only be extended beyond the third year by submitting an entirely new replacement protocol.

If you find that your research directions change, please notify the IACUC to amend your protocol. Outside inspectors visit VARI and compare the actual animal use with the animal use described in approved protocols. It is critical that currently approved protocols are accurate and up to date. If there are any questions, please contact me by phone (616-234-5684) or e-mail (pam.swiatek@vai.org).

cc: Bryn Eagleson, Laboratory Animal Resource Director
Joan Koelzer, DVM, VARI Veterinarian
Kaye Johnson, IACUC Administrative Assistant

BIBLIOGRAPHY

1. Goldstein, D. B., Tate, S. K., and Sisodiya, S. M. Pharmacogenetics goes genomic. *Nat Rev Genet*, 4: 937-947, 2003.
2. Baylin, S. B. and Ohm, J. E. Epigenetic gene silencing in cancer - a mechanism for early oncogenic pathway addiction? *Nat Rev Cancer*, 6: 107-116, 2006.
3. Kaelin, W. G., Jr. The concept of synthetic lethality in the context of anticancer therapy. *Nat Rev Cancer*, 5: 689-698, 2005.
4. Curtin, J. A., Fridlyand, J., Kageshita, T., Patel, H. N., Busam, K. J., Kutzner, H., Cho, K. H., Aiba, S., Brocker, E. B., LeBoit, P. E., Pinkel, D., and Bastian, B. C. Distinct sets of genetic alterations in melanoma. *N Engl J Med*, 353: 2135-2147, 2005.
5. Soengas, M. S. and Lowe, S. W. Apoptosis and melanoma chemoresistance. *Oncogene*, 22: 3138-3151, 2003.
6. Serrone, L., Zeuli, M., Sega, F. M., and Cognetti, F. Dacarbazine-based chemotherapy for metastatic melanoma: thirty-year experience overview. *J Exp Clin Cancer Res*, 19: 21-34., 2000.
7. Grossman, D. and Altieri, D. C. Drug resistance in melanoma: mechanisms, apoptosis, and new potential therapeutic targets. *Cancer Metastasis Rev*, 20: 3-11, 2001.
8. Polsky, D. and Cordon-Cardo, C. Oncogenes in melanoma. *Oncogene*, 22: 3087-3091, 2003.
9. Satyamoorthy, K., Chehab, N. H., Waterman, M. J., Lien, M. C., El-Deiry, W. S., Herlyn, M., and Halazonetis, T. D. Aberrant regulation and function of wild-type p53 in radioresistant melanoma cells [In Process Citation]. *Cell Growth Differ*, 11: 467-474, 2000.
10. Sharpless, N. E. and Chin, L. The INK4a/ARF locus and melanoma. *Oncogene*, 22: 3092-3098, 2003.
11. Vucic, D., Stennicke, H. R., Pisabarro, M. T., Salvesen, G. S., and Dixit, V. M. ML-IAP, a novel inhibitor of apoptosis that is preferentially expressed in human melanomas. *Curr Biol*, 10: 1359-1366, 2000.

12. Soengas, M. S., Capodiecici, P., Polsky, D., Mora, J., Esteller, M., Opitz-Araya, X., McCombie, R., Herman, J. G., Gerald, W. L., Lazebnik, Y. A., Cordon-Cardo, C., and Lowe, S. W. Inactivation of the apoptosis effector Apaf-1 in malignant melanoma. *Nature*, *409*: 207-211, 2001.
13. Fujimoto, A., Takeuchi, H., Taback, B., Hsueh, E. C., Elashoff, D., Morton, D. L., and Hoon, D. S. B. Allelic Imbalance of 12q22-23 associated with Apaf-1 locus correlates with poor disease outcome in cutaneous melanoma. *Cancer Res*, *64*: 2245-2250, 2004.
14. Tuveson, D. A., Weber, B. L., and Herlyn, M. BRAF as a potential therapeutic target in melanoma and other malignancies. *Cancer Cell*, *4*: 95-98, 2003.
15. Karasarides, M., Chioeches, A., Hayward, R., Niculescu-Duvaz, D., Scanlon, I., Friedlos, F., Ogilvie, L., Hedley, D., Martin, J., Marshall, C. J., Springer, C. J., and Marais, R. B-RAF is a therapeutic target in melanoma. *Oncogene*, *23*: 6292-6298, 2004.
16. Panka, D. J., Atkins, M. B., and Mier, J. W. Targeting the mitogen-activated protein kinase pathway in the treatment of malignant melanoma. *Clin Cancer Res*, *12*: 2371s-2375s, 2006.
17. Chin, L., Garraway, L. A., and Fisher, D. E. Malignant melanoma: genetics and therapeutics in the genomic era. *Genes Dev*, *20*: 2149-2182, 2006.
18. Bedogni, B., O'Neill, M. S., Welford, S. M., Bouley, D. M., Giaccia, A. J., Denko, N. C., and Powell, M. B. Topical treatment with inhibitors of the phosphatidylinositol 3'-kinase/Akt and Raf/mitogen-activated protein kinase kinase/extracellular signal-regulated kinase pathways reduces melanoma development in severe combined immunodeficient mice. *Cancer Res*, *64*: 2552-2560, 2004.
19. Zhang, X. D., Borrow, J. M., Zhang, X. Y., Nguyen, T., and Hersey, P. Activation of ERK1/2 protects melanoma cells from TRAIL-induced apoptosis by inhibiting Smac/DIABLO release from mitochondria. *Oncogene*, *22*: 2869-2881, 2003.
20. Boucher, M. J., Morisset, J., Vachon, P. H., Reed, J. C., Laine, J., and Rivard, N. MEK/ERK signaling pathway regulates the expression of Bcl-2, Bcl-X(L), and Mcl-1 and promotes survival of human pancreatic cancer cells. *J Cell Biochem*, *79*: 355-369, 2000.
21. Eisenmann, K. M., VanBrocklin, M. W., Staffend, N. A., Kitchen, S. M., and Koo, H. M. Mitogen-activated protein kinase pathway-dependent tumor-specific survival signaling in melanoma cells through inactivation of the proapoptotic protein bad. *Cancer Res*, *63*: 8330-8337, 2003.

22. Ley, R., Ewings, K. E., Hadfield, K., Howes, E., Balmanno, K., and Cook, S. J. Extracellular signal-regulated kinases 1/2 are serum-stimulated "Bim(EL) kinases" that bind to the BH3-only protein Bim(EL) causing its phosphorylation and turnover. *J Biol Chem*, 279: 8837-8847, 2004.
23. Erhardt, P., Schremser, E. J., and Cooper, G. M. B-Raf inhibits programmed cell death downstream of cytochrome c release from mitochondria by activating the MEK/Erk pathway. *Mol Cell Biol*, 19: 5308-5315, 1999.
24. Meier, F., Schitteck, B., Busch, S., Garbe, C., Smalley, K., Satyamoorthy, K., Li, G., and Herlyn, M. The RAS/RAF/MEK/ERK and PI3K/AKT signaling pathways present molecular targets for the effective treatment of advanced melanoma. *Front Biosci*, 10: 2986-3001, 2005.
25. Solit, D. B., Garraway, L. A., Pratilas, C. A., Sawai, A., Getz, G., Basso, A., Ye, Q., Lobo, J. M., She, Y., Osman, I., Golub, T. R., Sebolt-Leopold, J., Sellers, W. R., and Rosen, N. BRAF mutation predicts sensitivity to MEK inhibition. *Nature*, 439: 358-362, 2006.
26. Abi-Habib, R. J., Urieto, J. O., Liu, S., Leppla, S. H., Duesbery, N. S., and Frankel, A. E. BRAF status and mitogen-activated protein/extracellular signal-regulated kinase kinase 1/2 activity indicate sensitivity of melanoma cells to anthrax lethal toxin. *Mol Cancer Ther*, 4: 1303-1310, 2005.
27. Smalley, K. S., Haass, N. K., Brafford, P. A., Lioni, M., Flaherty, K. T., and Herlyn, M. Multiple signaling pathways must be targeted to overcome drug resistance in cell lines derived from melanoma metastases. *Mol Cancer Ther*, 5: 1136-1144, 2006.
28. Flaherty, K. T. Chemotherapy and targeted therapy combinations in advanced melanoma. *Clin Cancer Res*, 12: 2366s-2370s, 2006.
29. Satyamoorthy, K., Meier, F., Hsu, M. Y., Berking, C., and Herlyn, M. Human xenografts, human skin and skin reconstructs for studies in melanoma development and progression. *Cancer Metastasis Rev*, 18: 401-405, 1999.
30. Nikolovska-Coleska, Z., Wang, R., Fang, X., Pan, H., Tomita, Y., Li, P., Roller, P. P., Krajewski, K., Saito, N. G., Stuckey, J. A., and Wang, S. Development and optimization of a binding assay for the XIAP BIR3 domain using fluorescence polarization. *Anal Biochem*, 332: 261-273, 2004.
31. Fernandez, Y., Miller, T. P., Denoyelle, C., Esteban, J. A., Tang, W. H., Bengston, A. L., and Soengas, M. S. Chemical blockage of the proteasome inhibitory function of bortezomib: impact on tumor cell death. *J Biol Chem*, 281: 1107-1118, 2006.

32. Fernandez, Y., Verhaegen, M., Miller, T. P., Rush, J. L., Steiner, P., Opiari, A. W., Jr., Lowe, S. W., and Soengas, M. S. Differential regulation of noxa in normal melanocytes and melanoma cells by proteasome inhibition: therapeutic implications. *Cancer Res*, *65*: 6294-6304, 2005.
33. Cioca, D. P., Aoki, Y., and Kiyosawa, K. RNA interference is a functional pathway with therapeutic potential in human myeloid leukemia cell lines. *Cancer Gene Ther*, *10*: 125-133, 2003.
34. Jiang, M. and Milner, J. Bcl-2 constitutively suppresses p53-dependent apoptosis in colorectal cancer cells. *Genes Dev*, *17*: 832-837, 2003.
35. Brummelkamp, T. R., Bernards, R., and Agami, R. Stable suppression of tumorigenicity by virus-mediated RNA interference. *Cancer Cell*, *2*: 243-247, 2002.
36. Ohtsuka, T., Ryu, H., Minamishima, Y. A., Macip, S., Sagara, J., Nakayama, K. I., Aaronson, S. A., and Lee, S. W. ASC is a Bax adaptor and regulates the p53-Bax mitochondrial apoptosis pathway. *Nat Cell Biol*, *6*: 121-128, 2004.
37. Lois, C., Hong, E. J., Pease, S., Brown, E. J., and Baltimore, D. Germline transmission and tissue-specific expression of transgenes delivered by lentiviral vectors. *Science*, *295*: 868-872, 2002.
38. Juin, P., Hunt, A., Littlewood, T., Griffiths, B., Swigart, L. B., Korsmeyer, S., and Evan, G. c-Myc functionally cooperates with Bax to induce apoptosis. *Mol Cell Biol*, *22*: 6158-6169, 2002.
39. Perez, D. and White, E. TNF-alpha signals apoptosis through a bid-dependent conformational change in Bax that is inhibited by E1B 19K. *Mol Cell*, *6*: 53-63, 2000.
40. Favata, M. F., Horiuchi, K. Y., Manos, E. J., Daulerio, A. J., Stradley, D. A., Feeser, W. S., Van Dyk, D. E., Pitts, W. J., Earl, R. A., Hobbs, F., Copeland, R. A., Magolda, R. L., Scherle, P. A., and Trzaskos, J. M. Identification of a novel inhibitor of mitogen-activated protein kinase kinase. *J Biol Chem*, *273*: 18623-18632, 1998.
41. Harada, H., Quearry, B., Ruiz-Vela, A., and Korsmeyer, S. J. Survival factor-induced extracellular signal-regulated kinase phosphorylates BIM, inhibiting its association with BAX and proapoptotic activity. *Proc Natl Acad Sci U S A*, *101*: 15313-15317, 2004.
42. Chang, F., Steelman, L. S., Shelton, J. G., Lee, J. T., Navolanic, P. M., Blalock, W. L., Franklin, R., and McCubrey, J. A. Regulation of cell cycle progression

- and apoptosis by the Ras/Raf/MEK/ERK pathway (Review). *Int J Oncol*, 22: 469-480, 2003.
43. Letai, A. Pharmacological manipulation of Bcl-2 family members to control cell death. *J Clin Invest*, 115: 2648-2655, 2005.
 44. Degterev, A., Lugovskoy, A., Cardone, M., Mulley, B., Wagner, G., Mitchison, T., and Yuan, J. Identification of small-molecule inhibitors of interaction between the BH3 domain and Bcl-xL. *Nat Cell Biol*, 3: 173-182, 2001.
 45. Oltersdorf, T., Elmore, S. W., Shoemaker, A. R., Armstrong, R. C., Augeri, D. J., Belli, B. A., Bruncko, M., Deckwerth, T. L., Dinges, J., Hajduk, P. J., Joseph, M. K., Kitada, S., Korsmeyer, S. J., Kunzer, A. R., Letai, A., Li, C., Mitten, M. J., Nettesheim, D. G., Ng, S., Nimmer, P. M., O'Connor, J. M., Oleksijew, A., Petros, A. M., Reed, J. C., Shen, W., Tahir, S. K., Thompson, C. B., Tomaselli, K. J., Wang, B., Wendt, M. D., Zhang, H., Fesik, S. W., and Rosenberg, S. H. An inhibitor of Bcl-2 family proteins induces regression of solid tumours. *Nature*, 435: 677-681, 2005.
 46. Yin, H., Lee, G. I., Sedey, K. A., Rodriguez, J. M., Wang, H. G., Sebt, S. M., and Hamilton, A. D. Terephthalamide derivatives as mimetics of helical peptides: disruption of the Bcl-x(L)/Bak interaction. *J Am Chem Soc*, 127: 5463-5468, 2005.
 47. Willis, S. N. and Adams, J. M. Life in the balance: how BH3-only proteins induce apoptosis. *Curr Opin Cell Biol*, 17: 617-625, 2005.
 48. Danial, N. N. and Korsmeyer, S. J. Cell death: critical control points. *Cell*, 116: 205-219, 2004.
 49. Davies, S. P., Reddy, H., Caivano, M., and Cohen, P. Specificity and mechanism of action of some commonly used protein kinase inhibitors. *Biochem J*, 351: 95-105, 2000.
 50. Collisson, E. A., De, A., Suzuki, H., Gambhir, S. S., and Kolodney, M. S. Treatment of metastatic melanoma with an orally available inhibitor of the Ras-Raf-MAPK cascade. *Cancer Res*, 63: 5669-5673, 2003.
 51. Green, D. R. Apoptotic pathways: ten minutes to dead. *Cell*, 121: 671-674, 2005.
 52. Letai, A., Bassik, M. C., Walensky, L. D., Sorcinelli, M. D., Weiler, S., and Korsmeyer, S. J. Distinct BH3 domains either sensitize or activate mitochondrial apoptosis, serving as prototype cancer therapeutics. *Cancer Cell*, 2: 183-192, 2002.

53. Willis, S. N., Chen, L., Dewson, G., Wei, A., Naik, E., Fletcher, J. I., Adams, J. M., and Huang, D. C. Proapoptotic Bak is sequestered by Mcl-1 and Bcl-xL, but not Bcl-2, until displaced by BH3-only proteins. *Genes Dev*, *19*: 1294-1305, 2005.
54. Kuwana, T., Bouchier-Hayes, L., Chipuk, J. E., Bonzon, C., Sullivan, B. A., Green, D. R., and Newmeyer, D. D. BH3 domains of BH3-only proteins differentially regulate Bax-mediated mitochondrial membrane permeabilization both directly and indirectly. *Mol Cell*, *17*: 525-535, 2005.
55. Frantz, S. Lessons learnt from Genasense's failure. *Nat Rev Drug Discov*, *3*: 542-543, 2004.
56. Agarwal, M. L., Ramana, C. V., Hamilton, M., Taylor, W. R., DePrimo, S. E., Bean, L. J., Agarwal, A., Agarwal, M. K., Wolfman, A., and Stark, G. R. Regulation of p53 expression by the RAS-MAP kinase pathway. *Oncogene*, *20*: 2527-2536, 2001.
57. Martindale, J. L. and Holbrook, N. J. Cellular response to oxidative stress: signaling for suicide and survival. *J Cell Physiol*, *192*: 1-15, 2002.
58. Soengas, M. S., Alarcon, R. M., Yoshida, H., Giaccia, A. J., Hakem, R., Mak, T. W., and Lowe, S. W. Apaf-1 and caspase-9 in p53-dependent apoptosis and tumor inhibition. *Science*, *284*: 156-159, 1999.
59. Dai, D. L., Martinka, M., Bush, J. A., and Li, G. Reduced Apaf-1 expression in human cutaneous melanomas. *Br J Cancer*, *91*: 1089-1095, 2004.
60. Svingen, P. A., Loegering, D., Rodriguez, J., Meng, X. W., Mesner, P. W., Jr., Holbeck, S., Monks, A., Krajewski, S., Scudiero, D. A., Sausville, E. A., Reed, J. C., Lazebnik, Y. A., and Kaufmann, S. H. Components of the cell death machine and drug sensitivity of the National Cancer Institute Cell Line Panel. *Clin Cancer Res*, *10*: 6807-6820, 2004.
61. Zanon, M., Piris, A., Bersani, I., Vegetti, C., Molla, A., Scarito, A., and Anichini, A. Apoptosis protease activator protein-1 expression is dispensable for response of human melanoma cells to distinct proapoptotic agents. *Cancer Res*, *64*: 7386-7394, 2004.
62. Meyskens, F. L., Jr., Farmer, P., and Fruehauf, J. P. Redox regulation in human melanocytes and melanoma. *Pigment Cell Res*, *14*: 148-154, 2001.
63. Meyskens, F. L., Jr., McNulty, S. E., Buckmeier, J. A., Tohidian, N. B., Spillane, T. J., Kahlon, R. S., and Gonzalez, R. I. Aberrant redox regulation in human metastatic melanoma cells compared to normal melanocytes. *Free Radic Biol Med*, *31*: 799-808, 2001.

64. Meyskens, F. L., Jr., Buckmeier, J. A., McNulty, S. E., and Tohidian, N. B. Activation of nuclear factor-kappa B in human metastatic melanomacells and the effect of oxidative stress. *Clin Cancer Res*, 5: 1197-1202, 1999.